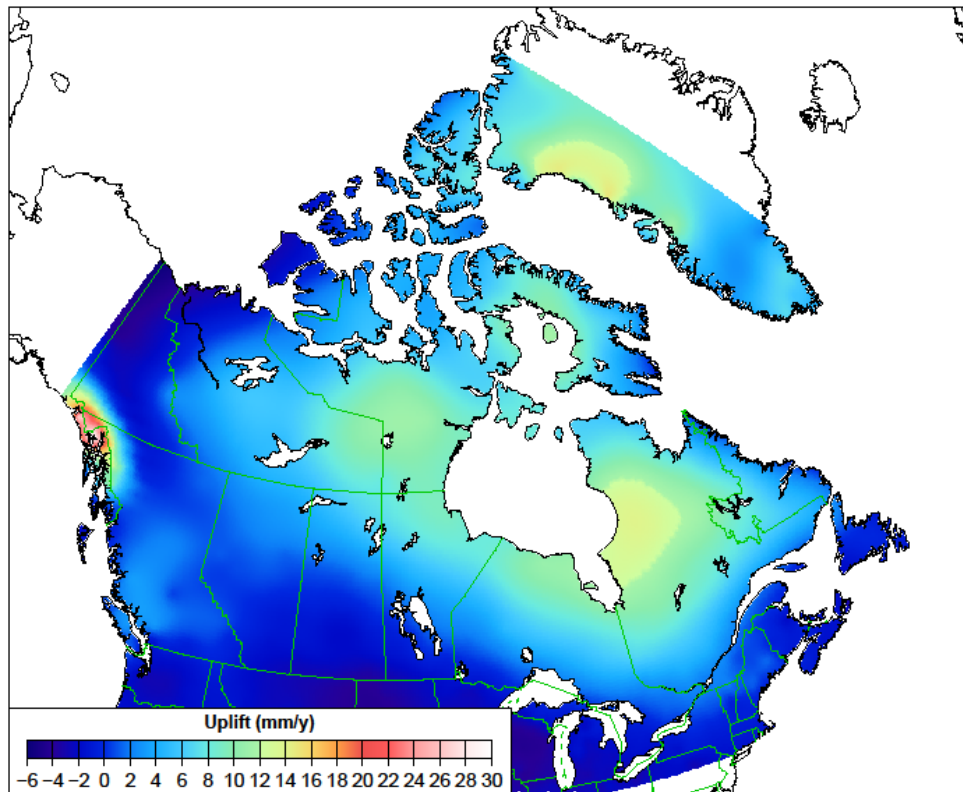




Natural Resources
Canada Ressources naturelles
Canada

GEOMATICS CANADA OPEN FILE 0062



NAD83v70VG: A new national crustal velocity model for Canada

C.M.I. Robin, M. Craymer, R. Ferland, T.S. James, E. Lapelle,
M. Piraszewski, and Y. Zhao

2020

Canada

GEOMATICS CANADA
OPEN FILE 0062

**NAD83v70VG: A new national crustal velocity
model for Canada**

**C.M.I. Robin¹, M. Craymer¹, R. Ferland¹, T.S. James², E. Lapelle¹,
M. Piraszewski¹, and Y. Zhao¹**

¹Canadian Geodetic Survey, 588 Booth Street, Ottawa, Ontario

²Geological Survey of Canada, 9860 West Saanich Road, Sidney, British Columbia

2020

© Her Majesty the Queen in Right of Canada, as represented by the Minister of Natural Resources, 2020

Information contained in this publication or product may be reproduced, in part or in whole, and by any means, for personal or public non-commercial purposes, without charge or further permission, unless otherwise specified.

You are asked to:

- exercise due diligence in ensuring the accuracy of the materials reproduced;
- indicate the complete title of the materials reproduced, and the name of the author organization; and
- indicate that the reproduction is a copy of an official work that is published by Natural Resources Canada (NRCan) and that the reproduction has not been produced in affiliation with, or with the endorsement of, NRCan.

Commercial reproduction and distribution is prohibited except with written permission from NRCan. For more information, contact NRCan at nrcan.copyrightdroitd'auteur.rncan@canada.ca.

Permanent link: <https://doi.org/10.4095/327592>

This publication is available for free download through GEOSCAN (<https://geoscan.nrcan.gc.ca/>).

Recommended citation

Robin, C.M.I., Craymer, M., Ferland, R., James, T.S., Lapelle, E., Piraszewski, M., and Zhao, Y., 2020. NAD83v70VG: A new national crustal velocity model for Canada; Geomatics Canada, Open File 0062, 1. zip file. <https://doi.org/10.4095/327592>

Publications in this series have not been edited; they are released as submitted by the author.

Abstract

A national-scale crustal velocity model has been developed for Canada as part of the current realisation of NAD83(CSRS), delivered as a set of 3 national grids, for each of the North, East and Up (N, E and U) components. It is used to propagate coordinates to different reference epochs, and to support scientific studies such as natural hazards, climate change, and groundwater change. The previous velocity model was based on continuous and campaign GPS data between 1994 and 2011.3. The new model includes new stations in key areas, six more years of data (to the end of 2017), and newly reprocessed historical data using the latest software and GPS products. We include data from continuous GPS sites in Canada, the northern portions of the US, all of Greenland, and a set of globally distributed sites used to define the reference frame; and from repeated high accuracy campaign surveys in Canada. A new type of model is introduced for the vertical grid. It incorporates GPS observations with the crustal uplift predictions of Glacial Isostatic Adjustment (GIA) and elastic rebound models, which are especially important in areas with sparse coverage. Gridded uncertainty estimates are provided for each component of NAD83v70VG.

Table of Contents

Abstract	3
Index of Figures	6
Index of Tables	6
1 Introduction.....	7
2 Data Sources.....	7
2.1 Velocity Field.....	7
2.1.1 Coordinate solutions at Active Control Stations (ACS's).....	8
2.1.2 Coordinate solutions at campaign stations.....	8
2.1.3 Multi-year combinations.....	8
2.1.4 Time series discontinuities	8
2.1.5 Periodic Signals.....	11
2.1.6 Outlier Detection.....	11
2.2 Geodynamic Models.....	14
2.2.1 ICE-6G_C (VM5a).....	16
2.2.2 LaurInnu.....	17
2.2.3 NAICE.....	18
2.2.4 Regional models for recent and present-day ice mass change.....	19
2.3 Geophysical model validation and selection	20
2.3.1 Velocity field subsets	21
2.3.2 Comparison of geophysical model predictions with observations	22
2.3.3 Geophysical model to observation residuals	23
2.3.4 Comparison of empirical semivariograms	23
2.3.5 The combined post-glacial geodynamic model	24
3 Input Data Integration.....	26
3.1 Model grid	26
3.2 Modelling approach	26
3.2.1 Interpolation method	26
3.2.2 Data integration: vertical component.....	27
3.2.3 Data integration: horizontal components	30
4 Uncertainty Model.....	32
4.1 Interpolation Uncertainty.....	33

4.2	Horizontal model uncertainties.....	33
4.3	Vertical model uncertainty.....	33
4.3.1	Combined Geodynamic Model Uncertainty.....	33
4.3.2	Total Uncertainty.....	34
5	Discussion.....	35
5.1	Comparison with NAD83v60VG.....	35
5.2	Data to model residuals	36
6	Future Work	39
7	User Summary.....	39
8	Acknowledgements.....	40
	Bibliography.....	40
	Appendix A. Interpolation technique cross-validation tests	46
	Appendix B. Weighted Ordinary Kriging.....	50
	Appendix C. Observations	53

Index of Figures

Figure 1 - Active and Passive Control Station locations.....	9
Figure 2 - Active Control Station time series.....	10
Figure 3 - Sites affected by post-seismic motion in BC.....	12
Figure 4 - Horizontal component of the full velocity field.....	13
Figure 5 - Vertical component Vu (mm/yr) of the full velocity field.....	14
Figure 6 - Vertical component of the full velocity field once outliers have been removed.....	15
Figure 7 - ICE-6G_C (VM5a)	17
Figure 8 - Laulinnu.....	18
Figure 9 - NAICE.....	19
Figure 10 - Regional uplift model predictions.....	20
Figure 11 - Subsets of stations used for testing glacial isostatic adjustment (GIA) models.....	21
Figure 12 - GIA to observation comparisons.....	22
Figure 13 - Empirical semivariograms for the three GIA models and all observations once outliers are removed	24
Figure 14 - Empirical semivariograms and models.....	25
Figure 15 - Interpolated observation to model residuals	28
Figure 16 - NAD83v70VG, vertical component.....	29
Figure 17 - Interpolated velocity field, vertical component.....	30
Figure 18 - NAD83v70VG, horizontal component.....	32
Figure 19 - NAD83v70VG, horizontal component, for the west coast of Canada	33
Figure 20 - NAD83v70VG uncertainty grid, vertical component.....	35
Figure 21 - NAD83v60VG, vertical component.....	36
Figure 22 - Residual field, vertical component.....	37
Figure 23 - Residual field, horizontal components.....	38
Figure A1 - Cross-validation test results.....	49

Index of Tables

Table 1 - GIA to observation comparisons.....	22
Table 2 - RMSE between observation and models.....	23
Table 3 - Residual Statistics.....	38
Table A1 - Interpolation and approximation methods tested	46
Table C1 - Velocity solutions analyzed for inclusion in the velocity field.....	53

1 Introduction

The Canadian Geodetic Survey (CGS) at Natural Resources Canada (NRCan) is the Government of Canada agency that defines the Canadian Spatial Reference System (CSRS) and provides access to it.

NAD83(CSRS) is the 3-dimensional realisation of the CSRS and is fundamentally tied to a high-precision three-dimensional international reference frame. The current realisation is NAD83(CSRS) v7, which was released in February 2019.

These systems enable the inter-operability of all geo-referenced data, including most geospatial data. Consequently, the accuracy of the CSRS limits the accuracy of georeferenced data in Canada. At the same time, the earth is dynamic and reference systems must account for position changes generated by crustal motion. In other words, providing an accurate CSRS requires ongoing monitoring of changes to the Canadian landmass. Indeed, the growing need for ubiquitous and increasingly precise georeferenced data in everyday life, including for safety-of-life applications, puts increasing demands on the CSRS and NRCan's Global Navigation Satellite System (GNSS) observation networks.

In addition to tracking crustal motion observations for the definition of the reference frame, CGS provides a gridded crustal velocity model with national coverage. Software such as the CGS's TRX and CSRS-PPP (freely available at [NRCan \(2020\)](#)) use the model to propagate users' coordinates in time, a critical capability for surveyors and engineers. The velocity model also supports scientific studies in fields of research such as natural hazards and sea level change (James, et al. in review). CGS velocity grids are periodically updated to provide users with current and accurate data. NAD83v70VG is a new version of the velocity model and accompanies the release of NAD83(CSRS) v7.

NAD83v70VG includes 3 grids for each of the north (N), east (E) and up (U) components. The grids extend from 41° to 85° North, and from 40° to 142° West, with grid spacing of 0.25°. While the model extends over marine areas, the data used to create it originates from terrestrial sites; thus, the model is only recommended for use on land. Unless stated otherwise, all data in this paper are in NAD83(CSRS) v7 (Canadian Geodetic Survey, 2020b)). NAD83v70VG is also available upon request in the latest realisation of International Terrestrial Reference Frame known as ITRF14 (Rebischung et al., 2017).

This document describes the data and modelling techniques used to calculate each of the N, E, and U components of NAD83v70VG and their error grids.

2 Data Sources

2.1 Velocity Field

A total of 1177 velocities were calculated from coordinate time series at 1076 GNSS sites. We refer to this set of observed velocities from GNSS stations as the velocity field. In addition to Canadian stations, the velocity field includes stations in the US and Greenland selected to constrain the model across its boundaries, as well as International GNSS Service (IGS) stations distributed globally, in order to align our results with a global reference frame. Coordinate estimates run from September 1994 to December 2017 (GPS week 1981). Canadian data sources include continuously operating Active Control Stations (ACS's) (Canadian Geodetic Survey, 2020a), as well as campaign stations (also referred to as passive

control stations (Canadian Geodetic Survey, 2020c). The distribution of active and passive control stations is plotted in Figure 1. Once edited as described below, 848 velocities are retained for use in creating the velocity model.

2.1.1 Coordinate solutions at Active Control Stations (ACS's)

ACS's are unattended tracking stations, equipped with high precision dual frequency GNSS receivers and geodetic-grade antennas, which continuously record carrier phase and pseudorange measurements for all GPS satellites within station view. Nine-hundred-thirty-nine weekly coordinate solutions (from 2000-01-02 to 2017-12-31) are calculated for these stations in the Bernese GNSS Software v5.2, using CODE repro2 precise orbits (Rebischung et al., 2016) and a number of environmental models. Fifty globally distributed IGS stations are included in the solution to ensure it is aligned to the IGS14 reference frame. Ionospheric-free baselines are used with tropospheric estimation for all baselines.

2.1.2 Coordinate solutions at campaign stations

Campaign stations include the Canadian Base Network (CBN) and stations installed for regional campaigns. The CBN is a network of stable pillar monuments anchored in bedrock, with force-centered antenna mounts. Observations at campaign stations include multiple (3-4) 24-hour occupations of each site for each campaign. This data set includes fifty-nine survey campaigns from 1994 to 2017. Regional campaigns include twenty-two campaigns (1999-2011) carried out by Geological Survey of Canada (GSC), twenty-two campaigns (2005-2016) from the Eastern Canada Deformation Array, nine campaigns (1998-2013) on Haida Gwaii, and five campaigns from the International Great Lakes Datum network. The same Bernese processing methodology is used as for the ACS's.

2.1.3 Multi-year combinations

The velocity field is estimated by linearly fitting all or sections of the observation time series at stations listed in Table C1 (Appendix C) using solution independent exchange (SINEX) analysis software designed in-house (R. Ferland, personal communication). All network solutions (station positions and velocities) are combined rigorously and simultaneously with full covariance information. Translations, rotations and scale (and their respective rates of change) are calculated with an alignment condition for the combined cumulative solutions, and a variance factor for each solution is estimated and applied to each weekly covariance matrix. Input station coordinates with residuals greater than 20 mm or 5σ are rejected. Station coordinate solutions which differ from their official IGS2014 coordinate solutions by more than 20 mm or 5σ (position) and 10 mm/yr or 5σ (velocity) are also rejected.

2.1.4 Time series discontinuities

Continuously operating stations may exhibit apparent offsets in position or changes in velocity. Significant offsets or changes in velocity which persist over a significant number of epochs are classified as position (P) or velocity (V) discontinuities respectively. Discontinuities may be caused by equipment changes (e.g., antenna replacements), changes to the station monument, and other physical changes (e.g., local infrastructure changes affecting multipath); or by geophysical events, such as earthquakes or

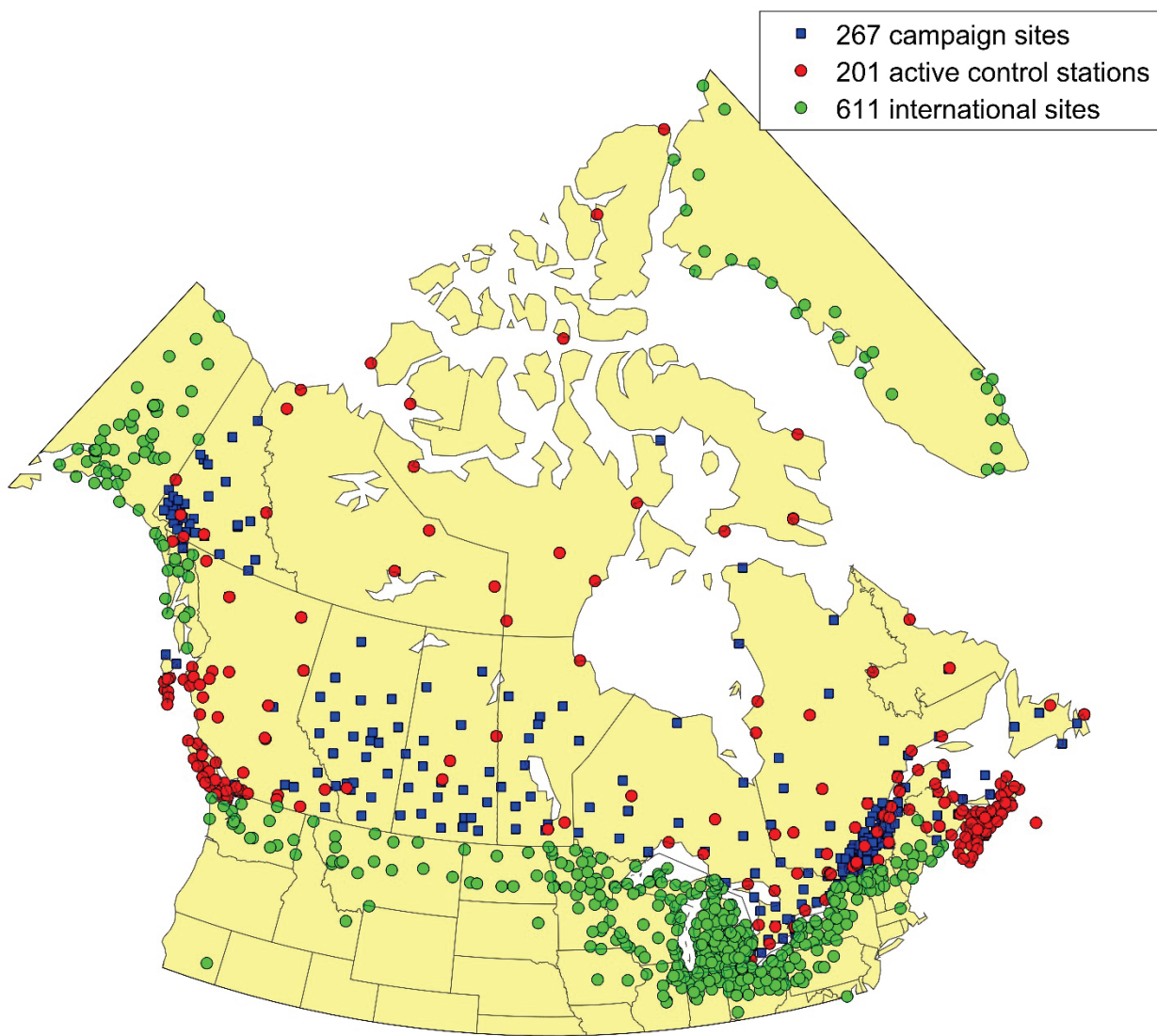


Figure 1 - Active and Passive Control Station locations. Velocities were analyzed at passive control (or campaign) stations (blue squares) and active control stations (red and green circles) at 1079 sites for the NAD83(CSRS) v7 velocity field. In addition, forty-nine sites distributed globally for alignment with the International Terrestrial Reference Frame (ITRF) are not shown.

long-term variability in water loading (including snow and ice) (see Figure 2). In some cases the cause of discontinuities is unknown. P or V discontinuities are introduced as parameters to correct time series offsets and to account for velocity changes. Both can significantly affect inferred velocities.

Identifying discontinuities in geodetic time series is an ongoing challenge. A test of the ability of a variety of methods (both automated and manual) to detect P and V offsets inserted into synthetic data with simulated noise levels (Gazeaux et al., 2013) indicate that manual methods generally outperform automated discontinuity identification software. Regardless of the methods used, however, discontinuity identification often remains a subjective exercise.

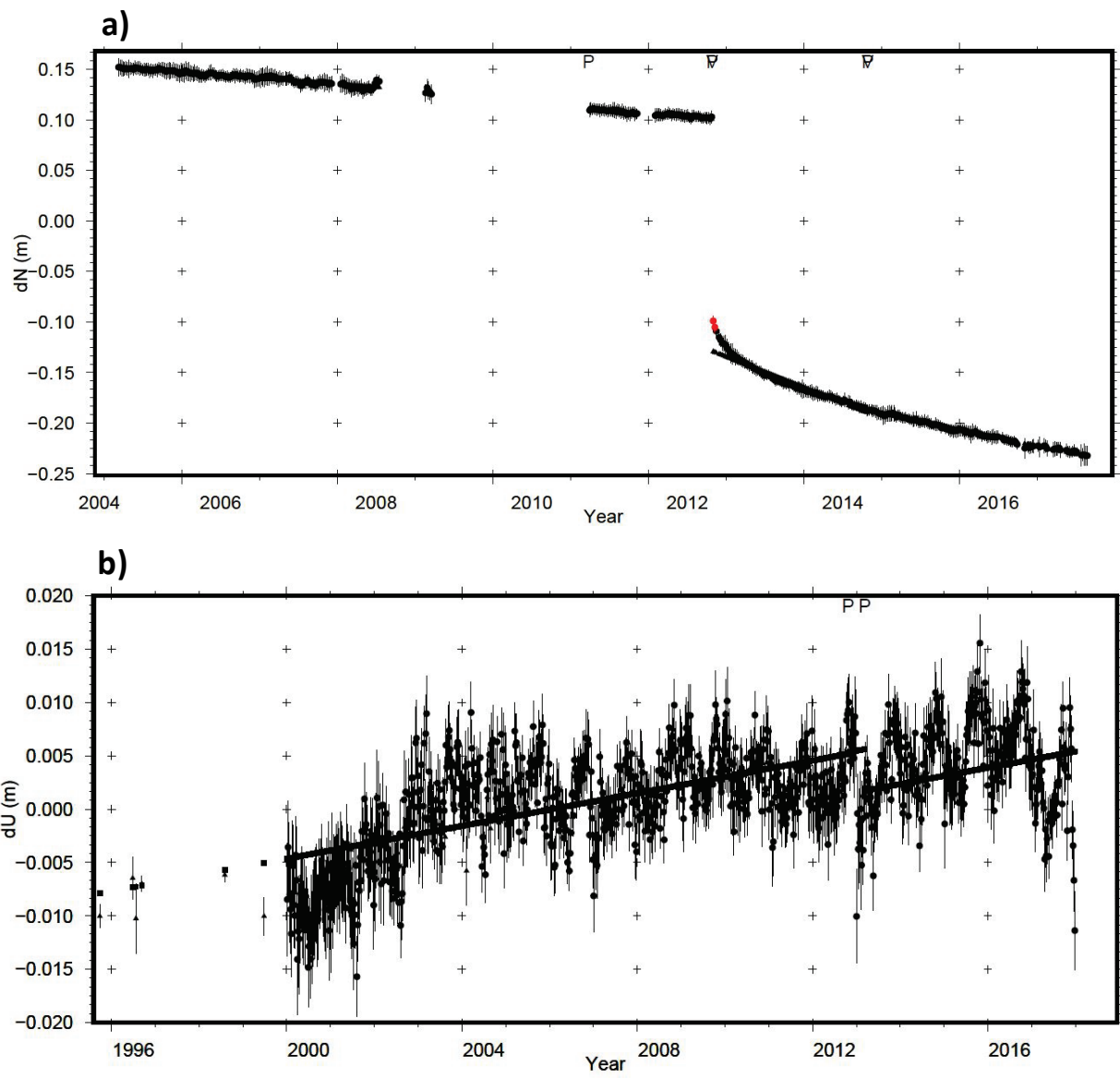


Figure 2 - Active Control Station time series in the IGS14 reference frame. Observations are displayed as circles with error bars; predicted velocities from a best fit to the data in a least squares sense are displayed with black squares (and appear linear). P marks where an offset discontinuity was applied, and V where a velocity discontinuity is applied. **Figure 2a** shows the weekly coordinates for the North component at the BCSS site on Haida Gwaii, BC, where there is a significant and ongoing post-seismic velocity change following a M7.8 earthquake on October 27, 2012. The first (pre-earthquake) velocity is used for the crustal velocity model as it represents long-term motion for that area. **Figure 2b** shows the weekly coordinates for the Up component at the DRAO site in southeast BC, where there are strong annual (seasonal) and multi-year signals.

The CGS determines its discontinuities manually, in some cases with the help of the time series visualization tool TSView (Herring, 2003). For consistency with the global reference frame to which NAD83(CRS) is aligned (IGS2014), P and V discontinuities for IGS reference stations employed in this realisation were chosen to be the same as those utilized in the realisation of IGS14.

Co-seismic discontinuities and post-seismic deformation from earthquakes are observed in geodetic time series which span these events (e.g., Altamimi et al., 2017). In Canada, these are most pronounced at ACS's along the tectonically active west coast. The Haida Gwaii earthquake of October 27, 2012 and the related Craig earthquake of January 5, 2013 caused position offsets of up to 20 cm and post-seismic velocity disturbances in BC and southeast Alaska which are ongoing (Figure 2a) (e.g., James et al., 2015; Nykolaishen et al., 2015). Crustal movement in periods of post-seismic relaxation is a long term non-linear process; however, users of NAD83v70VG require epoch transformations of up to 20 years, and longer for geoscience applications such as prediction of past relative sea level change (Simon et al., 2017) and projection of future relative sea-level change (Lemmen et al., 2016). Thus, only velocities estimating steady-state motion were adopted for NAD83v70VG. In order to extract steady-state velocities from earthquake-affected sites, the following two schemes were applied:

- for two ACS's nearest to the Haida Gwaii and Craig earthquakes (BCSS and AB48 - see Table 1), we imposed a V discontinuity at the time of the quake, and another 2 years later, resulting in 3 velocities for different portions of the time series; this piece-wise linear approximation we call this the V1V2V3 scheme (Figure 2a). The first represent long-term motion for that site, and this was the one adopted for the velocity model. An exponential fit to the post-seismic deformation was tested, but the computational expense outweighed the benefit over the V1V2V3 model for our purposes.
- At a group of sites further afield (Figure 3), earthquake-related discontinuities were identified. These have approached steady-state motion more quickly. For these sites, we isolated 2 years of data following the Craig earthquake, and constrained the velocities before and after to be the same. We call this the V1V2V1 scheme.

2.1.5 Periodic Signals

We tested the inclusion of parameters for annual and semi-annual signals to account for seasonal variations (Figure 2b). These could be due to hydrological and atmospheric pressure cycles, weather effects on the antenna (e.g., ice and hoar frost), or other incompletely modeled effects. They can have significant effects on velocity estimates for time series of short duration. Blewitt and Lavallee (2002) found that seasonal biases dominate velocity errors for data spanning less than 2.5 years, and that the bias drops off rapidly between 2 and 2.5 years. For the velocity model, we retain 30 time series with less than 2.5 years of data (3.4% of the total number) because they exhibit subtle seasonal signals and are consistent with regional motion. Generally, removing seasonal signals produced only small changes to estimated velocities. Nevertheless, gains in computational power may permit periodic signals to be estimated in the future.

2.1.6 Outlier Detection

NAD83V70VG is designed to capture regional and large-scale variations in crustal velocity. Observations which do not fit with surrounding velocities are removed from the model calculation, although in some cases they represent real motion with very limited spatial extent. All removed stations are referred to as model 'outliers'.



Figure 3 - Sites affected by post-seismic motion in BC. Shown here are the locations of the Oct. 27 2012 Haida Gwaii and Jan 4 2013 Craig earthquakes, and the ACS's where post-seismic position and velocity discontinuities were identified in the time series. The V1V2V3 scheme was used for BCSS and AB48 while the V1V2V1 schemes was used for other sites shown here to determine long-term motion (see Section 2.1.4, Appendix C, Table C1).

Horizontal and vertical components of all 1177 velocities calculated by the SINEX combination software are given in Figures 4 and 5, respectively. Of these, 848 velocities are retained for the crustal velocity model calculation. Velocity solutions are removed if they are duplicate, inconsistent with regional motion, or have high degrees of uncertainty, as described in detail below. In addition, for sites with multiple monuments, we de-cluster the velocity field using a weighted average of sites within a 100 meter radius. All sites, including those removed as outliers, are listed in Table C1 (Appendix C).

We identify velocity solutions as outliers in the following cases. Some outliers are inconsistent in only one or two of the components; however, at this time stations identified as outliers in only one or two components are removed from the calculation for all three components.

- At stations with multiple velocities (duplicates). Time series with one or more velocity discontinuities have two or more velocity estimates. The default is to select the most recent velocity. In some cases, such as stations affected by the Haida Gwaii earthquake of 2012, velocities other than the most recent are used. See Section 2.1.4 for a discussion on velocity (V) discontinuities and the treatment of sites affected by post-seismic deformation.

- At stations where only post-seismic transient motion is recorded (**PS** in Table C1).
- At stations with known local deformation not representative of regional motion (e.g., Goderich, ON, where the ACS is affected by local subsidence due to salt extraction). (**LD** in Table C1)
- At stations with known monument instability or other equipment problems. (**EP** in Table C1)
- At stations where the site is known to be (or have become) unsuitable, for reasons such as signal obstructions or unstable foundations (**US** in Table C1).
- At stations with velocities inconsistent with regional motion where no known cause can be identified. We remove these by visual inspection. These are most likely to be undocumented local or monument instabilities. (**NNC** in Table C1)

The vertical component of the velocity field once outliers are removed is given in Figure 6.

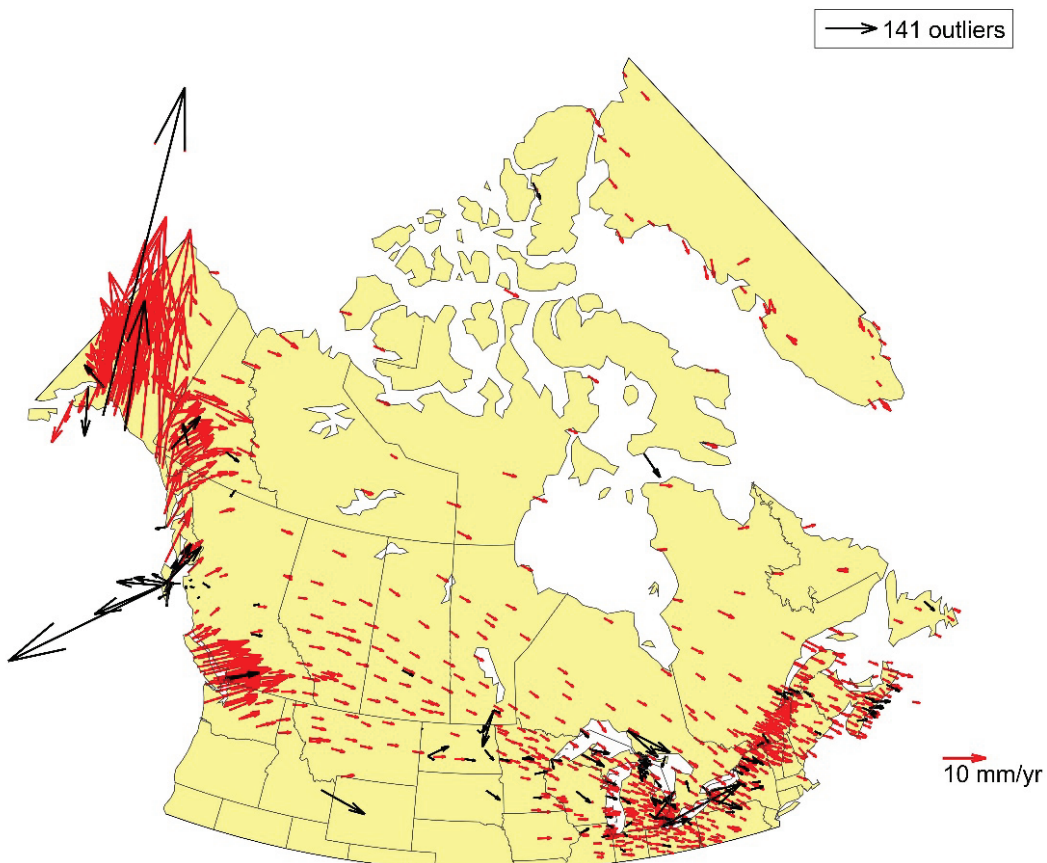


Figure 4 - Horizontal component of the full velocity field, in NAD83(CSRS). Outliers are marked in black. Outliers are velocity solutions that are duplicate, inconsistent with local motion, or that have high degrees of uncertainty, as described in the text. The general eastward trend in velocities seen in this figure are the residual plate rotation between observations and the plate rotation parameters adopted for the definition of NAD83(CSRS) in the 1990s. These are accounted for through the use of the velocity model.

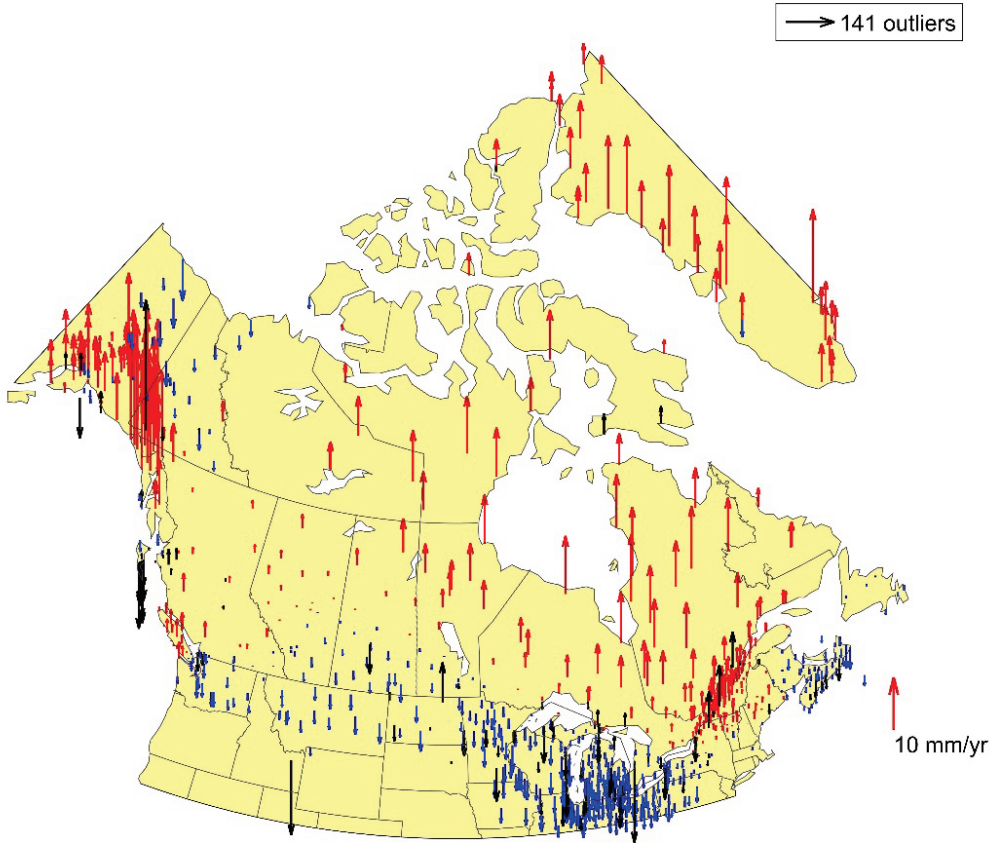


Figure 5 - Vertical component V_u (mm/yr) of the full velocity field, in NAD83(CSRS). Red arrows indicate uplift and blue arrows indicate subsidence. Outliers are marked in black.

2.2 Geodynamic Models

The distribution of ACS's in our network is relatively dense in southern Canada and the northern United States. In densely sampled areas a robust crustal velocity model could be created by simply interpolating the velocity field. In contrast, areas which are difficult to access and have little supporting infrastructure are less well sampled. Interpolating crustal motion over these greater distances does not capture the expected variability in crustal velocity known from geodynamic studies. This is particularly true for vertical crustal motion, which can exhibit high degrees of variability over short distances, for reasons ranging from anthropogenic activity (e.g., groundwater extraction) to long-term climate variability (e.g., melting of continental-scale ice sheets).

The method of integrating geodynamic model predictions with geodetic data has recently gained popularity for geodetic applications (e.g., Snay et al., 2016; Robin et al., 2017; Vestol et al., 2019). In this section we describe the geodynamic models considered for integration with the vertical component of NAD83v70VG.

Large-scale crustal motion for most of Canada east of the Rockies is dominated by the effects of glacial isostatic adjustment (GIA). GIA is the response of the solid earth to changes in surface load brought about by fluctuations in glaciers and ice sheets. In Canada, the largest GIA response arises from thinning and retreating of the continental-scale Laurentide ice sheets that covered most of Canada 20,000 years ago (e.g., Simon et al., 2016), and that had deglaciated to near-modern extent by the early Holocene

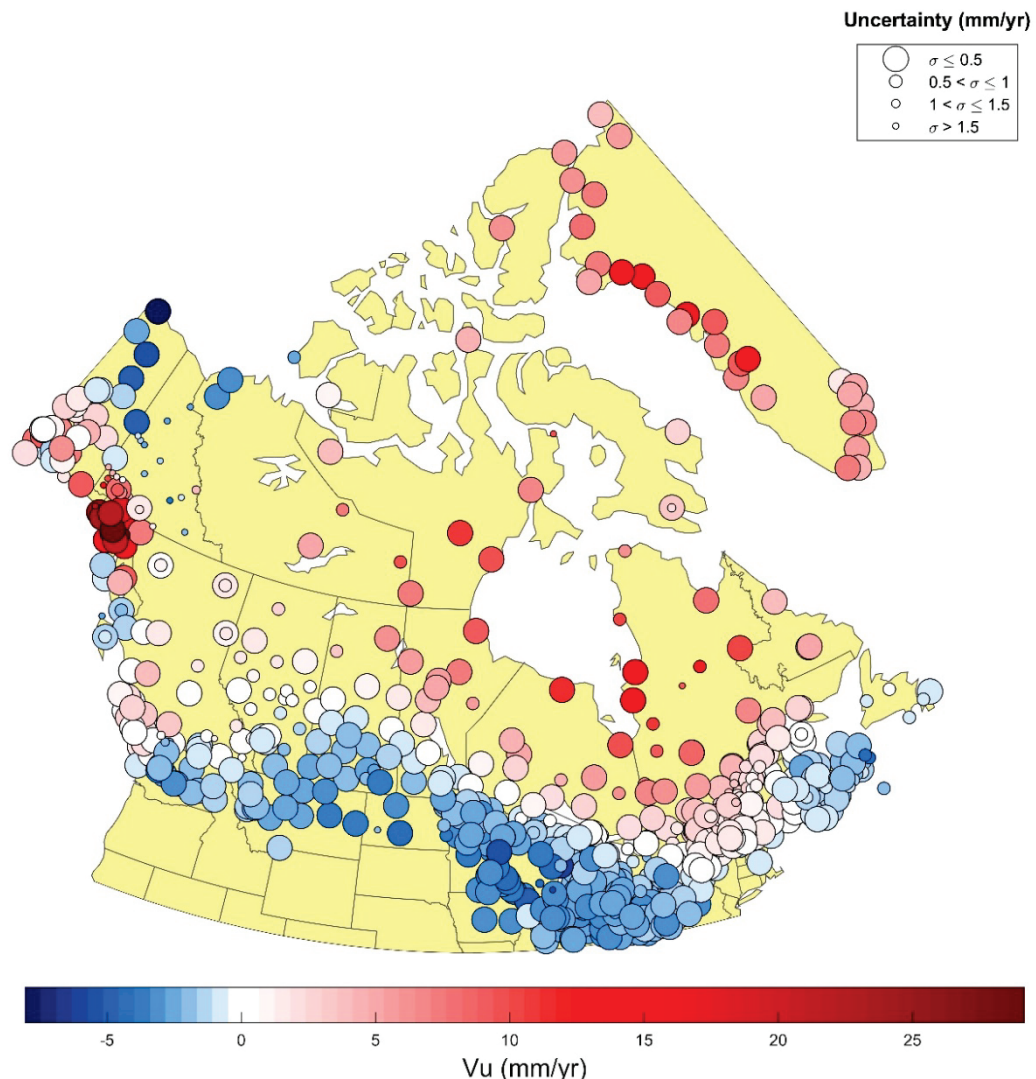


Figure 6 - Vertical component (in mm/yr) of the full velocity field, in NAD83(CSRS), once outliers have been removed. Vertical velocities are indicated by the colour, and uncertainties are indicated by the marker size.

(~7000 years ago). Further north, the Innuitian Ice Sheet (IIT) covered the Queen Elizabeth Islands (e.g., Simon et al., 2015), and has diminished to isolated ice caps and glaciers. Ongoing and more recent glacial fluctuations in western Canada, Alaska, and Greenland also generate crustal motions.

For Canada, several lines of evidence help constrain GIA models. This evidence includes shoreline migration and other indicators of relative sea level change (e.g., Peltier and Fairbanks, 2006), paleogeological records of ice advance and retreat (e.g., Dyke et al., 2003) and crustal velocities measured

with GNSS (e.g., Sella et al., 2007). Hence GIA models can provide valuable input to our crustal velocity model, with greatest impact in the north and other areas where the geodetic network is sparse. For the realisation of NAD83v70VG, GIA model predictions were used to supplement the velocity field for the vertical (U) component only. Generally, the crustal uplift rates predicted by GIA models are about a factor of ten larger than the horizontal motions in a plate-centered frame (e.g., James and Morgan, 1990; James and Ivins, 1998), and therefore we do not incorporate them in the horizontal components of NAD83v70VG at this time.

Three GIA models incorporating the thinning and retreat of the LIS and IIS were tested for use in NAD83v70VG. These are ICE-6G_C (VM5a) (Peltier et al., 2015), LaurInnu (Simon et al., 2015; Simon et al., 2016), and NAICE (Gowan et al., 2016). They are differentiated by their choice of models for ice history (extent, thickness, and temporal evolution) since the last glacial maximum, and for the earth structure parameters which define the earth's response to the changing ice load. The earth structure models are one-dimensional and radially stratified models and are calculated for a spherically symmetric earth. They account for the redistribution of meltwater, including the migration of shorelines and changes to earth rotation and the geoid (e.g., Mitrovica and Peltier, 1991). Their differences lie mainly in the focus of their study areas and the constraints used to reconstruct their ice histories. Uplift related to the Little Ice Age retreat in Alaska as well as current melting in the Arctic Archipelago and Greenland are included in two separate regional elastic models.

All tested geophysical models are described below. Figures show the models on a $2^\circ \times 2^\circ$ grid designed to cover all the velocity field stations used to create the velocity model, which is wider than the velocity model grid. Unless stated otherwise, models are plotted in their native reference frames, roughly equivalent to ITRF2014, and the accompanying observations are in IGS14. The NAD83v70VG grid is a subregion of this larger modelling grid and has smaller extent in all directions.

2.2.1 ICE-6G_C (VM5a)

ICE-6G_C (VM5a) (Peltier et al., 2015) is a global GIA model that includes a detailed retreat history of the LIS and IIS. ICE-6G_C refers to the ice history model; VM5a refers to the earth structure model. ICE-6G_C (VM5a) (referred to as ICE-6G hereon in) is a recent release of the ICE-xG (VMx) series that is constrained by GNSS uplift rates, including rates from Canadian ACS's, in addition to paleo-geographic and paleo-sea-level observations.

Uplift rates of ICE-6G superimposed with the NAD83v70VG velocity field are shown in Figure 7. The large-scale uplift structure in ICE-6G features three centers of uplift on the east, north and west sides of Hudson Bay. The hinge line (the zero contour where uplift changes to subsidence) runs roughly parallel to the Canada-US border before cutting across the Gulf of St. Lawrence. Differences between ICE-6G and the NAD83v70VG velocity field are seen over the domes of peak uplift. Data from GNSS ACS sites near these domes of uplift were not available at the time ICE-6G was being developed. Other important differences are in areas affected by more recent glacier and ice cap fluctuations.

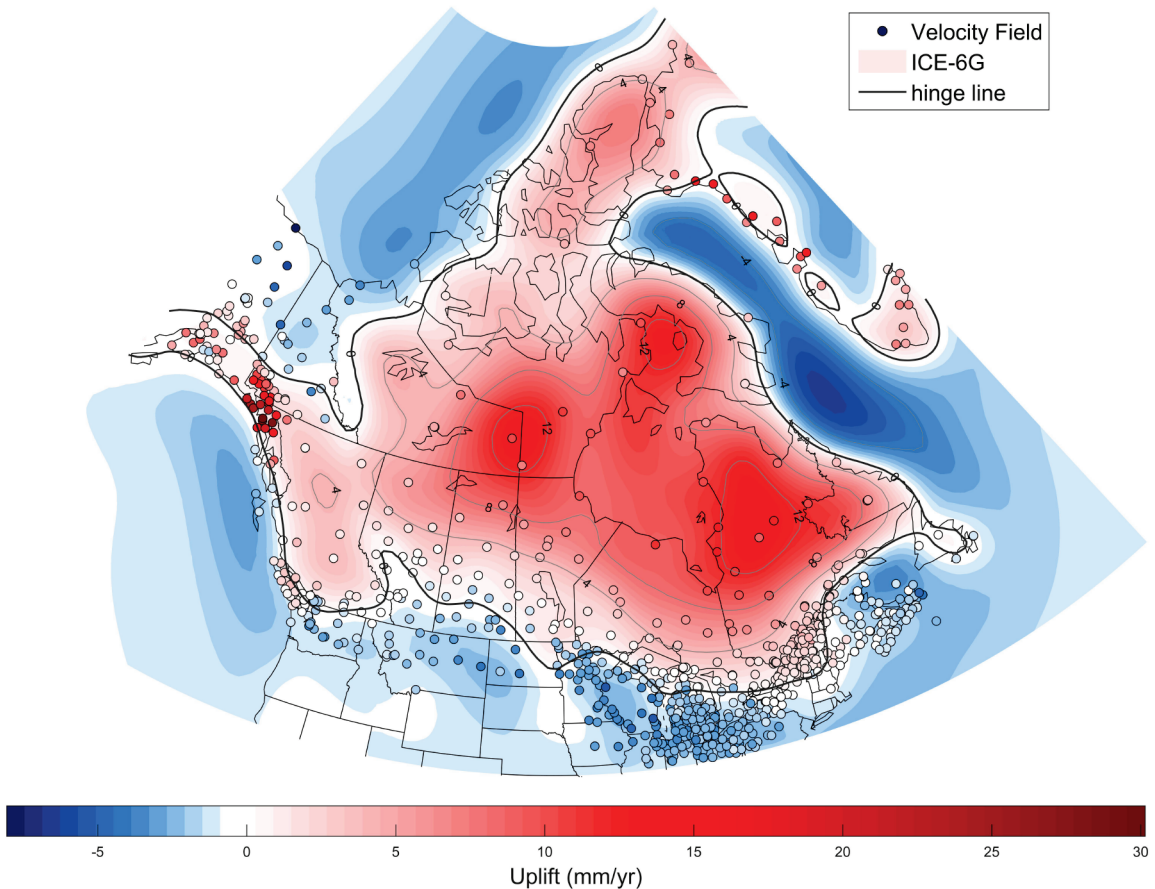


Figure 7 - ICE-6G_C (VM5a). Predicted uplift rates for the ICE-6G_C (VM5a) model of Peltier et al (2016) (shaded contours) superimposed by uplift rates from the observed velocity field (small coloured circles). The hinge line (thick black contour line) is the contour of zero vertical crustal motion across which uplift changes to subsidence.

2.2.2 LaurInnu

LaurInnu refers to the predictions of a GIA model which incorporates the Innuitian Ice Sheet (IIS) model of Simon et al. (2015) and the Laurentian ice sheet model (Laur16) of Simon et al. (2016), using modelling methods described in James and Ivins (1998) and Simon (2014). Both IIS and Laur16 were developed by tuning or altering the ICE-5G model of Peltier (2004) to improve its fit to updated sea level and GNSS data in northern Canada. ICE-5G was not tuned to GNSS observations and was found to overestimate ice thickness west of Hudson's Bay (Simon et al., 2014). The LaurInnu model utilizes the VM5a viscosity profile of Peltier and Drummond (2008).

Uplift rates of LaurInnu and the NAD83v70VG velocity field are shown in Figure 8. Differences between the velocity field and the model are similar to those noted for the ICE-6G model. In this model, the western dome is more prominent and the northern one less so relative to ICE-6G, and all three domes are less broad. Another difference is in southern Manitoba and the Dakotas where, contrary to observations, the model predicts significant uplift. This feature is inherited from the ICE-5G model, and remains in LaurInnu because it was outside of the IIS and Laur16 study areas (shown in Figure 8).

Comparison with Figure 7 shows that it has largely been corrected in the ICE-6G model. In addition, the hinge line between ICE-5G and ICE-6G is significantly different in eastern Canada.

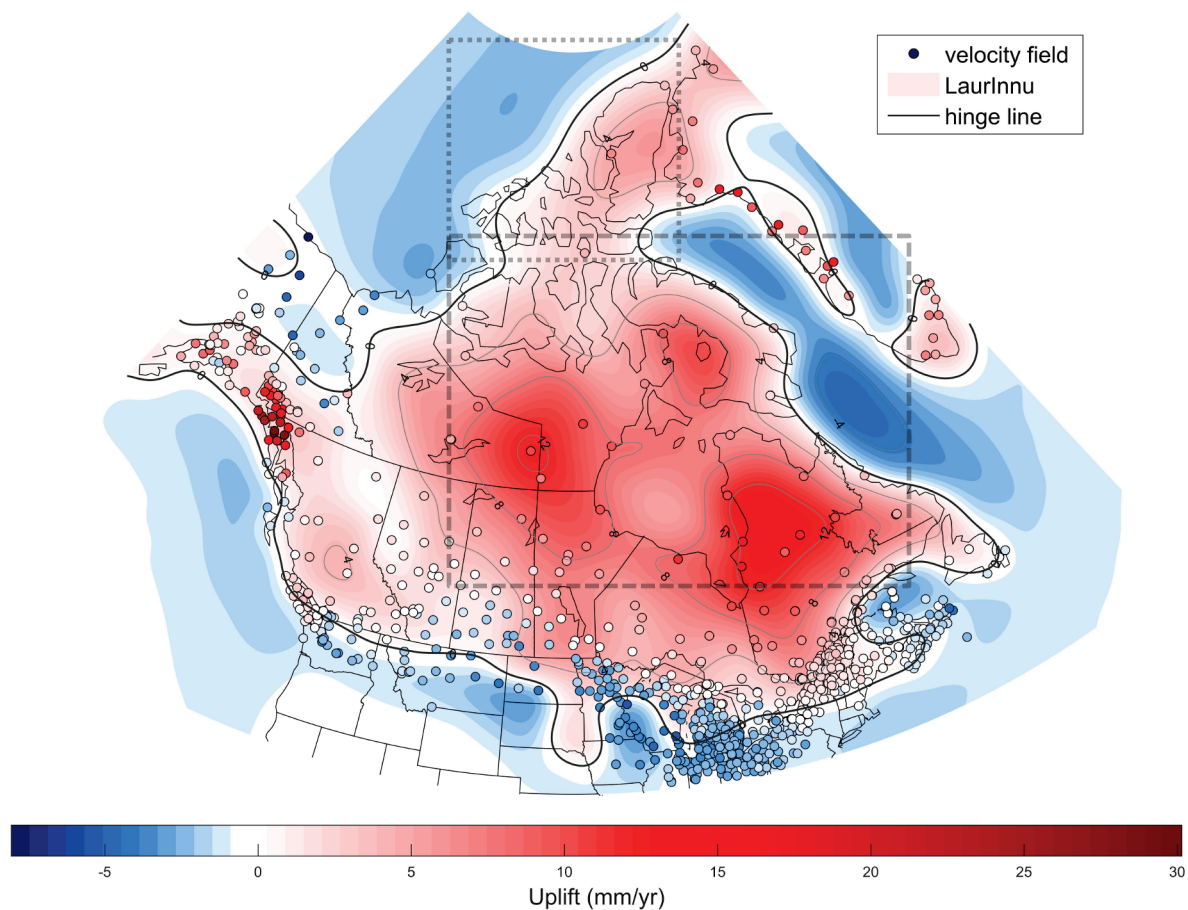


Figure 8 – Laurlinnu. Predicted uplift rates for the Laurlinnu model Simon et al. (2015, 2016) (shaded contours) superimposed by uplift rates from the observed velocity field (small coloured circles). The hinge line (thick black contour line) is the contour of zero vertical crustal motion across which uplift changes to subsidence. The dotted line indicates the study area of Simon et al. (2015), and the dashed line the study area of Simon, et al. (2016).

2.2.3 NAICE

Unlike the two models described above, the ice histories in the study area of Gowan et al. (2016) are constructed using a simple ice physics model constrained by GNSS uplift rates, modern-day and paleo-reconstructions of differential lake levels or tilts, and relative sea level indicators in the surrounding area. Far field ice histories are adopted from previous studies, and earth model parameters were developed for this study as described by Gowan et al. (2016).

Uplift rates for NAICE are shown in Figure 9. For this model as well, the most obvious discrepancies with the velocity field are on the uplift domes at the location of newer ACS's. This physics-based ice model produces a much smoother uplift field, including the hinge line.

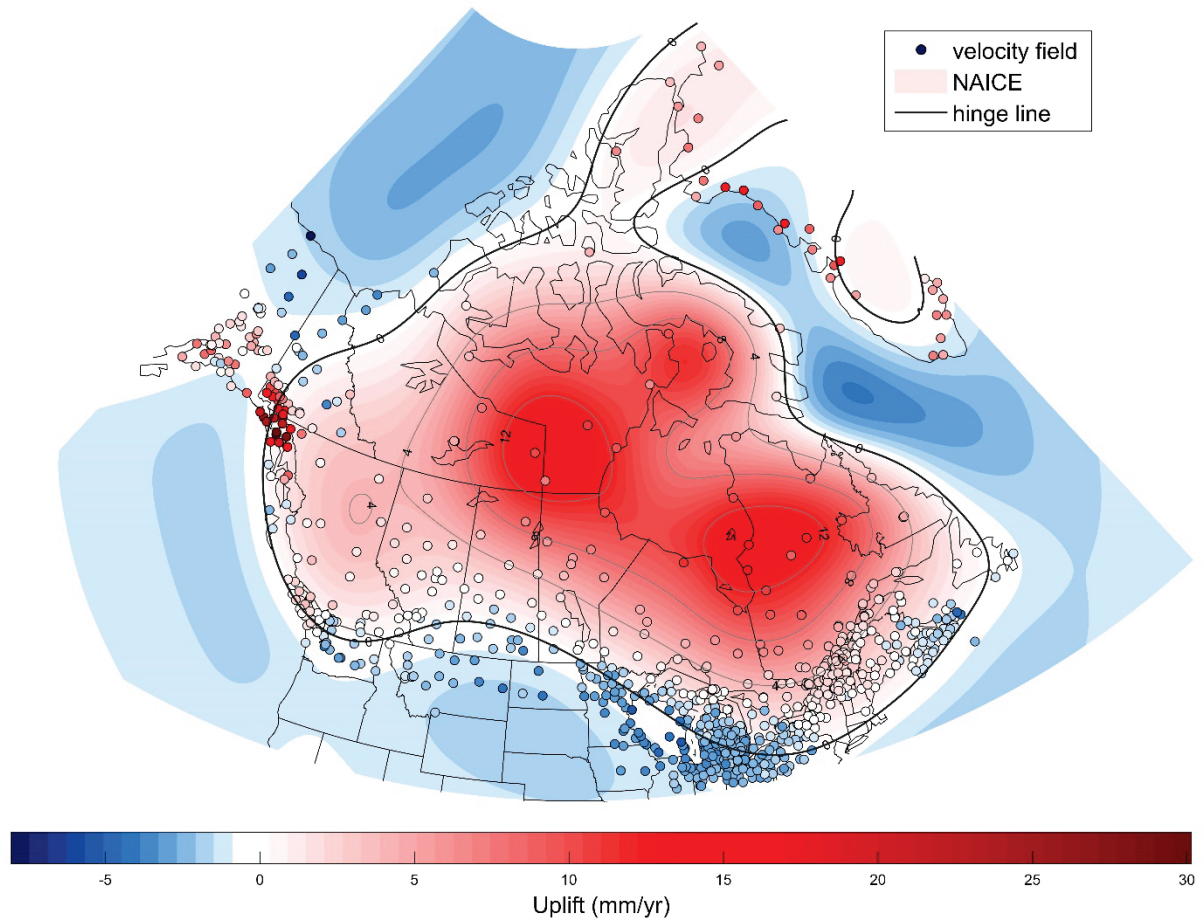


Figure 9 –NAICE. Predicted uplift rates for the NAICE model of Gowan et al. (2016)(shaded contours) superimposed by uplift rates from the observed velocity field (small coloured circles). The hinge line (thick black contour line) is the contour of zero vertical crustal motion across which uplift changes to subsidence.

2.2.4 Regional models for recent and present-day ice mass change

Changes to the surface load from more recent glacier and ice cap changes such as that following the Little Ice Age in Alaska (which began about 235 years ago (Larsen et al., 2005), and from present-day ice mass change in the Queen Elisabeth Islands of the Canadian Arctic Archipelago, are not included in the GIA models described above. For the high uplift rates in the Alaskan panhandle we use a regional model from Hu and Freymueller (2019). For northern Canada, we use a model for glacier and ice cap melting in the Arctic Archipelago and another for the Greenland Ice Sheet, both calculated by K. Simon using methods described in Simon et al. (2015). Both are shown in Figure 10.

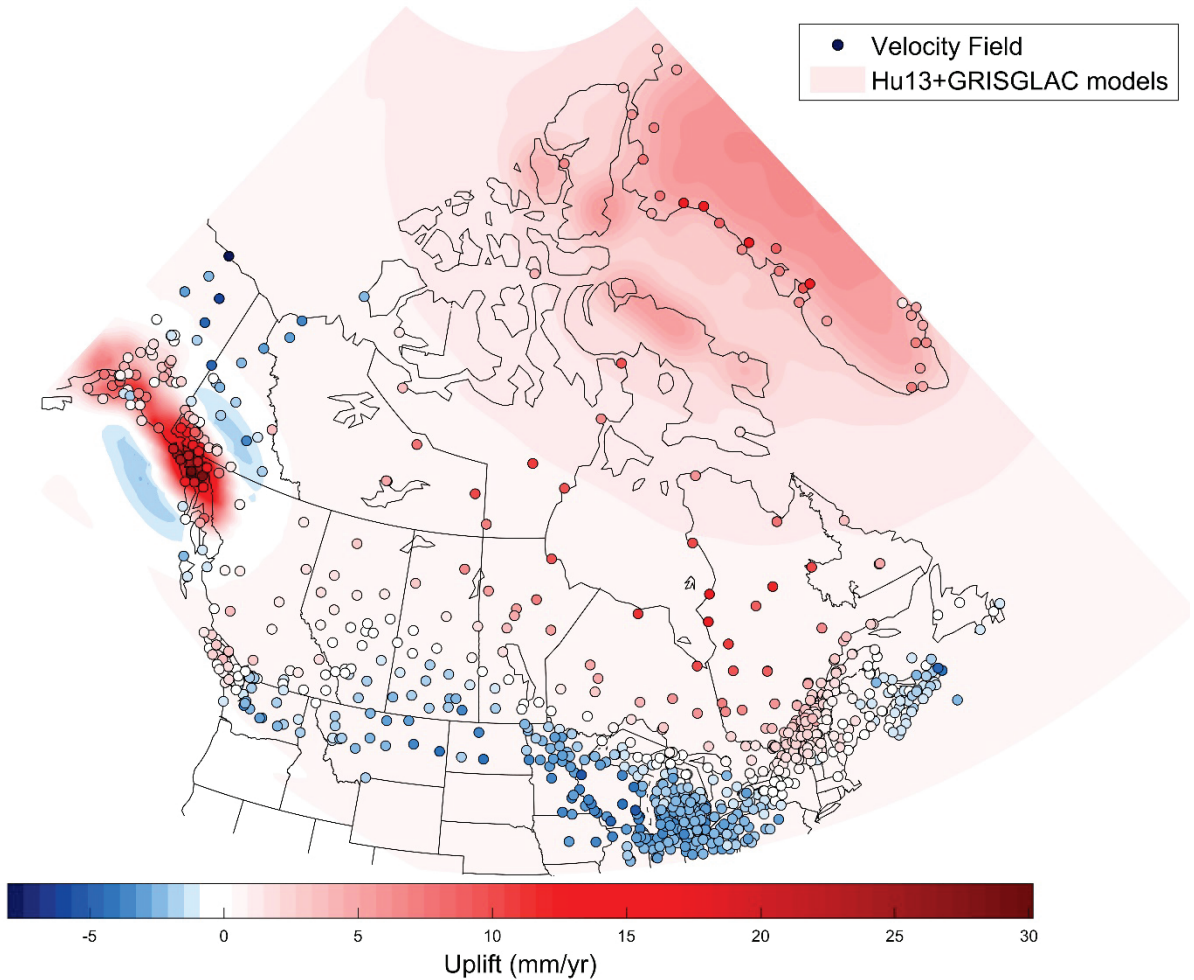


Figure 10 - Regional uplift model predictions. Predicted uplift rates from two regional models for recent and present-day ice mass change in Alaska (Hu and Freymueller, 2019) and for the Canadian Arctic Archipelago and Greenland (Simon et al., 2015) (shaded contours) superimposed by uplift rates from the observed velocity field (small coloured circles).

2.3 Geophysical model validation and selection

We leverage the paleo-geological and sea level history data in the geophysical models described above to supplement GPS observations for the vertical component of the velocity model. In essence, we use the geophysical models as an aid to interpolation by fitting the model predictions to the measured uplift rates. Thus, the models have the most influence where our observations are sparse, and where uplift rates are highest. Conversely, they will have very little influence where the GNSS measurements are spatially dense relative to the spatial variability of model-predicted uplift rates.

In this section we describe model validation procedures used to select the model(s) with the best fit to our velocity field. We focus our analysis in central and northern Canada, where data is sparse relative to the modeled uplift structures, and uplift rates are high. In particular we are interested in the model that best fits the area covered by the three uplift domes common to Figures 7, 8 and 9. Data-model

integration is facilitated by the fact that all three of the GIA models tested were constrained using GNSS data in the region. Both regional models described in Section 2.2.4 are used by default, since they were the only ones available to us for their respective regions.

2.3.1 Velocity field subsets

We test each GIA model against different subsets of our velocity field, shown in Figure 11. The ‘Core’ subset includes sites in the study areas of Simon et al. (2015) and Simon et al. (2016) (see Figure 8), including new sites that were not available for that study. The ‘Sparse’ sites extend to where station density in the south begins to make the inclusion of a GIA model less important. The ‘GIA’ subset

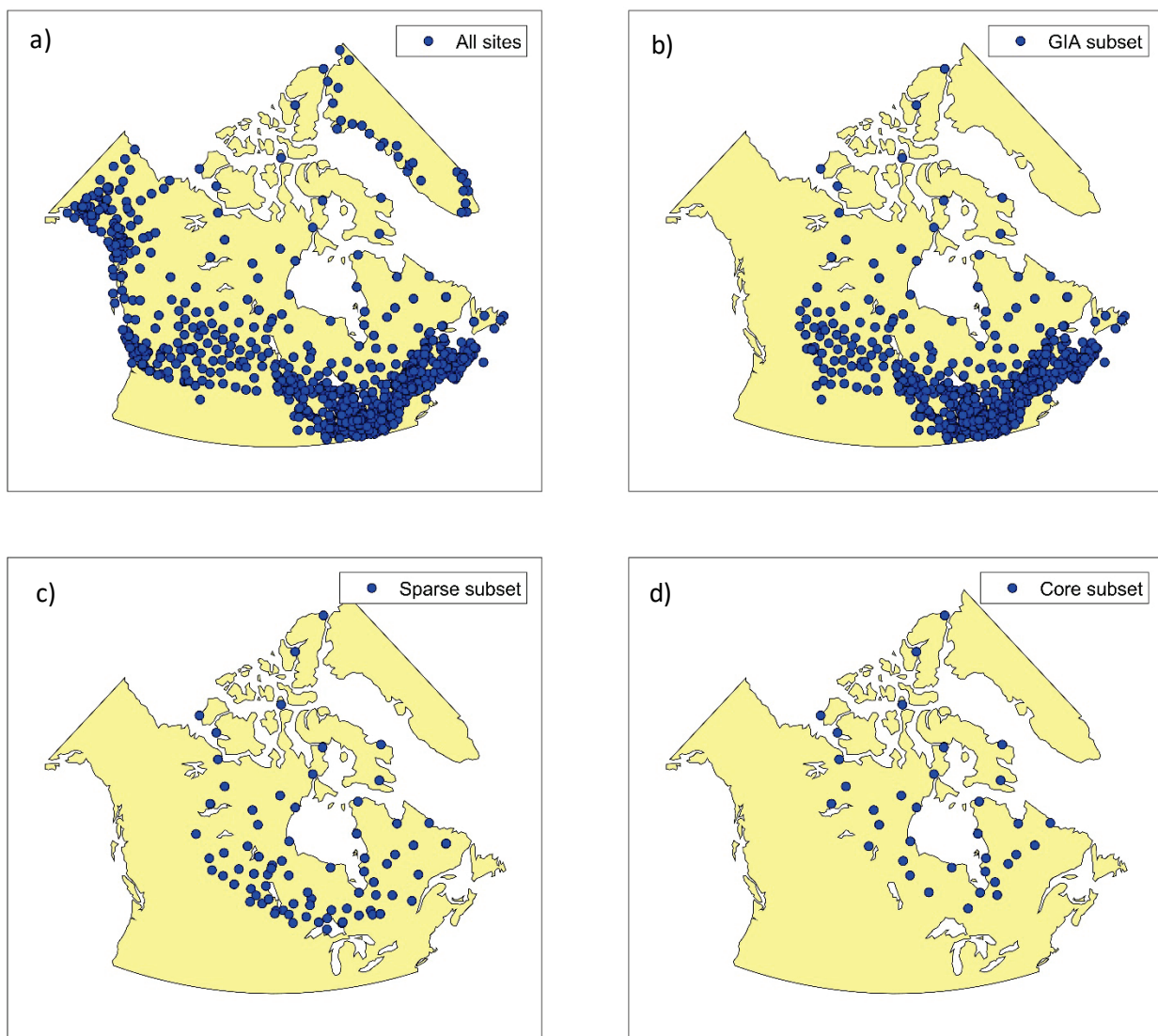


Figure 11 - Subsets of stations used for testing glacial isostatic adjustment (GIA) models. These are: a) All velocity field sites after outliers have been removed; b) GIA sites cover the area where crustal motion is expected to be dominated by GIA; c) Sparse sites are a subset of the velocity field where station density is relatively low; and d) Core test sites are a subset of the velocity field where station density is very low and post-Laurentian uplift is significant.

includes all sites outside of the tectonically active region west of the Rockies. Statistical tests are performed for all subsets and the full velocity field. However, test results for the ‘Core’ subset most heavily influence our model selection, since this is where GNSS network spacing is sparse and the influence of the model predictions most important.

Where GIA model predictions are not provided for our site coordinates, they are bilinearly interpolated to the sites for comparison between the two. All comparisons are in ITRF2014 (e.g., Simon et al., 2015; Peltier et al., 2015).

2.3.2 Comparison of geophysical model predictions with observations

Linear regression parameters for scatter plots between GIA model predictions and observations are summarized in Table 1, for each of the observation subsets described in Section 2.3.1. Figure 12 shows the scatter plots and fits for the Core subset. Core sites correspond to the study areas of Simon et al. (2015) and Simon et al. (2016), and therefore for this subset the fit is slightly better for LaurInnu (i.e., the slope of the linear fit is closer to 1). ICE-6G provides the best fit when all observations are included. For all models, there is a systematic difference with respect to the observations that is seen as a bias (the intercept) in the linear regressions. The bias changes with sample size and distribution and is more pronounced for the two models tuned to data in Canada. It is thought these biases may be due to differences in reference frame realization.

Table 1 - GIA to observation comparisons. Linear regression parameters (slope and intercept (in mm/yr)) of scatter plots of GIA model predictions and the velocity field for the four specified subsets of stations displayed in Figure 11. Scatter plots are shown for the Core subset in Figure 12.

	Core		Sparse		GIA		All	
	slope	intercept	slope	intercept	slope	intercept	slope	intercept
LaurInnu	0.82	0.44	1.01	-2.51	0.84	-1.89	0.94	-1.75
ICE-6G_C	0.78	0.58	0.95	-1.25	0.94	-0.84	0.97	-0.75
NAICE	0.74	0.64	0.92	-1.30	1.04	-2.53	1.08	-2.12

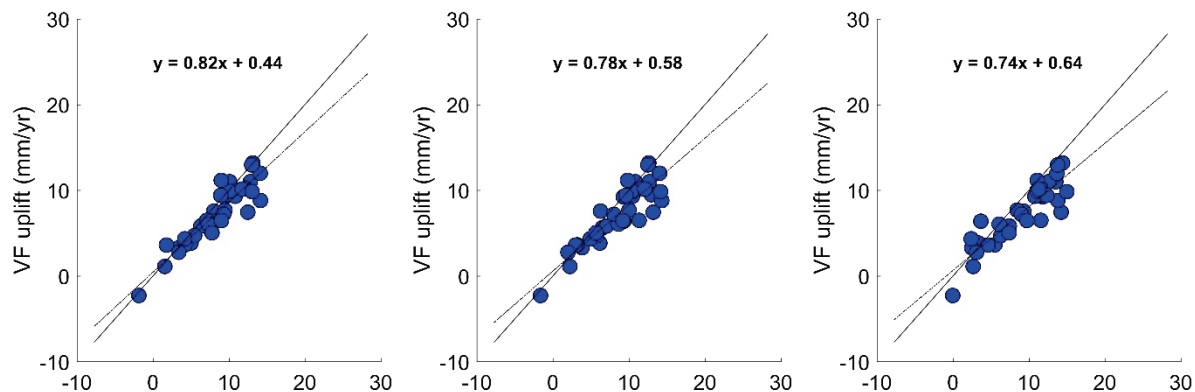


Figure 12 - GIA to observation comparisons. Scatter plots of the observed velocity field (VF) and the predictions of the three GIA models for the Core Sites. The derived fits are given with dashed lines and the 1:1 fit is shown as a solid line.

2.3.3 Geophysical model to observation residuals

A test of the fit between the models and the velocity field are listed in Table 2. These are calculated as RMS errors defined as

$$\text{RMSE} = \sqrt{\frac{\sum_{i=1}^N (V_i^o - V_i^m)^2}{N}} \quad (1)$$

where V_i^o is the observed uplift velocity, V_i^m is the model uplift velocity and N is the number of observations. Similar to the results described in Section 2.3.2, Table 2 reveals that for the Core subset, LaurInnu provides the best fit to our velocity field. For subsets that include southern sites, ICE-6G provides the best fit.

Table 2 - RMSE between observation and models. These are calculated for each of the subsets shown defined in Section 2.3.1 and shown in Figure 11. Units are mm/yr.

	Core	Sparse	GIA	All
ICE-6G	1.80	1.52	1.28	1.93
LaurInnu	1.60	2.70	2.14	2.37
NAICE	1.91	1.43	1.73	2.25

2.3.4 Comparison of empirical semivariograms

The final test compares the empirical semivariograms of the GIA models with that of the velocity field. Empirical semivariograms are used to understand the correlation structure of a stochastic field or variable as a function of distance using observations. In Section 3.2.1 we describe how models of the empirical semivariograms are in the geospatial interpolation method known as kriging. Here we use semivariograms to determine which geophysical model predictions best replicate the spatial correlation of the data.

The semivariogram ($\gamma(h)$) for this data set is defined as

$$\gamma(h) = \frac{1}{2 \cdot N(h)} \sum_{i=1}^{N(h)} (z(x_i) - z(x_i + h))^2 \quad (2)$$

where $N(h)$ is the number of pairs of sites separated by a distance (or lag) h , and $(z(x_i) - z(x_i + h))$ is the difference in uplift velocities for site pairs separated by lag, or distance, h . For n observations, the total number of site pairs is $N_{total} = n(n - 1)/2$. These are binned as a function of lag with at least 30 site pairs per bin. More information on semivariograms can be found in, e.g., Goovaerts (1997) and Webster and Oliver (2007).

Parameters used to characterize semivariograms are the range, the sill and the nugget. The range is the lag at which the semivariogram levels off, or the maximum lag where the data is correlated. The sill is the maximum variability of the data. The nugget is the y-intercept, and is indicative of small-scale variation including observation uncertainty.

Figure 13 shows the empirical semivariograms for the three GIA model uplift velocities (interpolated to velocity field sites) and the velocity field itself, for site pairs covering the entire data set which are binned into 40 lag increments. Coordinates are converted to a polyconic projection to preserve distance relationships, and h is in those units. The maximum lag of $h=0.6$ represents a separation of about 2700 km. For this set of empirical semivariograms, LaurInnu appears to correlate better than the others at the shorter lags in that range, whereas ICE-6G performs better at the longer distance (although none of them do particularly well past about $h = 0.4$).

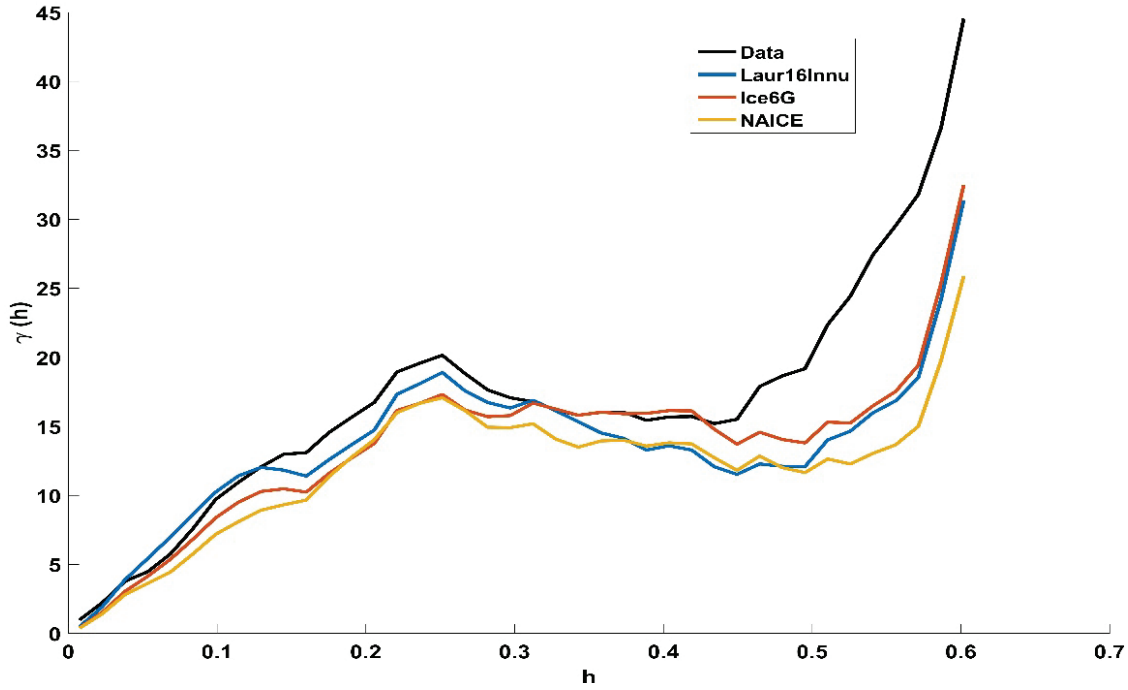


Figure 13 - Empirical semivariogram for the three GIA models and all observations once outliers are removed. The quantity h is the lag (distance) between stations, given in units of the polyconic projection used for this calculation, where $h=0.6$ is approximately 2700 km. The quantity $\gamma(h)$ is the semivariogram as defined in Section 2.3.4 (Equation (2)), for which the circular semivariogram model has been fit to observations.

Characteristic semivariogram parameters are illustrated in Figure 14 using a semivariogram model. In this case, the model is fit to an empirical semivariogram with a range of half the maximum site pair lag, representing a maximum distance of about 1400 km ($h=0.3$). This is also roughly the maximum separations of sites in our Core subset. The model used here is the circular semivariogram model because of the ones tested, it provides the clearest illustration of the range, sill and nugget; other models are listed in Table A1 (Appendix A). For the velocity field vertical velocity, these are: a sill of ~ 19 , a range of ~ 0.25 , and a nugget of 0. The nugget is held fixed at zero for all semivariograms in this plot (see Section 3.2.1). As seen in Figure 14, over this range, the LaurInnu model predictions appear to best approximate the semivariogram model parameters of the observations.

2.3.5 The combined post-glacial geodynamic model

In summary, we find through these comparisons that LaurInnu provides a better fit to our data in our primary area of interest as defined by the Core subset; this is not surprising as that model was tuned to

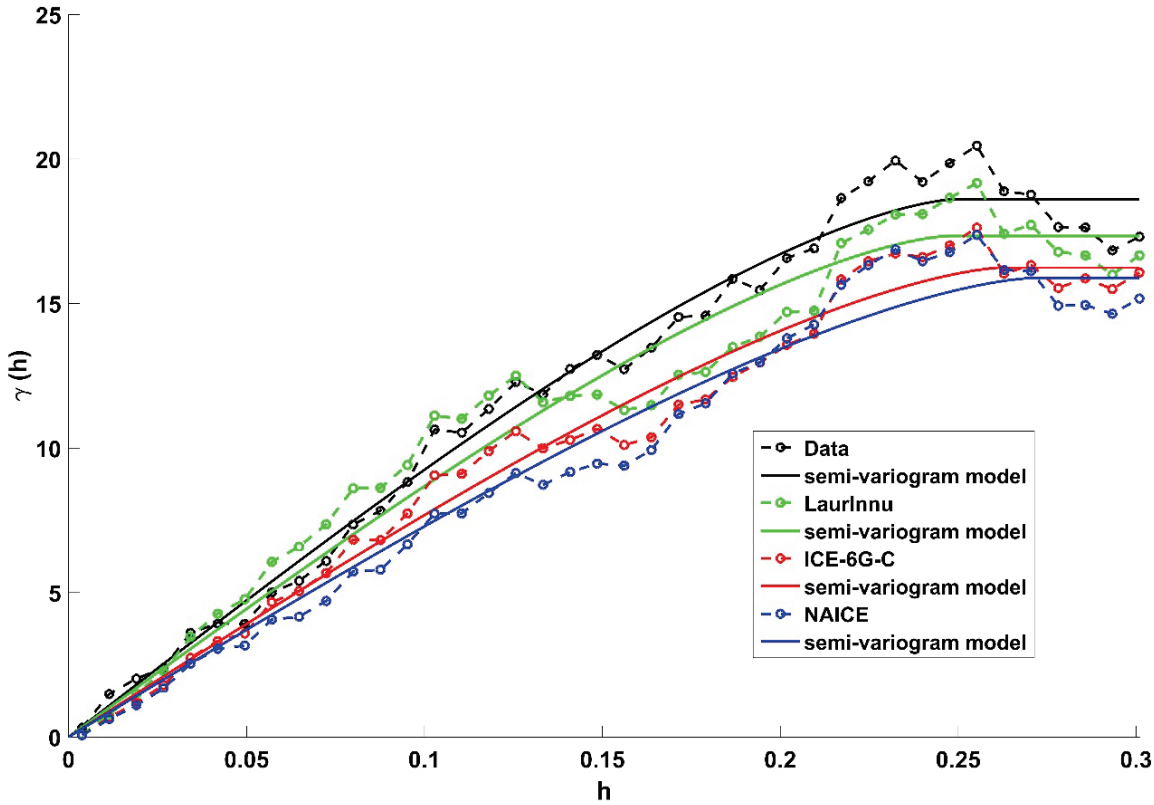


Figure 14 - Empirical semivariograms and models. Here the empirical semivariograms are for the same observations and geophysical models as in Figure 13, but limited to half of the maximum lag or point to point distance. A circular semivariogram model (Table A1, Appendix A) is fit to the observations for each semivariogram to illustrate the sill, the range and the nugget. The quantity h is the lag (distance) between stations, given in units of the polyconic projection used for this calculation, where $h=0.3$ is approximately 1400 km. The quantity $\gamma(h)$ is the semivariogram as defined in Section 2.3.4 (Equation (2)).

a densified and updated data set in that area. In the south, however, ICE-6G appears to be a better fit. If we had a dense network across all of the south, the data would override the input GIA model in the data integration process (Section 3). However, our velocity field has a gap west of the Great Lakes precisely in the area where LaurInnu has inherited a strong feature from ICE-5G (see Section 2.2.2 and Figure 8), which is much less prominent in ICE-6G. Thus we adopt LaurInnu above 52N and ICE-6G below 48N, which are smoothly transitioned across that band using a Gaussian transfer function.

Once these two models are merged, we add the regional models described in Section 2.2.4 to account for recent ice mass changes. We refer to this combination of four models as the ‘combined geodynamic model’. All three GIA models described above are used to devise an estimate of GIA model uncertainty (Section 3.4.2).

3 Input Data Integration

In this section we describe methods used to create the three components of the velocity model from the input data described above. This work was performed using the Mathwork's MATLAB and Mapping Toolbox (R2015b).

3.1 Model grid

The previous version of the velocity model (NAD83v60VG) was distributed on a set of grids at $0.25^\circ \times 0.25^\circ$ spacing, which extend from 50W to 140W, and 41N to 85N. For NAD83v70VG, we retain the same spacing but broaden the grid from 40W to 142W to cover the Grand Banks in the east and extend past the Yukon-Alaska border in the west.

3.2 Modelling approach

3.2.1 Interpolation method

The variable density of our GNSS station network poses a significant interpolation challenge. Moreover, as Canada is bordered by oceans on 3 sides, there is no data with which to constrain the model over Canada's offshore. One exception is the offshore Baffin Bay to Labrador Sea, for which we include Greenland data, although we note that western Greenland and eastern Baffin Island are under different geological and ice mass loading domains (see Sections 3.3 and 3.4). Thus, we require an interpolation tool which performs well for irregularly spaced data, and extrapolates over the oceans without introducing large artefacts. Other considerations include the ability to weigh the data by its uncertainty, and to provide an estimate of interpolation error.

We tested over 25 interpolation/extrapolation methods for this study, covering a wide range of interpolator types, including those listed in Table A1 as well as others not listed. While some are not extrapolators, we kept them for comparison in the validation process. Here we use the term 'interpolation' in a general sense, as some of these tools create a surface which weights or approximates the data.

Interpolators were evaluated using cross-validation techniques that test their ability to predict missing data for all three velocity components as described in Appendix A. The result of one cross-validation test is shown in Figure A1. In general, test results were similar for most of the tools tested, and for all velocity components. Differences in the RMS of the residuals for any one interpolation method are related to the distribution of the test subset.

Based on these results, we selected weighted ordinary kriging using an exponential model for the semivariogram fit (Appendix B). Ordinary kriging methods on average outperformed other tested methods, and weighted kriging methods in particular performed as well or better than their unweighted equivalents, confirming that using data weights provides a better estimate of the sampled crustal motion. In addition, and contrary to most other methods tested, weighted ordinary kriging provides an estimate of interpolation error, smooths noisy data, and performed well as an extrapolator in the offshore.

Kriging is a widely used tool in geostatistics which provides predicted values of an unknown field as a weighted average of discrete observations of it (Matheron, 1968). Unlike other inverse-distance weighting methods, kriging weights take into account the spatial correlation of the observations by modelling the empirical semivariogram defined in Section 2.3.4.

Variations of the kriging method make different assumptions about the underlying structure of the data. Ordinary kriging assumes the data is isotropic and that the data mean is constant but unknown. These assumptions may be reasonable when interpolation is performed on data from which large-scale trends are removed, as is the case for the vertical component of NAD83v70VG (Section 3.2.2). However, for the North and East components, no underlying trend or model is removed (Section 3.2.3), and ordinary kriging may not be optimal. This is particularly true in Western Canada which, unlike the rest of the country, is dominated by large and complex gradients in horizontal motion (Figure 4). Future work will address this issue (see Section 6).

The reader is referred to, e.g., Matheron (1968), Bailey and Gatrell (1995), Goovaerts (1997), and Webster and Oliver (2007) for detailed reviews of kriging theory and applications. For a description of the kriging procedure as applied in this study, see Appendix B.

Unless noted otherwise, discussions of interpolation for the remainder of this report refer to interpolation by weighted ordinary kriging.

3.2.2 Data integration: vertical component

For the vertical component of the velocity model, we integrate the combined geodynamic model with the velocity field using a simple remove-compute-restore (RCR) method. We subtract the combined geodynamic model from observations (remove), interpolate the resulting residuals (compute), and add the residual surface back to the combined post-glacial model (restore). If the residuals are small and evenly distributed, the final surface reproduces observations within their uncertainties, and where data is sparse it is shaped by the combined post-glacial model.

Figure 15 shows the residual at stations and as interpolated to the grid. Interpolation is done by weighted ordinary kriging (Section 3.2.1, Appendix B), with weights taken from velocity field uncertainty calculated by the SINEX combination software (Section 2.1.3). Where the velocity field is sufficiently dense, the interpolated residual surface reveals observation-to-model discrepancies on a sub-regional scale. Based on this, we note the following:

- Our current velocity field suggests that the combined geodynamic model underestimates crustal uplift west and south of Hudson's Bay, and overestimates it on the east side. However, our GNSS stations at these locations have relatively short time series, and this will be re-examined regularly in the coming years.
- A higher resolution regional model for uplift due to current melting in Greenland is needed, as well as more information on the status of stations in NW Greenland, which exhibit large variability over short distances.
- A broad and regionally consistent difference in the comparison over the southern Manitoba/Saskatchewan border suggests a shortcoming in the combined geodynamic model,

which may be due to the limited availability of ice history constraints in the prairies. Other possible contributions to the misfit include multi-year hydrological loading signals noted in ACS times series at stations in the area as well as other data (e.g., Lambert et al., 2013).

Nevertheless, new GIA models should be tested. Fortunately, in this region the observed velocity field is sampled densely and the RCR method will favour measured values over the predictions of a GIA model.

- Analysis of historical water levels from tide gauges suggests that vertical crustal motion is not well resolved by either the velocity field or the previous crustal velocity model (NAD83v60VG) in coastal British Columbia Robin et al. (2016). In contrast, a comparison of the predictions of our new velocity model NAD83v70VG to water level trends at Arctic tide gauges shows a marked improvement compared the same analysis using NAD83v60VG.

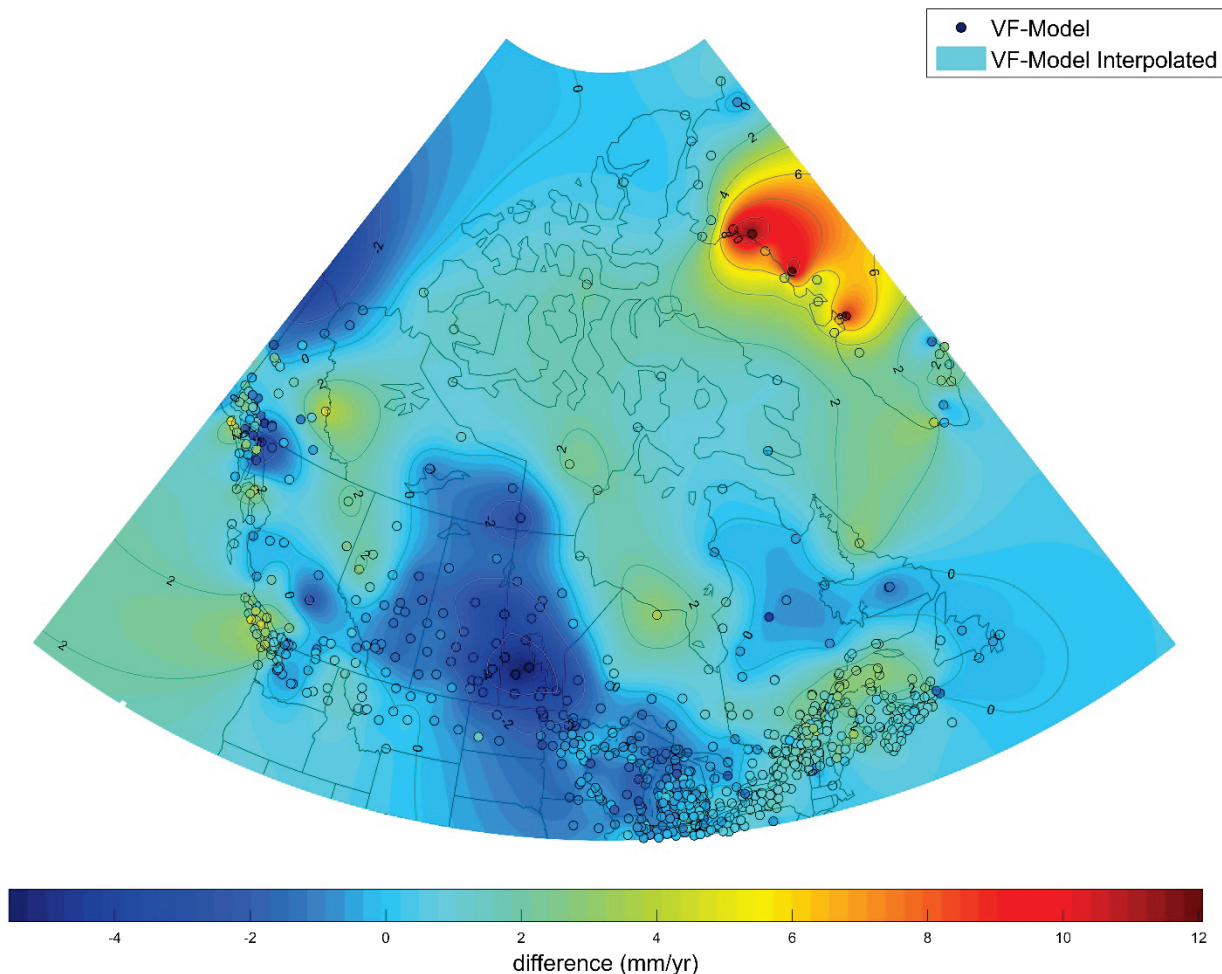


Figure 15 - Interpolated observation to model residuals. Residuals between the vertical velocity at stations and the combined geophysical model, plotted at all velocity field sites and as interpolated to the grid.

Figure 16 shows the contoured hybrid vertical crustal velocity model once the interpolated residuals have been restored to the combined geodynamic model. This is the vertical component of

NAD83v70VG. For comparison, we also include a vertical velocity model created by weighted kriging of the velocity field without any geodynamic model (Figure 17). These figures highlight the importance of the combined geodynamic model in defining crustal motion where data is sparse for both continental and coastal areas.

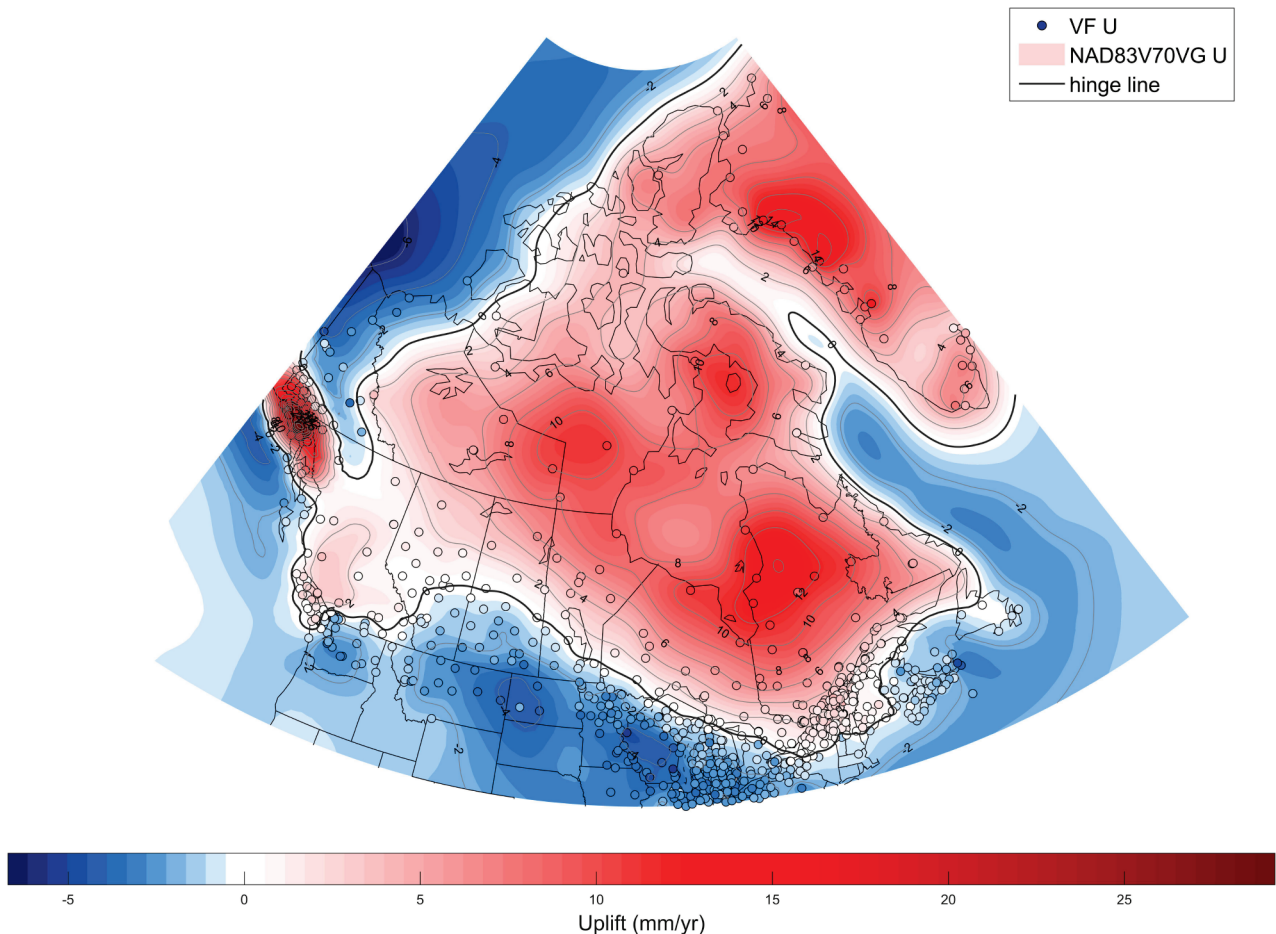


Figure 16 - NAD83v70VG, vertical component, in NAD83(CRS). The observed velocity field is shown with coloured circles and shaded contours represents the hybrid velocity model which integrates both the observed velocity field and a combined geophysical model.

In summary, integrating the combined geodynamic model with observations provides significant improvements compared to a simple interpolation of our velocity field. Challenges remain in British Columbia, and where the observed velocity field is sparse and GIA models diverge. These areas overlap, in part because the GIA models tested for this model are constrained with a similar set of GNSS crustal motion observations. Network densification and further GIA model testing are planned to address these gaps (see Section 6).

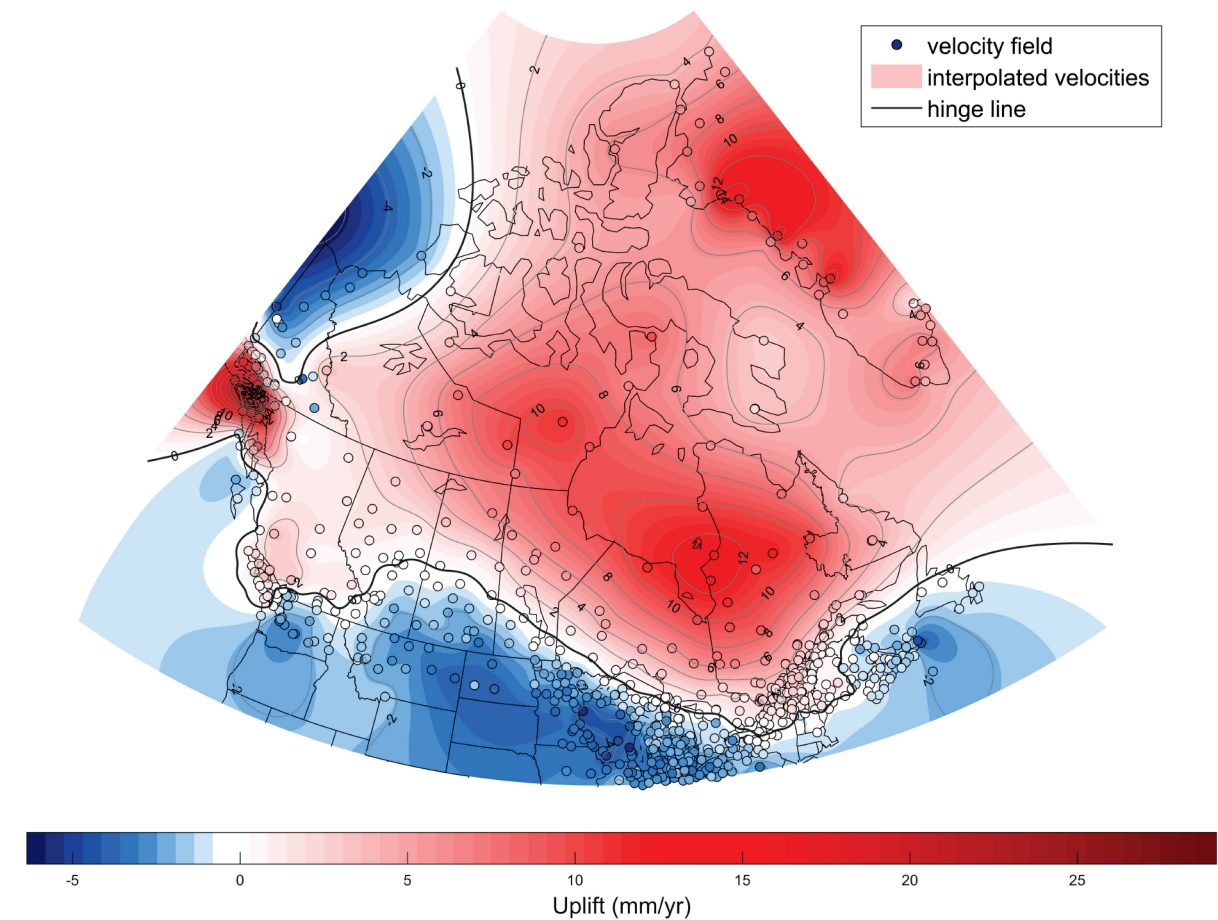


Figure 17 - Interpolated velocity field, vertical component, in NAD83(CSRS). In this model, there is no geophysical model supplementing the interpolation.

3.2.3 Data integration: horizontal components

As discussed in Section 2.2, the horizontal components of the velocity model are calculated by interpolation of the velocity field, with no input from geodynamic models. Thus, N and E models are calculated by weighted ordinary kriging of the velocity field directly, with weights taken from the velocity field uncertainties estimated by the SINEX combination software (Section 2.1.3).

In Figure 18 we plot the modeled horizontal velocities together with the velocity field from which it was calculated. From this plot we note the following:

- The generally eastward velocity is a result of the definition of NAD83(CSRS). NAD83(CSRS) is designed to remain stable relative to the North American plate, using rotation parameters from the NNR-Nuvel-1A model to account for plate motion relative to the ITRF (M. Craymer 2006). However, the parameters do not capture all of the rotation; the residual is the eastward velocity seen in Figure 18. This may be addressed in a future version of NAD83(CSRS), taking into consideration plans by the US National Geodetic Survey (NGS) to adopt a new reference frame

(NATRF2022) which will be defined using a new independent set of rotation parameters (Erickson et al., 2019; National Geodetic Survey, 2018).

- More careful treatment of the Greenland data is required (also noted in Section 3.3.2 for the vertical model).
- Patterns of seismicity and GIA modelling suggest that horizontal crustal motion in the eastern Arctic Archipelago is different from that in Greenland (e.g., Basham et al., 1977; James and Shamehorn, 2016). Because the observed velocity field has a large gap between Qikiqtarjuaq and Alert, velocities from western Greenland dominate the interpolated model in the eastern Arctic Archipelago. For the vertical component, this effect is somewhat mitigated by the combined geodynamic model (compare Figures 16 and 17).
- The tectonically active west coast requires better sampling. Figure 19 shows the horizontal velocity grid and velocity field in British Columbia. Crustal motion along the west coast of Canada varies over a range of spatial scales, reflecting the complexity of active plate boundary processes (e.g., Mazzotti et al., 2008). In particular, the sharp change in velocity between Vancouver Island and the mainland is not well constrained by observations.

In summary, horizontal crustal motion varies little and smoothly over central Canada, and therefore the observed velocity field captures horizontal crustal motion well for most of the country and a simple interpolation method is justified. However, challenges exist in the west coast due to the complexity of the plate boundaries, and in the Eastern Arctic Archipelago due to disparate and variable surface loading regimes. NRCan is actively working to densify the ACS and campaign networks in British Columbia and the Arctic Archipelago. We do not, however, expect to achieve the network coverage available in other jurisdictions (e.g., Vestol et al., 2019). Therefore, we are investigating the use of tectonic models to support interpolation for the horizontal component in the west (e.g., Pearson and Snay, 2012).

Horizontal velocities related to GIA and current ice mass change for the Eastern Archipelago are not yet well modeled (e.g., Sella et al., 2007; James and Shamehorn, 2016; Hermans et al., 2018). Inclusion of these models would allow us to use the compute-remove-restore method for the horizontal velocities, the advantages of which are described in Section 3.2.2.

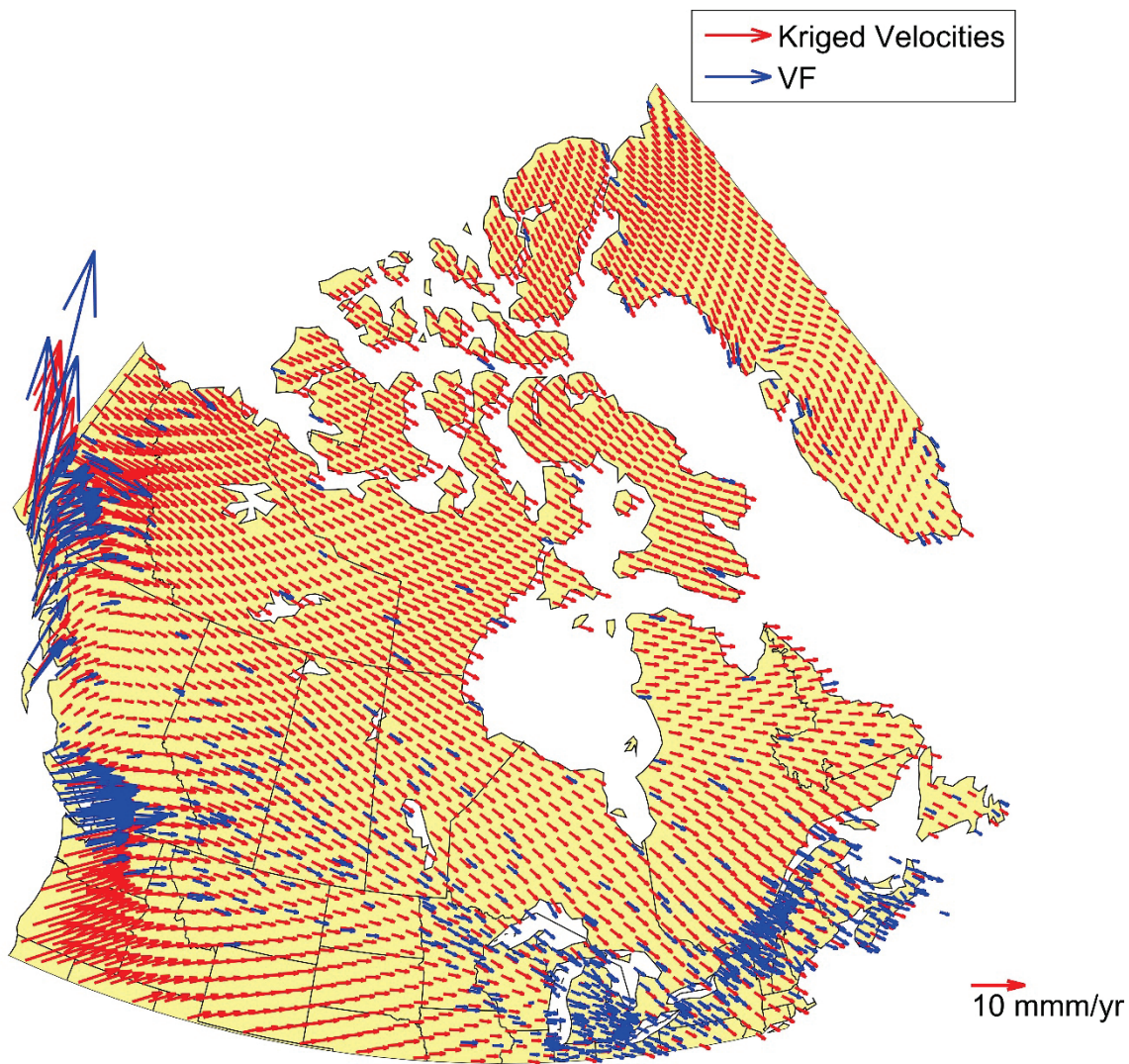


Figure 18 - NAD83v70VG, horizontal component, in NAD83(CSRS). The gridded model (red arrows) is decimated for easier visualization. The model is interpolated from the measured horizontal component of the velocity field (blue arrows).

4 Uncertainty Model

NAD83v70VG includes a set of gridded uncertainty estimates for each of the North, East and Up components. These are derived from a combination of statistical uncertainties associated with each velocity estimate, interpolation error as determined by the ordinary kriging procedure, and in the case of the vertical component, a simple estimate of GIA model error. Uncertainty estimates are available for each point of the grid on which NAD83v70VG is distributed.

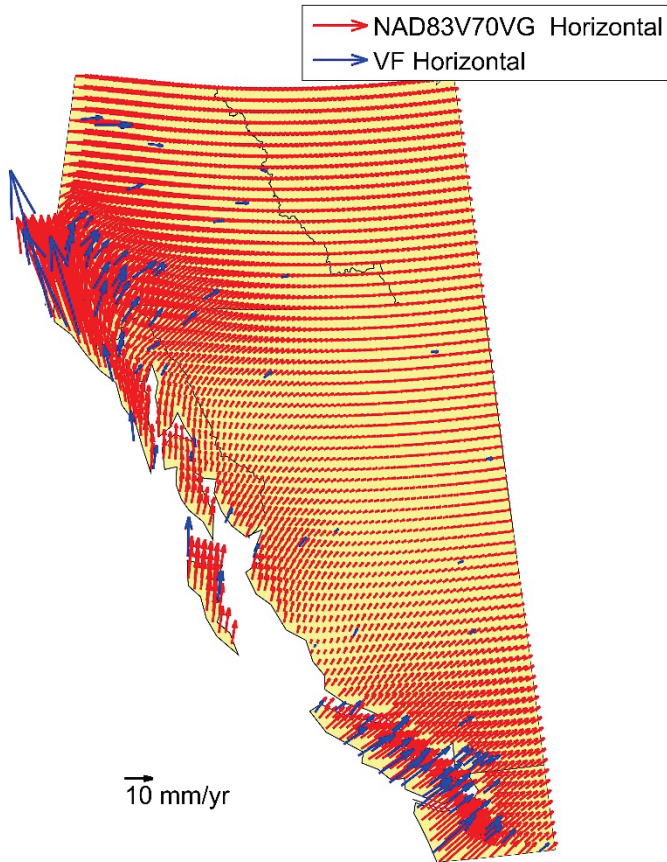


Figure 19 - NAD83v70VG, horizontal component, in NAD83(CSRS), for the west coast of Canada. The gridded model (red arrows) is displayed at its full density. The model is interpolated from the measure horizontal component of the velocity field (blue arrows).

4.1 Interpolation Uncertainty

Kriging provides an estimate of uncertainty as described in Appendix B. Since we weigh the interpolation using observation uncertainty, interpolation uncertainty includes data uncertainty.

4.2 Horizontal model uncertainties

As we calculate the horizontal components of the velocity model by directly interpolating the velocity field with no geodynamic model input, the interpolation uncertainty defines the horizontal uncertainty grids.

4.3 Vertical model uncertainty

4.3.1 Combined Geodynamic Model Uncertainty

Recent work in the GIA community suggests that GIA error models will soon be available (e.g., Caron et al., 2018; Simon et al., 2017), which could provide statistically rigorous uncertainty for our geodynamic model input. At this time, however, none of the geodynamic models used for the combined geodynamic model (Section 2.3.5) provide associated uncertainties. Instead we devise an approximate estimate of

geodynamic model uncertainty which takes into account that the geodynamic models are shifted to fit observed crustal motion. The procedure is:

1. Create hybrid models using each of the three models described in Section 2.2, using the method described in Section 3.
2. Determine the difference between each pair of models in that set.
3. Compute the standard deviation of those differences.

Using the standard deviation of the model differences rather than of the models themselves represents a cautious approach, and only affects the amplitude of the geodynamic model uncertainty, not its distribution.

4.3.2 Total Uncertainty

Calculation of the uncertainty grid for the horizontal components of NAD83v70VG is fully described in Section 4.2. The uncertainty grid for the vertical component is calculated by combining the interpolation and geodynamic model uncertainties in quadrature:

$$\sigma_{Total} = \sqrt{\sigma_{int}^2 + \sigma_{geo}^2} \quad (3)$$

where σ_{Total} is the standard deviation of the velocity model, and σ_{int} and σ_{geo} are the uncertainties coming from the interpolation method (Section 4.1) and the combined geodynamic model (Section 4.2). σ_{Total} is provided on the same grid as the velocity model. The vertical uncertainty model is shown in Figure 20.

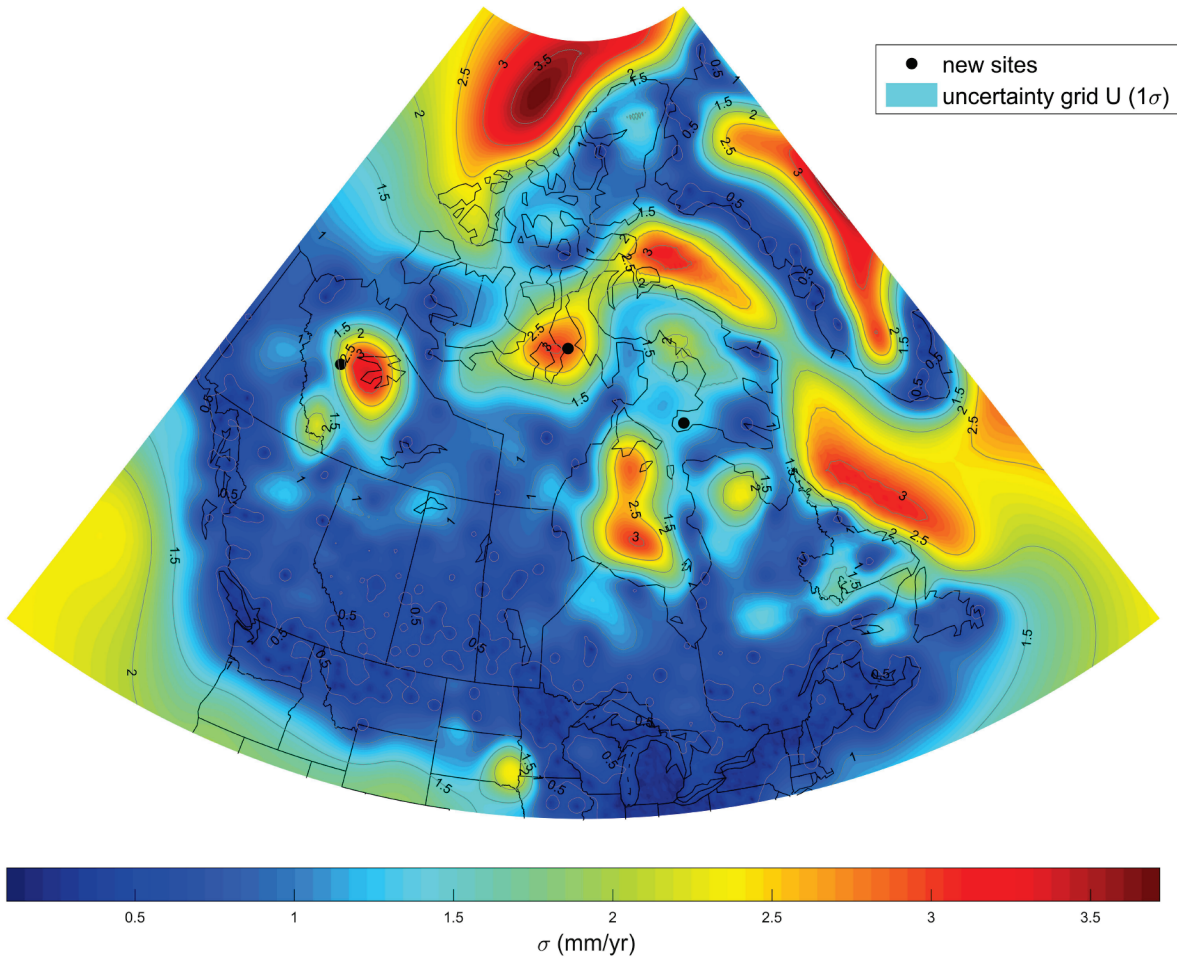


Figure 20 - NAD83v70VG uncertainty grid, vertical component. Uncertainty is at the 1σ level. Three newly installed sites (black circles) are anticipated to provide robust velocities in another few years.

5 Discussion

5.1 Comparison with NAD83v60VG

NAD83v70VG provides significant improvements over NAD83v60VG which was released in 2011 (Craymer et al., 2011; Figure 21). The v7 update includes 6 more years of data at existing sites, new sites in key locations, a new interpolation strategy, and a combined geodynamic model for the vertical component. New sites and the combined geodynamic model improve the central-northern region surrounding Hudson Bay. The new interpolation method and the combined geodynamic model improves the model over the Arctic Archipelago (see Figures 16 and 21). The CGS now recommends the use of the velocity model in northern and Arctic Canada (also see Section 3.2.1), which was not the case for NAD83v60VG.

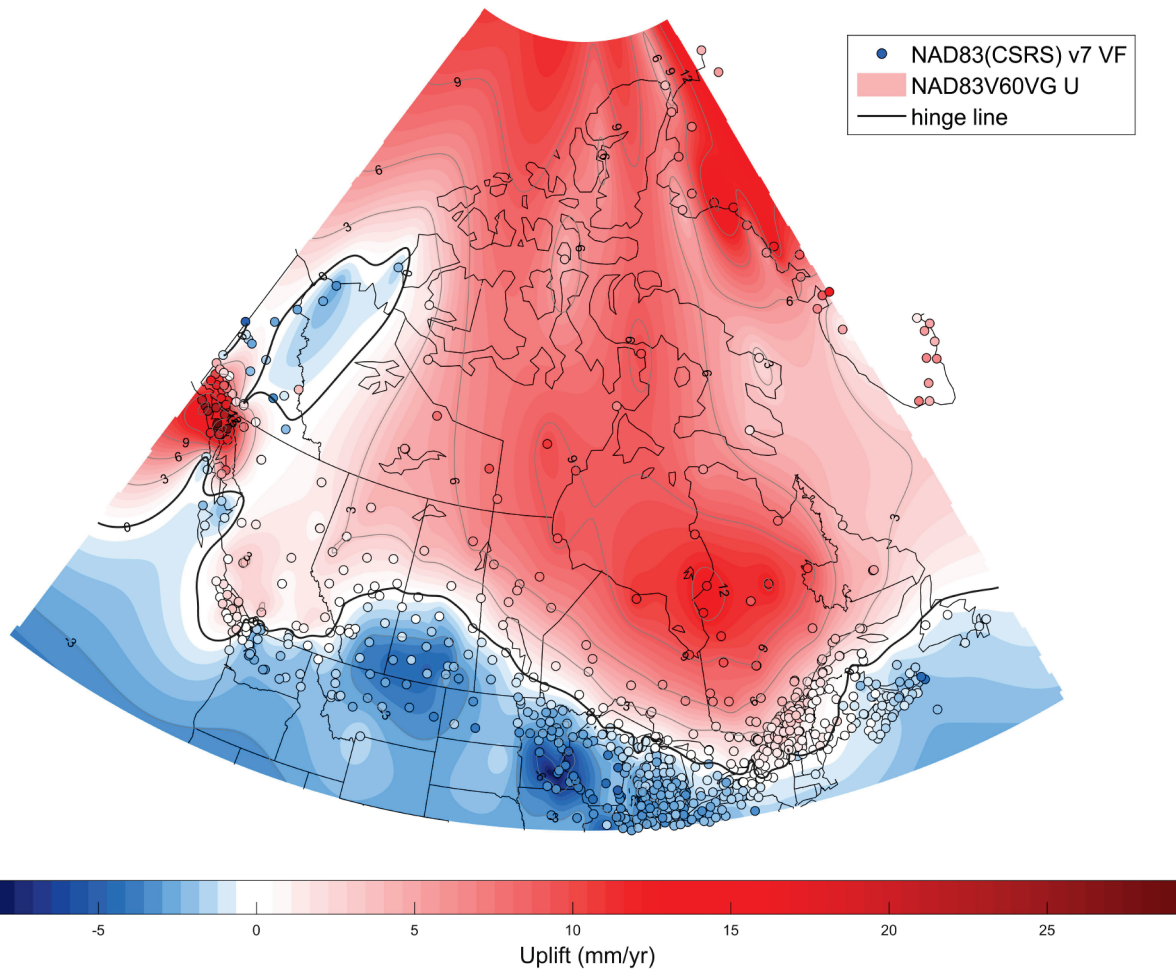


Figure 21 - NAD83v60VG, vertical component, in NAD83(CSRS). The vertical component of the 2011 NAD83v60VG model (shaded contours), superimposed by the more recent NAD83(CSRS) v7 velocity field (outliers removed) (coloured circles).

5.2 Data to model residuals

The data input and modelling methods described in this paper are designed to capture large-scale patterns of regional crustal motion. As such, not all observed velocity measurements are used (Section 2.1.6), and velocity field inputs to the model are weighted using their uncertainty estimates (Appendix B). Therefore, NAD83v70VG models are relatively smooth and only approximate the velocity field. The residuals between the observations and the models are summarized for different subsets of the velocity field in Table 3, and shown in Figures 22 and 23. Residuals are also listed for individual stations in Table C1 of Appendix C. From these we observe that:

- As expected, the residual statistics (Table 3) and the residual field (Figures 22 and 23) are dominated by sites removed as outliers.

- Residual velocity statistics at campaign sites are comparable on average to those at active control stations. In general, NRCan campaign stations have been observed consistently and rigorously, some since the early 1990's. Thus they are assigned a high level of confidence.
- Large residuals at other sites are generally in areas with very high uplift rates (e.g., the Alaskan panhandle) and/or post-seismic motion, in areas where the network is relatively dense, or where uncertainties are large and the site is down-weighted in the model.

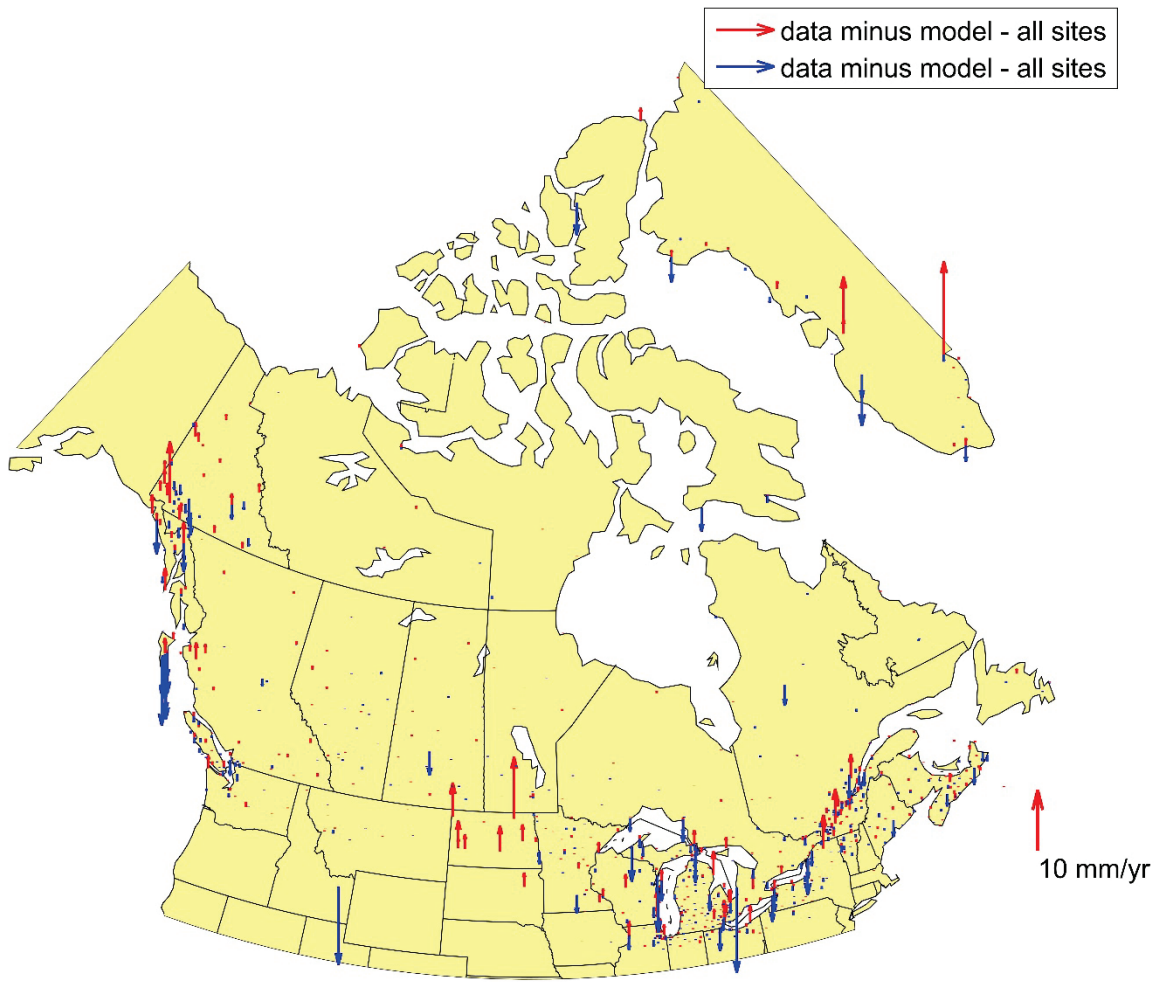


Figure 22 - Residual field, vertical component. Arrows map the residuals defined as station velocities minus the velocity model (as interpolated to site coordinates).

For coordinate epoch changes in areas near outlier stations it may be preferable in some cases to use the station velocity estimate directly rather than the velocity model. This would not be recommended for cases where site instability or other monument problems are suspected, or at new sites with short time series. Users are referred to Table C1 of Appendix 1 for site-specific information on why outliers were removed.

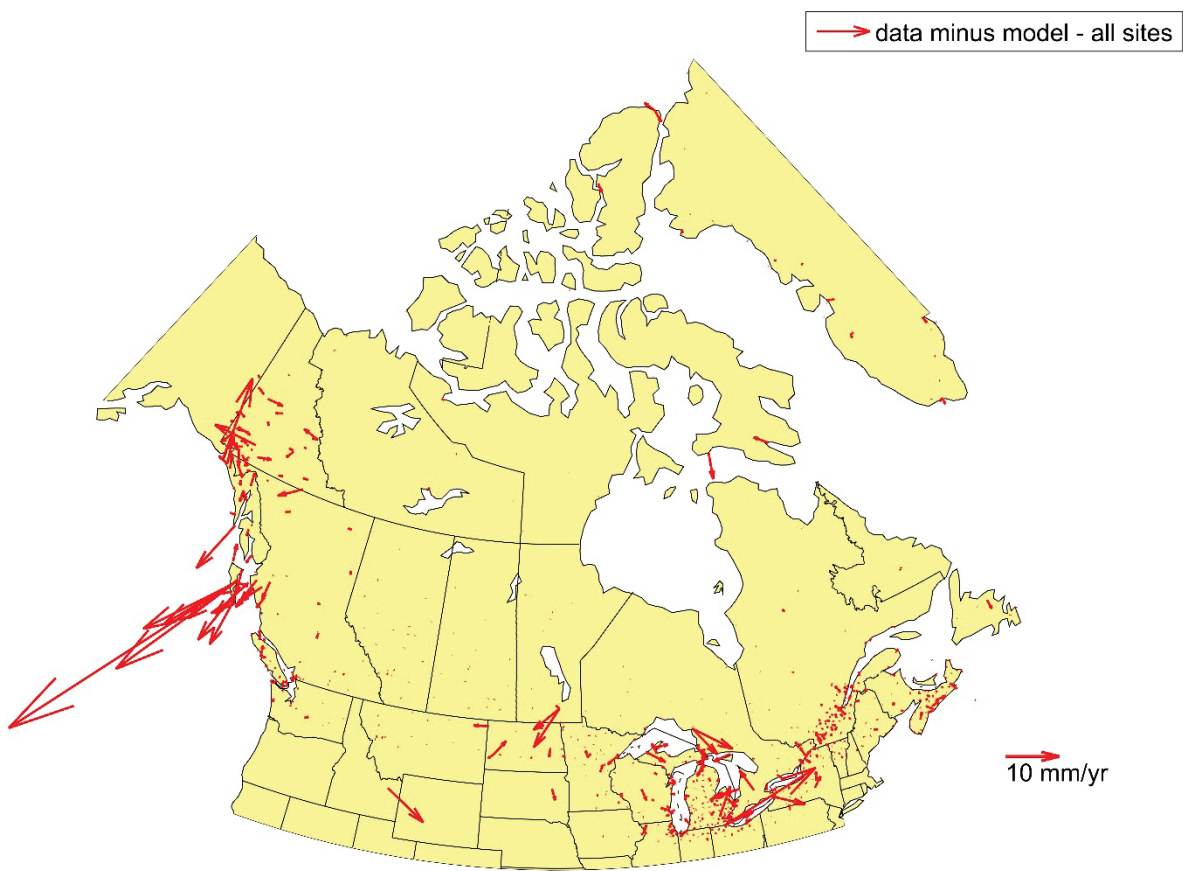


Figure 23 - Residual field, horizontal components. Arrows map the residuals defined as station velocities minus the velocity model (as interpolated to site coordinates) in two dimensions.

Table 3 - Residual Statistics. Statistics of the absolute value of the residuals (velocity field minus velocity model, in mm/yr) for different subsets of the velocity field.

	North		East		Up	
	Mean	σ	Mean	σ	Mean	σ
ACS*	0.17	0.31	0.15	0.24	0.26	0.38
Campaign*	0.19	0.37	0.23	0.44	0.43	0.53
Velocity Field*	0.18	0.66	0.17	0.33	0.39	0.89
All sites	0.5	2.05	0.41	1.41	0.74	1.52
Outliers	1.95	4.4	1.55	2.95	2.55	2.84

* Outliers removed

6 Future Work

In addition to maintaining its active control and campaign sites, CGS continues to expand its networks by installing new sites in key locations. The primary motivation for these activities is to improve the velocity model; hence, network expansion is guided in large part by consideration of the NAD83v70VG uncertainty grid. As seen in Figure 20, newly installed sites target areas where NAD83v70VG is the most uncertain.

CGS computes a new national velocity field and crustal velocity model every few years. Computation of the new velocity field includes a detailed review of discontinuities and outliers. New velocity models will be officially released if significant differences are found with respect to the previous one. These differences are expected to result from:

- Availability of robust velocities as new sites produce sufficiently long time series.
- Significant changes in velocities at existing sites.
- New and improved geodynamic model input, such as new GIA models, elastic models for recent loading changes, or tectonic block models for the west coast (which could be applied to all components).
- New and improved interpolation and error propagation methods.

7 User Summary

We summarize the following points for users of NAD83v70VG:

- NAD83v70VG is provided on a set of three grids, one for each of the **three components of crustal motion for all of Canada** (see Figures 16 and 18). It is officially released in the NAD83(CRS) v7 reference frame.
- NAD83v70VG includes **three uncertainty grids**, corresponding to the estimated standard deviation (1σ) for each of the three components of the velocity model (e.g., Figure 20). These are used by CGS to estimate epoch transformation errors by, e.g., CSRS-PPP services.
 - Until now, users performing large epoch changes may not have been aware of the error introduced by this process.
- **NAD83v70VG is intended to capture large-scale regional motion.** Horizontal velocities exhibit significantly less regional variability than vertical velocities.
- **Sites which appear to be affected by local motion have been removed** from the modelling process. However, users working in close proximity to these **outliers** may prefer to use station velocities directly rather than velocities interpolated from NAD83v70VG. These users are referred to Table C1 in Appendix C, which describes the reasons outliers were removed.
- NAD83v70VG provides velocities which are **stable in time**. Periodic (seasonal and multi-year) and post-seismic signals are not included in NAD83v70VG at this time (e.g., Figure 2).
- **CGS recommends the use of NAD83v70VG in northern Canada** for the first time. New data, longer time series, the introduction of geodynamic models in the vertical component, and a new

data interpolation method have contributed to significant improvements of the models since the 2011 release of NAD83v60VG (e.g., Figures 16 and 21).

- **CGS does not recommend using NAD83v70VG offshore**, as there are no crustal velocity constraints for the ocean floor at this time.
- **CGS does not recommend using NAD83v70VG outside of Canada**, as the models and velocity field have not been optimized for that purpose.
- **The velocity model will be updated on a semi-regular basis** when improvements to the data and modelling methods generate significant differences with the previous version.
- Online tools provided by the CGS (e.g., CSRS-PPP, TRX) use bilinear interpolation to perform epoch changes using NAD83v70VG velocities and uncertainties for any point inside the grid.
- The velocity grid is available in NAD83(CSRS) for download in ASCII and binary formats at <https://webapp.geod.nrcan.gc.ca/geod/tools-outils/nad83-docs.php>. The grids are available in IGS14 upon request.

8 Acknowledgements

We are grateful to Karen Simon for calculating the LaurInnu GIA model and the Greenland and Arctic Ice Sheet models on our model grid nodes; to CGS and provincial geodetic agencies for installation and operation of geodetic networks of the highest quality; and to CGS field survey personnel who have always maintained exceptional standards for GPS survey campaigns. We thank Dr. Joe Henton and Dr. Reza Ghoddousi-Fard for careful reviews which improved the quality of this submission.

Bibliography

- Altamimi, Z., P. Rebischung, L. Metivier, and X. Collilieux. 2017. "ITRF2014: A new release of the International Terrestrial Reference Frame modeling nonlinear station motions." *Journal of Geophysical Research: Solid Earth* 121: 6109-6131. doi:10.1002/2016JB013098.
- Bailey, T.C., and A.C. Gatrell. 1995. *Interactive spatial data analysis*. New York: Longman Scientific & Technical.
- Basham, P.W., D.A. Forsyth, and R.J. Wetmiller. 1977. "The seismicity of northern Canada." *Canadian Journal of Earth Science* 14 (7): 1646-1667.
- Blewitt, G., and D. Lavallee. 2002. "Effect of annual signals on geodetic velocity." *Journal of Geophysical Research* 107 (B7). doi:10.1029/2001JB000570.
- Canadian Geodetic Survey. 2020a. *Canadian Active Control Stations*. 08 07. Accessed 11 16, 2020.
<https://www.nrcan.gc.ca/earth-sciences/geomatics/geodetic-reference-systems/data/10923#cacs>.
- Canadian Geodetic Survey. 2020b. *NAD83(CSRS) v7*. 08 07.
<https://webapp.geod.nrcan.gc.ca/geod/tools-outils/nad83-docs.php>.

- Canadian Geodetic Survey. 2020c. *Passive Control Networks*. 08 07. Accessed 11 15, 2020.
<https://webapp.geod.nrcan.gc.ca/geod/data-donnees/passive-passif.php?locale=en>.
- Caron, L., E.R. Ivins, E. Larour, S. Adhikari, J. Nilsson, and G. Blewitt. 2018. "GIA Model Statistics for GRACE Hydrology, Cryosphere, and Ocean Science." *Geophysical Research Letters* 45: 2203-2212. doi:10.1002/2017GL076644.
- Craymer, M. R., J. A. Henton, M. Piraszewksi, and E. Lapelle. 2011. "An Updated GPS Velocity Field for Canada." *AGU Fall Meeting*. San Francisco, CA, USA: American Geophysical Union.
- Craymer, M.R. 2006. "The Evolution of NAD83 in Canada." *Geomatica* 60 (2): 151-164.
- Dyke, A. S., A. Moore, and L. Robertson. 2003. *Deglaciation of North America*. Ottawa: Geological Survey of Canada.
- Elliot, J.L., C.F. Larsen, J.T. Freymueller, and R.J. Motyka. 2010. "Tectonic block motion and glacial isostatic adjustment in southeast Alaska and adjacent Canada constrained by GPS measurements." *Journal of Geophysics* 115. doi:10.1029/2009JB007139.
- Erickson, C., G. Banham, R. Berg, J. Chessie, M. Craymer, B. Donahue, R. Tardif, Y. Theriault, and M. Veronneau. 2019. "The U.S. is replacing NAD83 with NATRF2022: what this means for Canada." *Geomatica* 73 (3): 74-80.
- Gazeaux, Julien, Simon Williams, Matt King, Machiel Bos, Rolf Dach, Manoj Doe, Angelyn Moore, et al. 2013. "Detecting offsets in GPS time series: First results from the detection of offsets in GPS experiment." *Journal of Geophysical Research - Solid Earth* 118: 2397-2407. doi:10.1002/jgrb.50152.
- Goovaerts, P. 1997. *Geostatistics for Natural Resource Evaluation*. New York: Oxford University Press.
- Gowan, E.J., P. Tregoning, A. Pucell, J.-P. Montillet, and S. McClusky. 2016. "A model of the western Laurentide Ice Sheet, using observations of glacial isostatic adjustment." *Quaternary Science Reviews* 139: 1-16.
- Hay, C, J.X. Mitrovica, N. Gomez, J.R. Creveling, J. Austermann, and R.E. Kopp. 2014. "The sea-level fingerprints of ice-sheet collapse during interglacial periods." *Quaternary Science Reviews* 87: 60-69.
- Hermans, T.H.J., W. van der Wal, and T. Broerse. 2018. "Reversal of the Direction of Horizontal Velocities Induced by GIA as a Function of Mantle Viscosity." *Geophysical Research Letters* 45: 9597-9604. doi:10.1029/2018GL078533.
- Herring, T. 2003. "Matlab Tools for viewing GPS velocities and time series." *GPS Solutions* 7: 194-199. doi:10.1007/s10291-003-0068-0.

- Hu, Y., and J. T. Freymueller. 2019. "Geodetic Observations of Time-Variable Glacial Isostatic Adjustment in Southeast Alaska and Its Implications for Earth Rheology." *Journal of Geophysical Research: Solid Earth* 9870–9889. doi:10.1029/2018JB017028.
- James, T. S., and E. Ivins. 1998. "Predictions of Antarctic crustal motions driven by present-day ice sheet evolution and by isostatic memory of the Last Glacial Maximum." *Journal of Geophysical Research* 103 (B3): 4993-5017.
- James, T. S., J. F. Cassidy, G. C. Rogers, and P. J. Haeussler. 2015. "Introduction to the Special Issue on the 2012 Haida Gwaii and 2013 Craig Earthquakes at the Pacific–North America Plate Boundary (British Columbia and Alaska)." *Bulletin of the Seismological Society of America* 105 (2B): 1053-1057. doi:10.1785/0120150044.
- James, T.S., and T.D. Shamehorn. 2016. *A comparison of seismicity to the crustal deformation predicted by a Glacial Isostatic Adjustment Model in northern Canada and western Greenland*. Open File 8106, Geological Survey of Canada. doi:10.4095/299098.
- James, T.S., and W.J. Morgan. 1990. "Horizontal motions due to post-glacial rebound." *Geophysical Research Letters* 17 (7): 957-960.
- James, T.S., C.M.I. Robin, J.A. Henton, and M. Craymer. in review. "Relative Sea-level Projections for Canada based on the IPCC Fifth Assessment report and the NAD83v70VG National Crustal Velocity Model." Geological Survey of Canada Open File.
- Junkins, D.R. 1990. "The National Transformation for Converting Between NAD27 and NAD83 in Canada." In *Moving to NAD '83: The New Address for Georeferenced Data in Canada*, edited by D.C. Barnes, 16-40. Ottawa: The Canadian Institute of Surveying and Mapping.
- Lambert, A., J. Huang, G. van der Kamp, J. Henton, S Mazzotti, T.S. James, N. Coutier, and A.G. Barr. 2013. "Measuring water accumulation rates using GRACE data in areas experiencing glacial isostatic adjustment: The Nelson River basin." *Geophysical Research Letters* 40 (23): 6118-6122. doi: <https://doi.org/10.1002/2013GL057973>.
- Larsen, C.F., R.J. Motyka, J.T. Freymueller, K.A. Echelmeyer, and E.R. Ivins. 2005. "Rapid viscoelastic uplift in southeast Alaska caused by post-Little Ice Age glacial retreat." *Earth and Planetary Science Letters* 237: 548– 560.
- Lemmen, D.S.; Waren, F.J., James, T.S.; Mercer Clarke, C.S.L. 2016. *Canada's Marine Coasts in a Changing Climate*. Ottawa, ON: Government of Canada, 274.
- Matheron, G. 1968. "Principles of Geostatistic." *Economic Geology* 58: 1246-1266.
- "MATLAB and Mapping Toolbox (R2015b)." (2015) Natick, Massachusetts: The MathWorks, Inc.
- Mazzotti, S., L.J. Leonard, R.D. Hyndman, and J.F. Cassidy. 2008. "Tectonics, Dynamics, and Seismic Hazard in the Canada-Alaska Cordillera." In *Active Tectonics and Seismic Potential of Alaska*,

edited by J.T. Freymueller, P.J. Haeussler, R.L. Wesson and G. Ekstrom, 297-319. American Geophysics Union. doi:10.1029/GM179.

Milne, G.A., J.L. Davis, J.X. Mitrovica, and H.-G. Scherneck. 2001. "Space-Geodetic Constraints on Glacial Isostatic Adjustment in Fennoscandia." *Science* 291.

Mitrovica, J.X., and W.R. Peltier. 1991. "On postglacial geoid subsidence over the equatorial oceans." *Journal of Geophysical Research* 96: 20053-20071.

National Geodetic Survey. 2018. *New Datums: Replacing NAVD 88 and NAD 83*. Accessed October 3, 2018. <https://www.ngs.noaa.gov/datums/newdatums/index.shtml>.

NRCan. 2020. *Tools and Applications*. 04 06. Accessed 05 06, 2020. <https://www.nrcan.gc.ca/maps-tools-publications/tools/geodetic-reference-systems-tools/tools-applications/10925>.

Nykolaishen, L., H. Dragert, K. Wang, T.S. James, and M. Schmidt. 2015. "GPS Observations of Crustal Deformation Associated with the 2012 Mw 7.8 Haida Gwaii Earthquake." *Bulletin of the Seismological Society of America* 105 (2B). doi:10.1785/0120140177.

Pearson, C., and R. Snay. 2012. "Introducing HTDP 3.1 to transform coordinates across time and spatial reference frames." *GPS Solutions* 17: 1-15. doi:DOI 10.1007/s10291-012-0255-y.

Peltier, W. R., D. F. Argus, and R. Drummond. 2015. "Space geodesy constrains ice age terminal deglaciation: The globe ICE-6G_C(VM5a) model." *Journal of Geophysical Research: Solid Earth* 120: 450-487.

Peltier, W.R. 2004. "Global glacial isostasy and the surface of the ice-age." *Annual Reviews of Earth and Planetary Sciences* 32: 111-149.

Peltier, W.R., and R. Drummond. 2008. "Rheological stratification of the lithosphere: a direct inference based upon the geodetically observed pattern." *Geophysical Research Letters* 35. doi:10.1029/2008GL034586.

Peltier, W.R., and R.G. Fairbanks. 2006. "Global glacial ice volume and Last Glacial Maximum duration from an extended Barbados sea level records." *Quaternary Science Reviews* 25: 3322–3337.

Rebischung, P. 2016. "[IGSMAIL-7399] Upcoming switch to IGS14/igs14.atx." lists.igs.org. 12 21. Accessed 2017. <https://lists.igs.org/pipermail/igsmail/2016/001233.html>.

Rebischung, P., R. Schmid, and A. Craddock. 2017. *IGS14 Reference Frame Transition*. February 7. <http://www.igs.org/article/igs14-reference-frame-transition>.

Rebischung, P., Z. Altamimi, J. Ray, and B. Garayt. 2016. "The IGS contribution to ITRF2014." *Journal of Geodesy* 90: 611-630.

- Robin, C. M. I., M. Craymer, R. Ferland, E. Lapelle, M. Piraszewski, and Y. Zhao. 2017. "Integrating GIA models with GNSS data: Testing models against a new Canadian velocity field." *2017 AGU Fall Meeting*. San Francisco: American Geophysical Union.
- Robin, C., S. Nudds, P. MacAulay, A. Godin, B. De Lange Boom, and J. Bartlett. 2016. "Hydrographic Vertical Separation Surfaces (HyVSEPs) for the Tidal Waters of Canada." *Marine Geodesy* 39 (2): 195-222. doi:10.1080/01490419.2016.1160011.
- Schwanghart, W. 2010. "variogramfit.m." *variogramfit*.
- Sella, G.F, S. Stein, T.H. Dixon, M. Craymer, T.S. James, S. Mazzotti, and R.K. Dokka. 2007. "Observation of glacial isostatic adjustment in "stable" North America." *Geophysical Research Letters* 34. doi:10.1029/2006GL027081.
- Simon, K. 2014. "Improved glacial isostatic adjustment models for northern Canada." *PhD Thesis*. University of Victoria.
- Simon, K. M., T. S. James, J.A. Henton, and A. S. Dyke. 2016. "A glacial isostatic adjustment model for the central and northerm Laurentide Ice Sheet based on relative sea level and GPS measurements." *Geophysical Journal International* 205: 1618-1636.
- Simon, K. S., T. S. James, and A. S. Dyke. 2015. "A new glacial isostatic adjustment model of the Innuitian Ice Sheet, Arctic Canada." *Quaternary Science Reviews* 119: 11-21.
- Simon, K.J., R.E.M. Riva, M. Kleinherenbrink, and N. Tangdamrongsub. 2017. "A data-driven model for constraint of present-day glacial isostatic adjustment in North America." *Earth and Planetary Science Letters* 474: 322-333. doi:10.1016/j.epsl.2017.06.046.
- Simon, K.M., T.S. James, D.S. Forbes, A.M. Telka, A.S. Dyke, and J.A. Henton. 2014. "A relative sea-level history for Arviat, Nunavut, and implications for Laurentide Ice Sheet thickness west of Hudson Bay." *Quaternary Research* 82: 185-197.
- Sjoberg, L.E. 2005. "A discussion on the approximations made in the practical implementation of the remove-compute-restore technique in regional geoid modeling." *Journal of Geodesy*. doi:DOI 10.1007/s00190-004-0430-1.
- Snay, R.A., J.T. Freymuelle, M.R. Craymer, C.F. Pearson, and J. Saleh. 2016. "Modeling 3-D crustal velocities in the United States and Canada." *Journal of Geophysical Research: Solid Earth* 121: 5365-5388.
- Vestol, O., J. Agren, H. Steffen, H. Kierulf, and L. Tarasov. 2019. "NKG2016LU: a new land uplift model for Fennoscandia and the Baltic Region." *Journal of Geodesy* 93: 1759–1779.
- Webster, R., and M. Oliver. 2007. *Geostatistics for Environmental Scientists*. Second. West Sussex: John Wiley & Sons, Ltd.

Whitehouse, P. 2018. "Glacial isostatic adjustment modelling: historical." *Earth Surface Dynamics* 6: 401–429.

Appendix A. Interpolation technique cross-validation tests

Interpolation methods which were subject to cross-validation are listed in Table A1. Others were tested, but the ones listed here were selected based on availability, ease of implementation (incorporating into automated testing routines), and performance (e.g., did not result in large excursions from the data or produce obvious artifacts).

Interpolators were evaluated using cross-validation techniques aimed at testing the interpolator's ability to predict missing data. We primarily used k -fold cross validation, where k validations are performed by removing an equal number of randomly selected subsets of the velocity field for each validation. Summary statistics of the predicted residuals (the difference between the interpolation results and the data) were compared across the set of tested interpolators.

The number k is determined by the size of the test data set and its division into subsets ($k = (\text{data set size}) / (\text{subset size})$). Optimal subset size for our velocity field was found to be between 3 and 10 data points. This permitted a sufficient number of validation tests for statistics to be meaningful and avoided clustering of the randomly selected test sites (which would be problematic for the sparse areas of our network). It also replicated the results of the leave-on-out cross-validation technique (LOO, where the number of validations (k) is equal to the size of the data set), which was found to be computationally expensive when testing more than 20 interpolation methods for nearly 1000 sites.

Results for one test are shown in Figure A1 for the north (N) component. Plotted are the RMS of the predicted residual for k comparisons and for each interpolator tested. For this test, the data set was limited to 446 Canadian sites, which were randomly removed in groups of six (i.e., subset size was 6 and $k = 74$). Cross-validation was performed for different data sets and subsets, and Figure 12 is representative of our analysis. In general, most of the tested interpolators performed in a consistent fashion, and performance for all interpolators depends on the distribution of the subset sites. Therefore, our selection was based on other performance parameters, including the ability to weigh the input data, to provide an estimate of interpolation error, and ability to extrapolate to the offshore (Section 3.2).

Table A1 - Interpolation and approximation methods tested for interpolation of the velocity field and/or the velocity geophysical model residuals.

Interpolator	Description	Source	Notes
Kriging (Exponential)	Ordinary kriging, exponential variogram model (unbounded): $\gamma(h) = c \left(1 - \exp \left(\frac{-h}{a} \right) \right)$	variogramfit.m (W. Schwanghart) kriging.m (W. Schwanghart)	- Good offshore interpolation - Interpolation error estimated
Kriging (Spherical)	Ordinary kriging, bounded spherical variogram model: $\begin{cases} \gamma(h) = c \left(\frac{3h}{2a} - \frac{1}{2} \left(\frac{h}{a} \right)^3 \right), & h \leq a \\ \gamma(h) = c, & h > a \end{cases}$	γ : variogram h : lag c : sill a : range	
Kriging (Pentaspherical)	Ordinary kriging, pentaspherical variogram model:		

	$\begin{cases} \gamma(h) = c \left(\frac{15h}{8a} - \frac{5}{4} \left(\frac{h}{a} \right)^3 + \frac{3}{8} \left(\frac{h}{a} \right)^5 \right), & h \leq a \\ \gamma(h) = c & , h > a \end{cases}$	See Section 2.3.4 and AppendixB for details.	
Kriging (Circular)	Ordinary kriging, circular variogram model: $\begin{cases} \gamma(h) = c \left(1 - \frac{2}{\pi} \cos^{-1} \left(\frac{h}{a} \right) + \frac{2h}{\pi a} \sqrt{1 - \left(\frac{h}{a} \right)^2} \right), & h \leq a \\ \gamma(h) = c & , h > a \end{cases}$		
Weighted Kriging (Exponential)	Weighted ordinary kriging, exponential variogram model (as above).	variogramfit.m (W. Schwanghart)	- data uncertainty taken into account, smoother model
Weighted Kriging (Spherical)	Weighted ordinary kriging, spherical variogram model (as above).	krigingw.m (modified from W. Schwanghart)	- better prediction at unsampled points than unweighted ordinary kriging
Weighted Kriging (Pentaspherical)	Weighted ordinary kriging, pentaspherical variogram model (as above).		
Weighted Kriging (Circular)	Weighted ordinary kriging, circular variogram model (as above).		
Griddata linear	Linear interpolation of 2D scattered data	griddata.m (Mathworks 2015b)	- No extrapolation
Griddata natural	Natural neighbour interpolation of 2D scattered data		- Interpolation (no smoothing or filtering)
Griddata cubic	cubic interpolation of 2D scattered data		
Griddata v4	v4 (biharmonic spline) interpolation of 2D scattered data		
RBF linear	Scattered data interpolation and approximation, Radial Base Function: linear	rbfcreate.m, rbfinterp.m, by Alex Chirokov	- Good fit for interpolation - Smoothing parameters arbitrary for approximation
RBF thinplate	Radial Base Function: thinplate		- large artefacts offshore
RBF cubic	Radial Base Function: cubic		- large artefacts offshore
NTV2 1	ntv2 distortion gridding, polynomial order 1	ntv2distgrid.m, by Catherine Robin, based on NTv2 by Don Junkins (Junkins 1990)	- artefacts likely from variable widths of the Gaussian distance weighting function
NTV2 2	same, polynomial order 2		- less noticeable in a denser network
NTV2 3	same, polynomial order 3		

			as was its original use. -offshore artifacts
Gridfit	estimates a surface on a 2d grid, based on scattered data	RegularizeData3D.m/Gridfit.m (J. D'Errico)	- smoothing parameters arbitrary - amplifies gradients offshore
Polyfitn 1	polynomial regression model in n dimensions, polynomial order 1	polyfitn.m (J. D'Errico)	- smoothing parameters arbitrary
Polyfitn 2	same, polynomial order 2		- extrapolation
Polyfitn 3	same, polynomial order 3		
Polyfitn 4	same, polynomial order 4		suffers with higher polynomial values

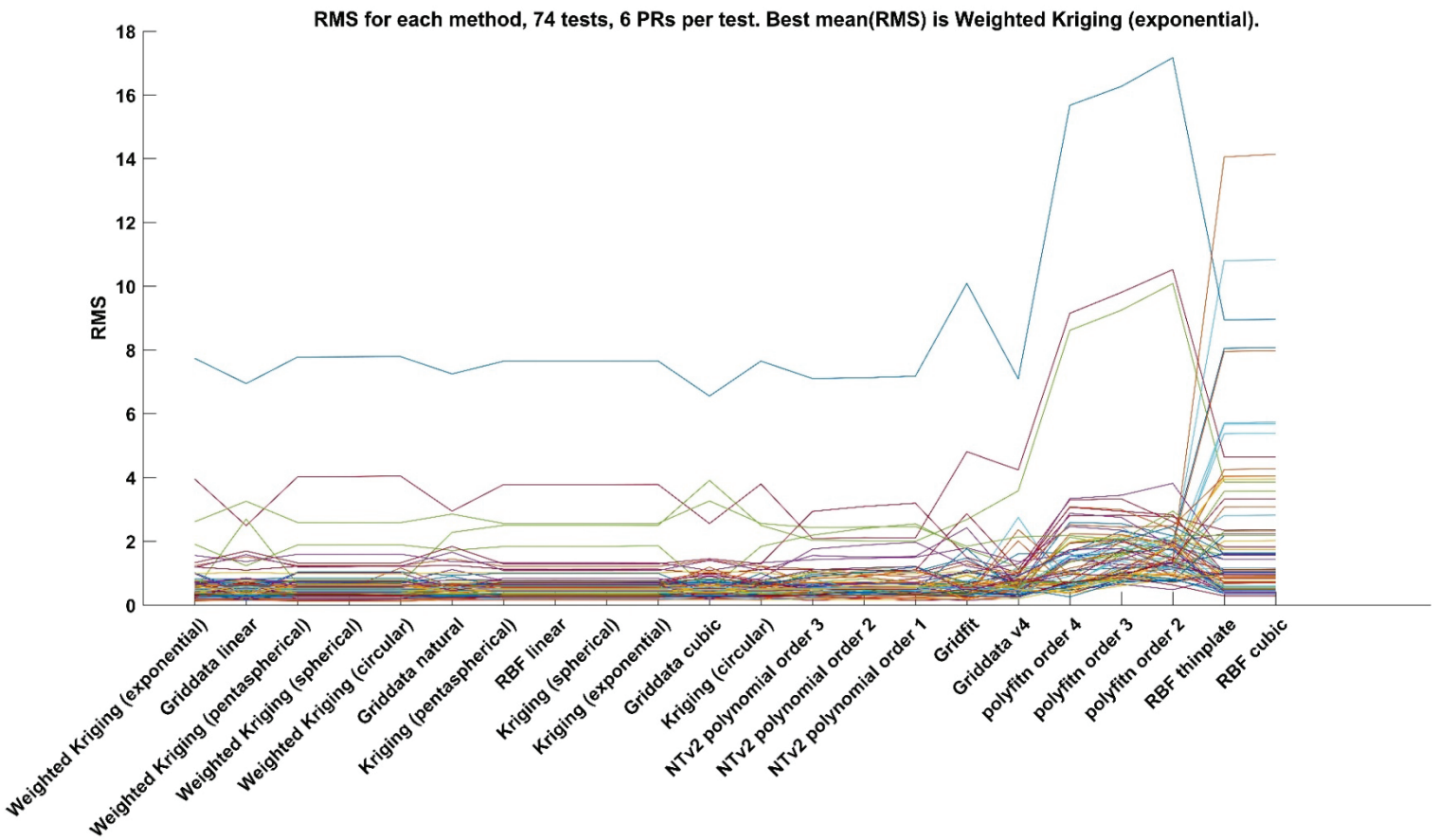


Figure A1 - Cross-validation test results for RMS residuals (in mm/yr) between observed and predicted vertical velocities for 23 interpolators, for the north component of the velocity. The number of tests is $k=74$. Each predicted subset consists of 6 randomly selected sites which were removed during the interpolation, then used to calculate the predicted residual. Each of k tests is a coloured line. In the case of the blue line, the large RMS is likely due to clustering of the sites removed, which created a large misfit over a small area. The performance of each interpolator for each test is evaluated as the RMS of the predicted residual. The mean of the RMS's was used to identify the 'best' interpolator, which for this test was Weighted Kriging using the exponential variogram model. Details of the method are given in Table A1.

Appendix B. Weighted Ordinary Kriging

Kriging is a geostatistical interpolation method developed by Daniel Krige and George Matheron in 1960 (Matheron, 1968). Many variations on the method and its applications exist, as described in, e.g., Bailey and Gatrell (1995), Goovaerts (1997), and Webster and Oliver (2007). Here we describe how it is formulated for the purpose of calculating the NAD83v70VG grids.

As with other interpolators, kriging calculates values at unobserved prediction points x_p as a weighted average of observed values z at observation points \mathbf{x} :

$$Z(x_{p_j}) = \sum_{i=1}^n w_i z_i = [w_1 \dots w_n] \begin{bmatrix} z_1 \\ \vdots \\ z_n \end{bmatrix} = \mathbf{w}' \mathbf{z} \quad (\text{C-1})$$

where w_i is the i^{th} weight, z_i the i^{th} sampled value at observation point x_i , x_{p_j} is the j^{th} prediction point, and $i = 1, \dots, n$ & $j = 1, \dots, p$. Similar to simpler inverse-distance interpolation schemes, kriging weights decrease as a function of distance (i.e., points closer together are assumed to be more similar than those further apart). However, instead of using a pre-defined function to define the inverse distance weights, kriging weights are based on observation statistics drawn from a model of the empirical semivariogram, introduced in Section 2.3.4.

The empirical semivariogram describes the spatial variability of a field or regional variable Z as a function of distance between pairs of observations. It is defined in Equation 2 (repeated here) as

$$\gamma(h) = \frac{1}{2 \cdot N(h)} \sum_{i=1}^{N(h)} (z(x_i) - z(x_i + h))^2$$

where $N(h)$ is the number of pairs of sites separated by a distance (or lag) h , and $(z(x_i) - z(x_i + h))$ is the difference in observation of the unknown field Z for each N pair of sites separated by lag h . A function fit to the empirical semivariogram provides a continuous model to define the weights for kriging interpolation. A number of standard functions are used; we have tested those listed in Table B1. Key parameters defining the fit are the range, the sill, and the nugget (see Section 2.3.4, and Table B1). Once a semivariogram model function is selected, model parameters are calculated by minimizing the mean squared error between the observed and modeled semivariogram, subject to the constraint that the weights sum to 1.

The exponential model delivered the best results for our data (Table B1). An empirical semivariogram and its exponential model fit are shown in Figure C1, where the data is the residual between the combined geophysical model and the vertical component of the velocity field. The exponential model provides a good fit at mid-distances, and less so outside of that range (see Section 2.3.4 for a description of the semivariogram plot). A non-zero y-intercept, or nugget, is caused by measurement error or small-scale variability, and can be applied as a correction to all the data. However, we have set the model nugget to zero, and instead individually weigh each data point using its uncertainty as described below.

Thus three exponential semivariogram models provide kriging weights for interpolation in equation C-1, one for each of the three components of velocity. For the vertical component, Z is the residual between observations and the combined geophysical model. For the horizontal components, Z is the velocity field itself.

Kriging performs under the assumption that the regional variable is intrinsically stationary; that is, that the mean and variance are constant, and that $z(x_i) - z(x_i + h)$ depends only on lag, independent of location. These assumptions may not be strictly true of the data, but permit the calculation of a semivariogram function; the applicability of these assumptions for our data is discussed briefly below. We use ordinary kriging, which assumes the mean is constant but unknown. Other options include simple kriging where the mean is assumed to be zero, or universal kriging where a trend (usually a polynomial) is removed from the data as well. In addition, our kriging tool also assumes that the sampled field is isotropic, and that one semivariogram model fit to the entire data set is sufficient.

Kriging applies the semivariogram model to formulate the design matrix, which is inverted to calculate the interpolation weights \mathbf{w} (equation C-1). For n sample points \mathbf{x} with observed values \mathbf{z} , and p unobserved locations \mathbf{x}_p where we seek predictions $Z(\mathbf{x}_p)$, we solve the kriging equations $\mathbf{Aw} = \mathbf{b}$ using the method of Lagrange multipliers as follows:

1. Calculate the $n \times n$ matrix \mathbf{D} which contains the distance between all observation point pairs.
2. Define the design matrix \mathbf{A} by applying the semivariogram model to \mathbf{D} :

$$\mathbf{A} = \begin{bmatrix} \gamma(x_1, x_1) & \gamma(x_1, x_2) & \dots & \gamma(x_1, x_n) \\ \gamma(x_2, x_1) & \gamma(x_2, x_2) & \dots & \gamma(x_2, x_n) \\ \dots & \dots & \dots & \dots \\ \gamma(x_n, x_1) & \gamma(x_n, x_2) & \dots & \gamma(x_n, x_n) \end{bmatrix} \quad (\text{C-2})$$

Since we have set the nugget to be zero (e.g. Figure 14), the diagonal elements are zero. This can be understood from the relationship between the semivariogram γ and the covariance C which is

$$\gamma(\mathbf{h}) = C(0) - C(\mathbf{h}) \quad (\text{C-3})$$

where $C(0) = \sigma^2$ is assumed to be constant (the assumption of stationarity).

3. To account for the condition that the weights must sum to 1 using the method of Lagrange multipliers, \mathbf{A} becomes $\begin{bmatrix} \mathbf{A} & 1 \\ 1' & 0 \end{bmatrix}$;
4. Weight the interpolation using individual observation errors by including velocity field uncertainties σ_{obs} in \mathbf{A} , such that $\mathbf{A} = \mathbf{A} - \sigma_{\text{obs}}^2$ on the diagonal elements only. This assumes that the observation uncertainty is uncorrelated. (Note that σ_{obs}^2 is subtracted because of the relationship between γ and the covariance as seen in Equation (C-3)).
5. Create an $n \times p$ distance matrix \mathbf{b} for all observation to prediction point pairs as in Step 1, expanding it with ones as in Step 2.
6. Solve for $\mathbf{w} = \mathbf{A}^{-1}\mathbf{b}$.

7. Expand the observation point vector \mathbf{z} with a zero and perform the interpolation

$$Z(\mathbf{x}_p) = \mathbf{w}' \mathbf{z}$$

Steps 6 and 7 are done in blocks for computational efficiency.

8. Calculate the kriging variance, or the interpolation error, as

$$\sigma_{x_p}^2 = \mathbf{w}' \mathbf{b}$$

This procedure performs a standard interpolation by ordinary kriging, with the addition of data uncertainties in the design matrix \mathbf{A} . This smooths the interpolated surface where data is noisy, and, as shown by the results of our cross-validation tests (Appendix A), provides better predictions than the unweighted version.

It is important to note that removal of the combined geophysical model from the data for the vertical component of NAD83v70VG (Section 2.3.5) is an important step towards ensuring that the interpolated data is free of trends and randomly distributed, for optimal kriging performance. The lack of geophysical models for the horizontal components is somewhat mitigated by the fact that horizontal velocity varies smoothly over most of Canada east of the Rockies. On the west coast this shortcoming is more problematic, although less so on Vancouver Island, southwest mainland BC, and the Alaskan panhandle, where the observed velocity field is relatively dense (Figures 4 and 5). Future work will focus on integrating geophysical models into the horizontal components of NAD83v70VG and densifying the ACS network on mainland BC.

Additional improvements to our kriging method could include taking into account anisotropy, trends (universal kriging), and defining separate semivariogram models for sub-regions of the data. However, the highly variable density of the velocity field may limit the achievement of significant improvements with these methods.

Appendix C. Observations

Table C1 lists the sites in the cumulative solution used to create NAD83v70VG, including those removed as model outliers (see Section 2.1). Coordinates and velocities are in NAD83(CSRS).

The table includes site coordinates (**Lat**, **Lon**), the 3 components of velocity and their $1-\sigma$ uncertainties (V_N , σ_N , V_E , σ_E , V_U , σ_U), and types (**Type**) using the acronyms defined below.

Stations removed as model outliers are indicated by an entry in the '**Out**' column, which also gives the reason for removal using the acronyms defined below.

Sites with velocity discontinuities have 2 or more velocity solutions, listed in the '**Soln**' column. The default is to use the most recent solution, in which case previous solutions are not listed (to shorten the table). If a solution other than the most recent is used, subsequent solutions are listed as outliers to indicate the reason the default was not used.

For all sites covered by the NAD83v70VG grid, Table C1 lists residuals between the velocity model and the station velocities, for all solutions and all components of velocity (res_N , res_E , res_U). Large residuals are generally at stations in areas with very high rates of uplift (e.g. the Alaskan panhandle) and/or post-seismic motion, stations with high uncertainty, stations in areas where the network is relatively dense, or stations which have been removed as model outliers.

Site types are:

ACS (*Active Control Stations*): continuously operating stations operated by NRCan, including CGS.

CBN (*Canadian Base Network*): campaign stations operated by CGS.

CAMP: campaign sites operated by the Canadian federal government not part of the CBN network.

CORS (*Continuously Operating Reference Stations*): continuously operating stations operated by international partners.

The following acronyms are used to identify model outliers types:

NED: not enough data (e.g. insufficient time span or large gaps).

EP: equipment problem (e.g. monument instability, undocumented antenna changes, site disturbance).

LD: Local deformation (e.g. over an active salt mine).

PS: post seismic (e.g. site dominated by transient motion).

US: unsuitable site (e.g. signal obstruction, unstable foundation).

NNC: no known cause.

The acronym **DC** (for declustered) is used for sites that are not outliers but are in close proximity and are combined using a weighted average, in order to de-cluster the velocity field for improved interpolation (Section 2.1.6).

Table C1. Velocity solutions analyzed for inclusion in the velocity field. See text for details.

Site	Solution	Type	Latitude	Longitude	Velocities (mm/yr) and Uncertainties (1σ , mm/yr)						Outlier rationale	Residuals (mm/yr)		
					v_{North}	σ_{North}	v_{East}	σ_{East}	v_{Up}	σ_{Up}		$\text{res}_{\text{North}}$	res_{East}	res_{Up}
044L	1	CORS	46.875	-89.323	-3.41	0.68	4.96	0.61	-7.18	2.63	NNC	-2.14	3.24	-5.85
3RIV	1	CBN	46.315	-72.576	-2.16	0.09	2.1	0.07	1.83	0.28		0.21	-0.08	-0.69
3RV2	1	CBN	46.316	-72.573	-2.02	0.68	1.87	0.55	2.11	2.13		0.35	-0.31	-0.40
489F	1	CAMP	59.973	-136.819	8.37	1.04	3.98	0.69	20.69	3.42		-0.67	-0.30	2.30
AASI	1	CORS	68.719	-52.793	-3.12	0.05	-0.16	0.04	6.56	0.12		-0.02	-0.01	-0.06
AB33	1	CORS	67.251	-150.173	-2.38	0.06	3.49	0.05	-2.88	0.12				
AB35	1	CORS	60.079	-142.390	34.49	0.06	-18.26	0.05	9.08	0.11				
AB36	1	CORS	65.030	-150.744	-4.75	0.07	2.68	0.05	0.1	0.16				
AB37	4	CORS	62.967	-145.452	9.62	0.11	-11.18	0.08	4.47	0.28				
AB39	1	CORS	66.559	-145.213	-1.52	0.07	2.74	0.05	-4.81	0.14				
AB41	2	CORS	64.777	-141.158	0.46	0.12	3.27	0.08	-4.95	0.33		0.04	-0.32	-0.70
AB42	2	CORS	59.340	-138.899	32.37	0.12	-19.45	0.08	24.72	0.32		0.11	-1.91	1.66
AB43	1	CORS	58.199	-136.641	12.56	0.1	-4.41	0.07	14.94	0.25		0.23	-0.25	-0.25
AB44	1	CORS	59.528	-135.228	6.4	0.06	4.18	0.05	16.4	0.13		0.17	-0.10	-0.56
AB45	1	CORS	68.761	-148.871	-1.29	0.06	3.14	0.05	-2.39	0.12				
AB46	1	CORS	68.121	-145.568	-0.7	0.06	3.83	0.05	-5.7	0.13				
AB48	1	CORS	56.245	-134.647	8.58	0.08	0.66	0.06	-0.66	0.2		-0.02	0.15	0.05
AB48	2	CORS	56.245	-134.647	-1.69	0.3	-2.17	0.19	2.78	0.79	PS	-10.29	-2.68	3.50
AB48	3	CORS	56.245	-134.647	-1.64	0.19	-2.14	0.12	3.01	0.5	PS	-10.24	-2.65	3.72
AB50	1	CORS	58.417	-134.545	3.73	0.08	1.74	0.05	15.49	0.19		0.05	-0.12	-0.83
AB51	1	CORS	56.798	-132.914	3.46	0.07	-0.73	0.05	8.88	0.16		-0.04	-0.22	0.39
AC09	2	CORS	59.869	-144.524	39.13	0.29	-21.6	0.19	1.64	0.77				
AC09	3	CORS	59.869	-144.524	27.51	0.46	-13.72	0.31	4.25	1.3	PS			
AC11	2	CORS	61.807	-148.332	13.33	0.11	-9.66	0.07	6.53	0.26				
AC14	1	CORS	60.849	-148.000	37.44	0.07	-14.77	0.05	0.93	0.13				
AC15	4	CORS	60.481	-149.724	17.26	0.13	-6.98	0.09	8.16	0.37				
AC16	1	CORS	60.518	-148.093	42.97	0.07	-16.06	0.05	-1.01	0.17				
AC20	4	CORS	60.929	-149.353	14.6	0.14	-8.51	0.09	8.81	0.4				
AC30	1	CORS	59.856	-147.739	71.97	7.78	-31.38	5.19	-7.7	20.98				
AC43	1	CORS	59.521	-149.629	36.31	0.07	-9.6	0.05	1.99	0.11				
AC44	2	CORS	61.242	-149.567	12.69	0.1	-6.15	0.07	1.1	0.25				
AC48	1	CORS	60.646	-147.343	41.69	0.06	-16.87	0.05	-1.62	0.11				
AC53	3	CORS	61.769	-150.069	3.77	0.12	-6.33	0.09	4.35	0.34				
AC57	1	CORS	61.139	-145.743	28.89	0.06	-12.58	0.05	7.51	0.11				
AC62	3	CORS	63.084	-146.313	7.41	0.1	-10.28	0.07	3.14	0.27				
AC63	4	CORS	63.502	-145.847	1.77	0.11	3.07	0.08	6.21	0.3				
AC64	4	CORS	62.714	-144.304	15.71	0.16	-9.15	0.1	3.38	0.59				
AC65	3	CORS	62.832	-143.704	13.68	0.14	-7.12	0.11	-0.52	0.51				
AC70	1	CORS	63.305	-148.188	2.2	0.06	-7.14	0.05	1.42	0.11				
AC72	1	CORS	63.695	-145.888	-0.66	0.07	5.87	0.05	2.86	0.14				
AC74	1	CORS	63.464	-148.807	1.66	0.06	-3.4	0.05	0.9	0.12				
AC75	1	CORS	62.999	-149.609	0.3	0.06	-5.15	0.05	2.54	0.11				
AC76	1	CORS	63.040	-143.259	3.91	0.06	7.82	0.05	2.27	0.12				
AC77	1	CORS	62.688	-145.426	11.52	0.06	-10.93	0.05	4.67	0.13				
ACHT	1	ACS	45.513	-61.027	-1.32	0.15	1.79	0.11	-1.24	0.43		0.05	0.00	0.32
ACTO	1	CAMP	45.711	-72.575	-1.11	0.32	1.65	0.25	2.25	1.06		0.75	0.02	0.07
ADLK	1	CAMP	60.717	-138.358	8.96	0.97	1.12	0.64	10.93	2.9		-0.73	-1.39	-0.64
ADRI	1	CORS	41.919	-84.024	-0.65	0.05	1.66	0.03	-2.68	0.1		0.04	-0.22	-0.20
ADVT	1	ACS	45.341	-64.788	-1.46	0.27	1.54	0.2	-0.76	0.8		0.08	-0.04	0.16
AIS1	1	CORS	55.069	-131.600	5.42	0.07	2.44	0.05	-1.19	0.16	DC	-0.02	0.36	-0.04
AIS5	1	CORS	55.069	-131.600	3.87	0.18	1.79	0.12	-2.15	0.5	DC	-1.56	-0.29	-1.00
AISH	1	CAMP	61.194	-136.999	3.82	2.83	-3.65	1.93	-2.67	8.67	NED	-0.43	-8.55	-4.58
ALBH	1	ACS	48.390	-123.488	5.32	0.05	8.1	0.04	-0.92	0.08		-0.06	-0.42	0.04
ALEC	1	CORS	44.332	-75.935	-1.96	0.56	2.06	0.46	-2.11	2.11	NNC	-0.01	0.20	-3.28
ALEX	1	CORS	44.323	-75.957	-0.98	0.46	1.55	0.4	-4.76	1.76	NNC	0.95	-0.30	-5.91
ALGO	1	ACS	45.956	-78.071	-2.36	0.05	1.57	0.04	2.15	0.12		-0.04	-0.04	0.02
ALIF	1	CAMP	53.186	-131.995	10.86	0.79	3.57	0.55	1.2	2.58	NED	0.28	2.59	2.47
ALRT	1	ACS	82.494	-62.340	-4.74	0.06	0.41	0.06	3.49	0.21	DC	-2.45	0.13	-0.07
ALRT	2	ACS	82.494	-62.340	-0.17	0.09	-0.82	0.08	5.61	0.48	DC	2.12	-1.10	2.05
ALSC	1	CORS	59.186	-138.318	33.35	0.17	-13.88	0.11	23.89	0.46		2.62	-0.83	0.76
AMHT	1	ACS	45.832	-64.188	-1.12	0.26	1.98	0.2	-1	0.75		0.18	0.16	-0.13
ANDR	1	CAMP	47.652	-69.733	-2.66	0.21	2.74	0.16	1.1	0.65		-0.21	0.54	-0.63

Site	Solution	Type	Latitude	Longitude	Velocities (mm/yr) and Uncertainties (1σ , mm/yr)						Outlier rationale	Residuals (mm/yr)		
					v_{North}	σ_{North}	v_{East}	σ_{East}	v_{Up}	σ_{Up}		$\text{res}_{\text{North}}$	res_{East}	res_{Up}
ANDS	1	CORS	41.596	-87.132	-0.18	0.05	1.98	0.04	-2.84	0.13		-0.01	-0.01	0.19
ANNE	1	ACS	49.128	-66.495	-2.61	0.06	2.35	0.04	1.55	0.15		-0.02	0.05	-0.01
ANTG	1	ACS	45.617	-62.011	-1.58	0.24	0.49	0.18	-1.18	0.68		-0.13	-0.27	0.31
ASBL	1	CBN	49.633	-106.027	-0.96	0.16	3.19	0.11	-2.06	0.48		-0.06	0.04	0.41
ASCS	1	CORS	42.255	-77.797	-1.4	0.1	1.71	0.08	-2.13	0.31		0.02	0.01	-0.37
ASKY	1	CORS	75.726	-58.257	-1.74	0.05	-0.13	0.05	14.7	0.16		0.03	-0.02	0.30
ATLI	1	ACS	59.590	-133.714	5.07	0.09	4.68	0.06	7.48	0.23		0.26	0.08	0.04
ATRI	1	ACS	46.848	-71.262	-2.41	0.05	1.71	0.04	2.16	0.13		-0.57	0.01	-0.01
ATW2	4	CORS	61.598	-149.132	12.35	0.11	-10.92	0.08	1.24	0.29				
AUBN	1	CORS	41.366	-85.054	-0.4	0.06	1.81	0.04	-2.1	0.14		0.16	0.05	0.35
AVCA	1	CORS	43.061	-82.688	-1.08	0.04	1.75	0.03	-2.18	0.08		-0.31	0.21	0.02
BAIE	1	ACS	49.187	-68.263	-2.41	0.04	2.42	0.03	3.16	0.07		0.09	0.02	0.06
BAKE	1	ACS	64.318	-96.002	-0.99	0.04	3.24	0.03	10.99	0.07		0.01	0.01	0.07
BAMF	1	ACS	48.835	-125.135	7.52	0.06	11.4	0.05	0.62	0.15		-0.01	-0.09	-0.19
BARH	1	CORS	44.395	-68.222	-1.54	0.05	2	0.03	-0.17	0.07		0.10	0.02	-0.09
BARI	1	CAMP	52.576	-131.753	8.29	0.48	-0.68	0.33	-6.26	1.27	PS	-1.28	-1.74	-4.98
BARN	1	CORS	44.099	-71.160	-2.6	0.06	2.19	0.04	0.03	0.13		-0.07	0.17	-0.21
BARR	1	ACS	43.580	-65.615	-1.4	0.18	1.95	0.14	-1.1	0.53		0.21	0.14	0.06
BASS	1	ACS	45.415	-63.781	-2.26	0.27	1.62	0.2	-1.72	0.79		-0.42	-0.05	-0.55
BATH	1	ACS	47.649	-65.693	-3.14	0.1	2.18	0.07	0.02	0.28		-0.46	0.36	0.46
BAYR	1	CORS	43.446	-83.892	-1.09	0.05	1.76	0.03	-2.17	0.09		-0.04	0.02	0.09
BCCG	1	ACS	49.312	-117.653	0.93	0.07	3.41	0.05	-0.12	0.15		0.01	-0.05	0.09
BCDI	1	ACS	52.158	-128.110	1.03	0.06	0.5	0.04	0.05	0.11		-0.36	-0.13	-0.27
BCDL	1	ACS	58.426	-130.026	1.8	0.06	2.02	0.04	0.27	0.1		-0.04	-0.24	-0.03
BCES	1	ACS	48.429	-123.429	5.46	0.07	8.67	0.04	-1.91	0.13		0.19	0.29	-0.76
BCFJ	1	ACS	56.246	-120.749	-0.43	0.05	2.24	0.04	0.99	0.08		-0.06	0.01	-0.01
BCFN	2	ACS	58.840	-122.585	-0.26	0.11	2.2	0.08	1.49	0.29		-0.03	-0.09	0.17
BCFT	1	CBN	45.044	-77.889	-2.17	0.14	1.84	0.12	1.64	0.52		-0.03	0.00	0.28
BCIN	1	ACS	50.509	-116.029	0.13	0.06	4.16	0.04	-0.38	0.14		0.01	0.02	-0.08
BCLC	1	ACS	49.104	-122.657	3.48	0.07	5.46	0.05	-2.29	0.14	EP?	-0.33	-0.62	-0.78
BCLI	1	ACS	49.115	-123.147	3.69	0.06	7.24	0.04	-3.74	0.11	EP?	-0.83	0.63	-2.58
BCMR	1	ACS	49.221	-122.539	3.16	0.05	5.95	0.04	-1.85	0.09		-0.14	0.06	-0.30
BCNS	3	ACS	48.649	-123.451	5	0.13	7.34	0.09	-1.19	0.33	DC	-0.18	0.21	1.01
BCOM	1	CBN	49.265	-68.157	-2.66	0.12	2.4	0.09	2.99	0.36		-0.09	0.00	-0.11
BCOV	1	ACS	50.544	-126.843	5.01	0.06	3.88	0.04	0.48	0.13		0.44	-0.18	-0.64
BCPG	1	ACS	53.908	-122.796	0.68	0.06	1.35	0.04	0.63	0.12	EP?	-0.02	-0.59	-1.25
BCPH	2	ACS	50.686	-127.375	2.6	0.1	3.7	0.07	2.14	0.25		-0.51	0.09	0.63
BCPR	1	ACS	54.277	-130.435	4.76	0.08	1.71	0.05	-1.09	0.17		-0.09	-0.02	-0.10
BCRK	1	ACS	62.414	-140.860	3.81	0.08	4.12	0.05	-0.16	0.19		-0.42	-0.68	0.32
BCSF	1	ACS	49.192	-122.860	4.28	0.05	6.62	0.04	-1.35	0.09		0.19	0.35	0.04
BCSL	1	ACS	49.565	-119.644	1.69	0.1	3.86	0.07	-1.18	0.25		0.04	0.07	-0.48
BCSM	1	ACS	48.560	-123.800	4.89	0.1	9.17	0.07	-0.23	0.25		-0.29	0.18	0.01
BCSS	1	ACS	53.254	-131.807	10.42	0.17	0.56	0.12	-1.24	0.48		0.10	-0.32	-0.05
BCSS	2	ACS	53.254	-131.807	-14.15	0.37	-12.37	0.26	-7.89	0.87	PS	-24.47	-13.25	-6.70
BCSS	3	ACS	53.254	-131.807	0.1	0.23	-4.4	0.17	-5.15	0.59	PS	-10.22	-5.27	-3.96
BCTE	1	ACS	54.515	-128.627	3.32	0.06	2.73	0.04	0.58	0.13		0.08	0.11	0.00
BCVC	1	ACS	49.276	-123.089	4.33	0.07	6.13	0.04	-1.31	0.13		0.01	-0.19	-0.25
BCWA	1	ACS	52.187	-122.064	0.38	0.11	2.52	0.08	0.76	0.29	NNC	-1.04	0.00	0.11
BDCK	1	ACS	46.114	-60.775	-1.93	0.07	1.59	0.05	-1.77	0.19		-0.02	-0.06	0.20
BEA2	1	ACS	62.408	-140.863	4	0.08	5.87	0.05	-1.02	0.18		-0.28	1.08	-0.56
BECA	1	CAMP	46.303	-72.276	-2.76	0.26	2.46	0.2	4.03	0.86		-0.23	0.14	1.50
BEL3	1	CBN	44.228	-77.188	-1.81	0.13	1.88	0.1	0.44	0.42		-0.01	0.02	-0.18
BEUT	1	CAMP	59.582	-136.465	9.04	0.4	5.23	0.28	21.65	1.24		0.30	0.53	-1.82
BFNY	1	CBN	42.878	-78.890	-1.26	0.05	1.58	0.04	-1.13	0.13	DC	0.18	-0.18	0.16
BGOH	1	CORS	41.380	-83.643	-0.47	0.06	1.54	0.04	-1.46	0.14		0.16	-0.24	0.48
BIGR	1	CORS	43.679	-85.488	-0.74	0.05	1.4	0.03	-1.43	0.11		0.00	-0.11	0.17
BIS1	1	CORS	56.855	-135.539	10.63	0.12	-1.24	0.08	-0.63	0.32	DC	0.10	0.67	-0.29
BISS	1	CORS	56.855	-135.539	10.47	0.11	-2.33	0.07	-1.46	0.26	DC	-0.06	-0.43	-1.11
BKSD	1	ACS	44.562	-63.732	-1.89	0.23	0.71	0.17	-0.98	0.66	NNC	-0.05	-0.97	0.54
BLCL	1	ACS	52.388	-126.589	2.57	0.11	1.31	0.07	3.6	0.3		0.16	0.00	0.54
BLFD	1	CBN	46.751	-64.191	-1.92	0.12	1.29	0.09	-1.44	0.34		-0.03	-0.05	-0.17
BLOM	1	CORS	40.496	-89.000	-0.26	0.06	1.56	0.05	-2.14	0.17				
BLRW	1	CORS	43.230	-90.531	-0.51	0.06	2.16	0.04	-3.11	0.17		-0.04	0.01	0.27

					Velocities (mm/yr) and Uncertainties (1σ , mm/yr)						Outlier rationale	Residuals (mm/yr)		
Site	Solution	Type	Latitude	Longitude	v_{North}	σ_{North}	v_{East}	σ_{East}	v_{Up}	σ_{Up}		$\text{res}_{\text{North}}$	res_{East}	res_{Up}
BMCP	1	CORS	58.783	-136.480	5.96	0.08	0.97	0.05	27.15	0.2		-0.50	0.08	-0.17
BMTN	1	CBN	51.014	-93.766	-1.66	0.1	2.02	0.07	1.22	0.3		0.00	0.00	-0.10
BNAB	1	ACS	53.493	-130.637	-0.89	0.22	-2.02	0.16	-0.38	0.62	NED	-7.77	-3.24	0.38
BNKB	1	ACS	53.332	-129.901	0.71	0.19	-0.4	0.13	-0.37	0.49	NED	-4.63	-1.65	-0.06
BNYV	1	CBN	54.563	-110.976	-0.59	0.19	3.28	0.13	0.27	0.53		0.03	0.02	-0.14
BOIB	1	CAMP	45.599	-73.862	-3.25	0.14	1.92	0.11	1.3	0.46		-0.94	-0.03	-0.53
BRCH	1	CORS	43.251	-83.867	-0.84	0.05	1.98	0.03	-2.46	0.08		0.24	0.11	-0.04
BRDN	1	CBN	49.886	-99.911	-1	0.1	2.46	0.07	-1.85	0.31		0.00	0.04	-0.01
BREW	1	CORS	48.132	-119.683	1.91	0.05	3.67	0.03	-2.06	0.07		0.02	0.03	-0.03
BRIG	1	CORS	42.520	-83.757	-0.69	0.05	1.97	0.03	-2.41	0.1		0.02	0.03	0.01
BRKS	1	CBN	50.665	-112.117	-0.61	0.17	3.26	0.12	-1.95	0.5		-0.04	-0.02	-0.39
BRU1	1	CORS	43.890	-69.947	-2.28	0.07	1.54	0.05	-0.63	0.17		0.00	0.00	-0.30
BRW1	1	CORS	71.283	-156.790	-0.11	0.07	3.41	0.05	-3	0.16				
BSHW	1	CBN	52.692	-113.245	-0.75	0.18	3.3	0.12	-0.69	0.51		-0.04	0.00	-0.13
BSLR	1	CBN	45.399	-75.922	-2.17	0.1	1.95	0.07	2.62	0.31		-0.08	0.06	0.56
BSMK	1	CORS	46.821	-100.817	0.04	0.05	2.34	0.04	-4.03	0.13		0.02	-0.01	0.00
BTHT	1	CBN	47.622	-65.784	-2.57	0.11	1.67	0.08	-0.54	0.33		0.04	-0.09	-0.06
BUFF	1	CORS	42.877	-78.890	-1.81	0.13	1.55	0.1	-1.41	0.4	DC	-0.36	-0.21	-0.12
BUTB	1	ACS	53.063	-128.464	0.56	0.23	0.35	0.16	1.32	0.62	NED	-2.34	-0.74	0.57
C293	1	CORS	46.501	-84.343	-1.58	0.77	1.58	0.61	2.82	2.76	NED	0.24	-0.06	2.36
CACU	1	CBN	47.905	-69.477	-2.59	0.1	1.97	0.07	2.13	0.3		-0.24	-0.07	0.20
CAGS	1	ACS	45.585	-75.807	-2.25	0.05	2.05	0.03	2.14	0.09		-0.21	0.00	-0.02
CAL4	1	CBN	51.096	-114.373	-0.31	0.14	3.38	0.1	-0.54	0.41		-0.04	0.00	-0.10
CALU	1	CORS	41.730	-87.538	-0.35	0.05	2.03	0.03	-3.43	0.09	DC	-0.03	0.08	-0.17
CAMB	1	ACS	45.059	-64.631	-1.94	0.1	1.67	0.07	-0.96	0.27		-0.12	0.03	0.03
CANY	1	CAMP	60.859	-137.063	5.41	0.26	4.36	0.17	3.82	0.8		-0.13	-0.26	-1.56
CAPL	1	ACS	48.094	-65.653	-1.96	0.05	1.05	0.04	0.01	0.12		0.18	-0.26	0.02
CARI	1	CAMP	62.424	-131.428	-0.03	1.2	4.85	0.73	-0.97	3.67		-0.05	0.46	-1.43
CASV	1	CORS	43.602	-83.161	-1.14	0.06	1.74	0.04	-1.87	0.13		-0.06	-0.11	0.17
CBRG	1	ACS	43.957	-78.164	-1.02	0.1	1.05	0.07	0.11	0.3	DC	0.27	-0.36	0.04
CBRK	1	CBN	48.944	-57.950	-1.78	0.2	1.44	0.14	-0.62	0.6		-0.02	0.02	-0.01
CCMI	1	CBN	48.480	-71.199	-2.43	0.12	2.45	0.08	3.92	0.37		0.03	0.05	-0.45
CCMK	1	CORS	41.590	-87.693	0.08	0.08	2.22	0.06	-2.3	0.22		0.28	0.27	0.45
CCRM	1	CORS	42.088	-88.007	-0.02	0.1	1.83	0.08	-2.8	0.28		0.18	-0.02	-0.09
CCSK	1	CORS	42.064	-87.767	0.02	0.1	2.14	0.08	-2.95	0.3		0.24	0.17	-0.02
CDOR	1	ACS	64.229	-76.529	-6.38	0.81	2.17	0.56	4.03	2.49	NED	-4.90	-0.47	-3.92
CENA	1	CORS	65.498	-144.678	-1.93	0.06	4.01	0.05	-1.5	0.12				
CHAR	1	CAMP	46.707	-71.256	-2.7	0.24	2.03	0.19	1.3	0.82		-0.94	0.58	-0.66
CHB1	1	CORS	45.654	-84.466	-2.23	0.06	2.1	0.04	-0.32	0.16	NED	-0.54	0.26	0.78
CHB2	1	CORS	45.654	-84.466	-3.67	0.13	0.33	0.1	-1.44	0.41	NED	-1.98	-1.51	-0.34
CHB5	2	CORS	45.654	-84.466	1.03	0.1	2.21	0.08	-4.88	0.3	NED	2.72	0.37	-3.78
CHB6	2	CORS	45.654	-84.466	-3.03	0.19	1.38	0.14	-3.57	0.58	NED	-1.34	-0.46	-2.47
CHCM	1	CORS	48.011	-122.776	4.75	0.08	7.4	0.06	-1.21	0.21		-0.02	0.00	0.12
CHEN	1	CAMP	47.200	-70.730	-2	0.29	2.27	0.23	1.61	1		0.14	0.15	-0.53
CHET	1	ACS	46.625	-61.014	-1.81	0.16	2.16	0.12	-0.83	0.45		-0.15	0.25	0.69
CHI3	1	CORS	60.238	-146.647	29.97	0.15	-10.7	0.1	-0.98	0.41	DC			
CHI5	1	CORS	60.238	-146.647	31.06	0.12	-13.02	0.08	-0.71	0.31	DC			
CHIB	1	ACS	49.913	-74.367	-2.53	0.04	2.22	0.03	8.64	0.07		-0.08	0.02	-0.03
CHIC	1	ACS	48.414	-71.255	-2.56	0.05	2.22	0.04	4.57	0.13		-0.07	-0.17	0.20
CHRI	1	CAMP	46.994	-71.024	-2.1	0.25	2.11	0.2	1.91	0.87		0.07	0.03	-0.23
CHSN	1	CORS	43.190	-84.123	-1.82	0.05	2.08	0.03	-2.61	0.1		-0.53	0.24	-0.11
CHSR	1	ACS	44.600	-64.321	-1.73	0.15	1.64	0.11	-0.76	0.43		0.05	-0.02	0.31
CHTG	1	CAMP	45.342	-73.696	-2.07	0.17	1.18	0.13	1.68	0.54		0.17	-0.54	-0.20
CHUR	1	ACS	58.759	-94.089	-1.52	0.05	2.74	0.04	9.25	0.13		0.00	0.00	0.04
CHWK	1	ACS	49.157	-122.008	2.93	0.05	4.78	0.04	-0.43	0.1		0.01	-0.12	0.23
CLDA	1	ACS	44.373	-65.033	-0.63	0.19	2.46	0.14	-1.2	0.55	EP?	1.17	0.85	-0.35
CLEV	1	CORS	41.540	-81.634	-0.7	0.32	1.36	0.24	-2.51	1.08		0.27	-0.53	0.54
CLGO	2	CORS	64.874	-147.861	-2.3	0.06	3.58	0.05	-1.15	0.1				
CLK1	1	CORS	44.936	-97.961	-2.24	0.07	3.32	0.04	-0.5	0.17	EP?	-2.17	0.63	2.35
CLRE	1	CORS	42.724	-82.596	-0.94	0.06	1.75	0.04	-1.98	0.14		0.21	0.08	0.15
CLRS	1	ACS	48.820	-124.131	5.52	0.06	8.5	0.04	0.31	0.12		0.02	-0.25	-0.11
CMBR	1	CBN	50.053	-125.326	5.51	0.31	6.21	0.23	2.78	1.01		0.31	0.05	-0.33
CMOU	1	CBN	49.913	-74.390	-2.31	0.12	2.18	0.08	8.79	0.36		0.12	-0.01	0.11

			Velocities (mm/yr) and Uncertainties (1σ , mm/yr)						Outlier rationale	Residuals (mm/yr)				
Site	Solution	Type	Latitude	Longitude	v_{North}	σ_{North}	v_{East}	σ_{East}	v_{Up}	σ_{Up}	$\text{res}_{\text{North}}$	res_{East}	res_{Up}	
CNDA	1	CBN	48.382	-64.561	-2.19	0.12	1.88	0.08	-0.35	0.34		-0.05	0.05	0.03
CNMC	1	CBN	45.408	-73.354	-2.34	0.09	1.84	0.07	2.35	0.26		-0.01	-0.01	0.25
CNSO	1	ACS	45.332	-61.029	-1.52	0.25	2.07	0.18	-1.04	0.71		-0.11	0.16	0.58
CNT2	1	CBN	43.543	-80.518	-1.49	0.16	1.61	0.12	-0.94	0.51		0.00	-0.02	0.32
COLA	1	CAMP	61.901	-132.411	-0.76	0.94	3.66	0.58	1	2.85	NED	-1.51	-0.74	2.13
COU2	1	CAMP	47.399	-70.414	-2.33	0.27	1.65	0.2	2.84	0.86		-0.10	-0.25	0.68
CP32	1	CBN	50.833	-113.919	-0.21	0.17	3.34	0.12	-0.99	0.5		0.02	-0.01	-0.21
CPAC	1	CORS	43.011	-82.934	-0.7	0.05	1.5	0.03	-2.61	0.1		0.07	-0.01	-0.16
CRLV	1	ACS	47.550	-70.327	-1.45	0.6	1.91	0.43	2.61	1.85		0.70	-0.04	0.36
CRNB	1	CBN	49.600	-115.670	0.17	0.35	3.61	0.24	-0.06	1.22		-0.01	0.00	0.57
CVAR	1	CBN	46.377	-62.136	-0.17	0.13	1.25	0.09	-2.09	0.39		0.38	-0.01	-0.38
DAUP	1	CBN	51.081	-99.997	-1.2	0.1	2.28	0.07	-1.06	0.3		0.00	-0.02	-0.14
DAWS	1	CAMP	64.052	-139.435	1.75	1.13	7.43	0.73	-1.51	3.44		0.50	-1.12	1.50
DEFI	1	CORS	41.277	-84.414	0.05	0.05	1.87	0.03	-2.99	0.09		0.20	0.08	-0.12
DEST	1	CAMP	61.217	-138.722	6.15	0.62	5.32	0.42	5.18	2.01		-0.74	0.83	-0.73
DET1	1	CBN	42.297	-83.095	-1.4	0.12	2.24	0.09	-0.45	0.37	NNC	-0.63	0.55	2.21
DET2	1	CORS	42.297	-83.096	-1.38	0.11	2.23	0.08	-1.6	0.34		-0.61	0.54	1.06
DET5	1	CORS	42.297	-83.095	-0.92	0.05	1.73	0.04	-2.93	0.12		-0.15	0.04	-0.26
DET6	1	CORS	42.297	-83.096	-0.94	0.06	1.78	0.04	-3.14	0.15		-0.16	0.10	-0.48
DETO	1	CORS	45.999	-83.901	-1.6	0.25	1.72	0.18	0.72	0.78		-0.02	-0.02	0.78
DEZA	1	CAMP	60.376	-137.054	7.66	0.28	4.29	0.19	14.21	0.87		-0.23	0.05	1.47
DFOE	1	CBN	51.750	-104.510	-1.18	0.11	2.65	0.08	-1.9	0.33		0.00	0.00	-0.07
DGBY	1	ACS	44.621	-65.760	-2.17	0.1	1.73	0.07	-0.17	0.27		-0.10	-0.02	0.38
DKSG	1	CORS	76.352	-61.678	-1.73	0.05	0.83	0.05	14.12	0.15		0.05	0.06	0.56
DONJ	1	CAMP	61.078	-139.402	10.56	0.83	1.81	0.57	10.21	2.54		0.13	-0.17	1.22
DP1A	1	CORS	41.867	-88.143	-0.25	0.05	2.12	0.04	-2.68	0.13		-0.05	0.35	-0.14
DP2A	1	CORS	41.900	-87.965	-0.18	0.05	1.89	0.04	-3.06	0.13		0.08	0.05	-0.42
DP3A	1	CORS	41.765	-88.177	0.06	0.08	1.87	0.07	-2.49	0.26		0.12	0.00	0.32
DP4A	1	CORS	41.714	-87.932	-0.19	0.17	1.64	0.14	-2.38	0.57		0.04	-0.32	0.42
DPSA	1	CORS	41.990	-88.157	-0.33	0.07	1.43	0.06	-1.22	0.2		-0.09	-0.23	1.12
DRAO	1	ACS	49.323	-119.625	1.55	0.05	3.68	0.03	-0.66	0.07		-0.06	-0.05	0.12
DRNG	1	ACS	64.864	-111.581	-0.69	0.2	1.76	0.14	7.57	0.59		0.00	-0.07	0.46
DSLK	1	CBN	58.437	-130.029	2.17	0.27	2.91	0.18	0.78	0.78		0.33	0.63	0.51
DSPT	1	CAMP	60.489	-138.605	10.06	1	1.95	0.69	25.01	3.07	NED	-2.84	1.59	10.11
DUBO	1	ACS	50.259	-95.866	-1.4	0.04	2.07	0.02	-0.52	0.06		0.00	-0.01	-0.07
DULU	1	CORS	46.775	-92.094	-2.51	0.21	0.42	0.15	-2.49	0.66	EP?	-1.30	-1.78	0.20
EAGL	1	CAMP	65.772	-137.846	1.18	0.52	5.53	0.34	-2.52	1.63		0.15	0.07	0.92
EDMD	1	CBN	47.401	-68.364	-2.14	0.12	1.98	0.09	0.31	0.37		-0.09	-0.01	-0.18
EDMN	1	CBN	53.571	-113.174	-0.67	0.18	3.19	0.12	0.28	0.51		-0.04	0.01	0.16
EDOC	1	CORS	70.310	-148.318	1.27	0.06	2	0.05	-8.06	0.14				
EDON	1	ACS	47.363	-68.326	-1.98	0.07	1.31	0.05	1.09	0.17	NNC	0.07	-0.67	0.64
EGMT	1	CBN	54.036	-113.155	-0.32	0.19	3.14	0.13	0.2	0.54		0.05	-0.01	-0.22
EIL3	1	CORS	64.688	-147.113	-2.38	0.38	4.32	0.26	-0.8	1.13				
ELDC	2	CORS	58.972	-135.222	3.18	0.2	4.03	0.14	27.97	0.57		-0.20	0.09	3.49
ELGI	1	CAMP	47.251	-70.154	-2.59	0.24	1.72	0.18	1.16	0.74		-0.17	-0.23	-0.63
ELIZ	1	ACS	49.873	-127.123	5.78	0.06	8.59	0.04	0.25	0.1		-0.02	-0.05	-0.44
ENNA	1	ACS	60.767	-101.696	-1.52	0.15	3.32	0.1	7.44	0.39		-0.01	0.01	-0.51
EPRT	1	CORS	44.909	-66.992	-1.96	0.05	1.93	0.04	-1	0.11		0.09	0.00	-0.25
ERIE	1	CORS	42.153	-80.079	-0.96	0.25	1.89	0.19	-2.26	0.86		0.00	0.06	-0.12
ESCO	1	CAMP	47.467	-69.232	-1.38	0.21	1.46	0.17	0.82	0.68		0.23	-0.25	-0.25
ESCU	1	ACS	47.073	-64.799	-1.84	0.05	1.86	0.04	-1.14	0.11		0.06	0.08	0.08
ESSE	1	CORS	43.629	-83.838	-1.67	0.14	2.17	0.11	-2.23	0.48		-0.44	0.29	-0.10
ESTM	1	CBN	52.111	-77.200	-2.05	0.17	2.3	0.12	11.01	0.5		-0.01	0.03	-0.37
EUR2	1	ACS	79.989	-85.938	-2.38	0.05	0.76	0.05	6.39	0.14		0.00	-0.01	0.00
EURK	1	ACS	79.989	-85.940	-4.11	0.2	1.16	0.16	1.08	1.05	NED	-1.73	0.39	-5.31
EYAC	1	CORS	60.549	-145.750	29.35	0.07	-10.42	0.06	0.93	0.16				
FAI1	2	CORS	64.810	-147.847	-1.98	0.08	3.5	0.06	-1.56	0.17				
FAIR	2	CORS	64.978	-147.499	-2.19	0.06	3.88	0.05	-0.85	0.1				
FALL	1	ACS	44.817	-63.617	-1.59	0.24	3.24	0.18	-1.05	0.69	NED	0.25	1.52	0.55
FARD	1	CBN	51.624	-98.736	-1.29	0.1	2.3	0.07	-0.18	0.3		0.01	0.00	-0.23
FERM	1	CORS	41.959	-83.261	-1.16	0.22	2.11	0.17	-4	0.75		-0.20	0.19	-1.24
FLAT	1	CAMP	63.959	-138.694	1.52	0.93	13.34	0.6	-2.59	3.41		0.28	3.08	0.33
FLIN	1	ACS	54.726	-101.978	-1.46	0.05	2.28	0.03	1.55	0.08		0.00	-0.01	-0.04

			Velocities (mm/yr) and Uncertainties (1σ , mm/yr)						Outlier rationale	Residuals (mm/yr)				
Site	Solution	Type	Latitude	Longitude	v_{North}	σ_{North}	v_{East}	σ_{East}	v_{Up}	σ_{Up}	$\text{res}_{\text{North}}$	res_{East}	res_{Up}	
FLM2	1	CBN	45.506	-63.541	-1.24	0.32	1.47	0.24	-1.07	1.01		0.20	-0.14	0.16
FLMT	1	CBN	45.506	-63.541	-1.7	0.29	1.79	0.22	0.24	0.96	NNC	-0.26	0.18	1.47
FNEL	1	CBN	58.842	-122.578	-0.03	0.25	2.49	0.17	1.35	0.71		0.20	0.20	0.03
FRDN	1	ACS	45.934	-66.660	-2.11	0.06	1.68	0.04	-0.44	0.12	DC	-0.24	-0.08	0.20
FRDT	1	CBN	45.933	-66.660	-1.98	0.11	2.01	0.08	-0.53	0.3	DC	-0.11	0.25	0.10
FREO	1	CORS	40.202	-81.258	-0.44	0.05	1.74	0.03	-2.54	0.11				
FRTG	1	CORS	43.038	-82.488	-0.94	0.05	1.57	0.04	-1.92	0.13		-0.23	0.13	0.10
FRTG	2	CORS	43.038	-82.488	-0.68	0.12	1.54	0.1	0.06	0.4	NED	0.03	0.10	2.08
FSRH	1	CBN	49.138	-122.288	3.17	0.37	5.27	0.26	-1.83	1.13		0.02	-0.12	-0.63
FTGR	1	CORS	43.006	-82.422	-1.45	0.47	1.38	0.38	0.1	1.73	NNC	-0.75	-0.04	2.11
FTRS	1	CBN	50.829	-115.200	-0.46	0.19	3.73	0.14	-0.09	0.59		-0.10	0.02	0.15
FTSJ	1	CBN	56.247	-120.730	0.23	0.2	2.09	0.14	1.59	0.57		0.58	-0.13	0.58
FTVM	1	CBN	58.515	-116.151	-0.67	0.18	3.37	0.12	2.71	0.51		0.00	0.02	-0.03
FTWA	1	CORS	42.297	-83.094	-2.22	0.33	1.73	0.27	0.09	1.14	NNC	-1.44	0.04	2.76
FXCR	1	CBN	54.383	-116.775	-0.2	0.18	3.03	0.12	1.04	0.52		-0.03	0.01	0.35
GANG	1	CBN	44.346	-76.171	-1.93	0.16	2.06	0.12	1.12	0.53		0.01	0.13	0.01
GARF	1	CORS	41.416	-81.615	-1.2	0.04	2.21	0.03	-3.83	0.07		-0.17	0.25	-0.76
GAS2	1	ACS	48.803	-64.488	-1.95	0.13	1.77	0.09	0.34	0.36		0.02	-0.16	0.16
GASP	1	ACS	48.829	-64.487	-1.72	0.25	2.5	0.18	0.31	0.76		0.25	0.53	0.09
GATI	1	ACS	45.481	-75.689	-1.94	0.06	2.24	0.04	2.07	0.14		0.00	0.23	-0.06
GATZ	1	ACS	44.777	-63.205	-0.95	0.3	2.02	0.22	-1.89	0.87	NED	0.68	0.27	-0.22
GDLK	1	CBN	54.555	-94.484	-1.59	0.21	2.26	0.14	5.62	0.64		0.00	0.00	0.28
GDMA	1	CBN	47.749	-90.341	-1.56	0.04	1.55	0.03	-0.58	0.08		-0.02	-0.08	0.02
GDPR	1	CBN	55.187	-118.539	0.26	0.18	2.15	0.12	1.72	0.5		0.04	-0.06	0.63
GDRM	1	CBN	46.672	-75.987	-2.38	0.11	1.8	0.09	3.47	0.39		-0.05	-0.05	-0.24
GEOR	1	CAMP	46.130	-70.687	-2.5	0.07	1.4	0.05	0.38	0.19		-0.22	-0.29	-0.32
GFAL	1	CBN	48.929	-55.671	-1.36	0.22	1.02	0.17	-0.49	0.8		0.03	-0.02	-0.29
GIBR	1	CORS	42.095	-83.191	-0.57	0.6	0.62	0.53	-4.29	2.29		0.28	-1.18	-1.54
GLAB	1	CAMP	42.144	-83.114	-0.26	0.38	1.93	0.3	-1.94	1.35		0.54	0.19	0.84
GLBP	1	CAMP	42.061	-83.103	-0.93	0.22	1.68	0.18	-2.37	0.77		-0.05	-0.14	0.49
GLBR	1	CAMP	42.296	-82.711	-0.99	0.38	1.79	0.3	-2.9	1.33		0.07	-0.05	-0.21
GLBV	1	CAMP	44.587	-75.682	-3.76	0.27	3.27	0.23	1.76	1.04		-0.98	0.92	0.25
GLCO	1	CAMP	43.956	-78.164	-2.18	0.42	2.05	0.32	1.3	1.44	DC	-0.89	0.65	1.23
GLCR	1	CAMP	45.015	-74.712	-2.59	0.37	2.77	0.3	1.72	1.27		-0.24	0.48	-0.16
GLCW	1	CAMP	44.510	-80.220	-2.01	0.35	1.24	0.27	-2.17	1.17		-0.05	-0.08	-1.51
GLDN	1	CBN	51.301	-116.984	0.26	0.25	3.78	0.18	1.65	0.77		-0.01	-0.02	0.69
GLDR	1	ACS	49.682	-126.127	5.31	0.12	8.54	0.11	1.64	0.43		-0.29	-0.45	-0.65
GLER	1	CAMP	42.260	-81.915	-1.12	0.51	2.02	0.47	-2.34	1.97		-0.01	0.07	0.22
GLGC	1	CAMP	46.528	-84.582	-1.89	0.22	1.62	0.16	0.61	0.7		-0.05	-0.09	0.07
GLIL	1	CAMP	44.837	-75.310	-2.39	0.36	2.32	0.28	2.22	1.2		0.24	0.39	0.41
GLIU	1	CAMP	44.822	-75.321	-3.16	0.39	1.47	0.3	2.16	1.28		-0.51	-0.46	0.36
GLMC	1	CAMP	47.962	-84.903	-1.79	0.34	2.19	0.23	2.92	1.07		0.04	0.05	0.30
GLPC	1	CAMP	42.876	-79.250	-4.34	0.35	7.43	0.28	-5.83	1.18	US	-2.95	5.80	-4.35
GLPD	1	CAMP	42.782	-80.201	-0.98	0.37	1.63	0.29	-1.36	1.24		0.09	-0.04	0.41
GLPE	1	CAMP	42.991	-82.421	-0.36	0.37	0.55	0.29	-2.82	1.25		0.33	-0.86	-0.81
GPLL	1	CAMP	42.730	-82.477	-1.11	0.24	1.76	0.18	-2.09	0.83		-0.18	0.06	0.02
GLRM	1	CAMP	48.478	-68.511	-2.89	0.24	2.19	0.17	1.79	0.73		-0.42	-0.10	-0.37
GLSS	1	CAMP	46.513	-84.354	-2.07	0.37	1.17	0.29	0.22	1.23		-0.24	-0.48	-0.27
GLST	1	CAMP	45.060	-74.554	-1.89	0.36	1.95	0.28	1.25	1.22		0.22	-0.11	-0.65
GLTB	1	CAMP	48.407	-89.222	-2.11	0.23	1.73	0.17	-1.5	0.74	EP	-0.36	-0.16	-2.21
GLTH	1	CAMP	46.254	-83.553	-1.56	0.22	1.81	0.16	0.21	0.73		0.02	0.03	-0.24
GLTM	1	CAMP	45.224	-81.636	-1.78	0.22	1.91	0.16	-0.03	0.72		-0.01	0.02	-0.02
GLTO	1	CAMP	43.639	-79.377	-2.53	0.39	1.44	0.3	-2.26	1.49	US	-1.06	-0.30	-1.08
GNAA	3	CORS	62.112	-145.970	13.3	0.13	-6.08	0.09	0.19	0.39				
GNFD	1	CBN	53.599	-114.721	-0.17	0.18	3.25	0.12	0.25	0.51		0.03	-0.01	-0.06
GOAT	1	CAMP	60.277	-137.900	9.78	0.89	4.59	0.59	16.59	2.68		-1.27	1.92	-0.43
GOD2	1	ACS	43.745	-81.728	-1.87	0.13	-2.86	0.09	-15.59	0.39	LD	-0.46	-4.77	-14.08
GODR	1	ACS	43.745	-81.728	-2.06	0.29	-3.39	0.22	-15.58	0.93	LD	-0.65	-5.30	-14.07
GRAM	1	CORS	47.745	-90.335	-1.55	0.19	1.9	0.14	-0.11	0.6		-0.01	0.26	0.49
GRAP	1	CBN	53.272	-99.333	-1.33	0.11	2.33	0.08	1.58	0.33		0.01	0.00	0.03
GRAR	1	CORS	42.989	-85.674	-0.8	0.05	1.61	0.03	-2.45	0.09		-0.06	-0.09	0.11
GREN	1	CAMP	45.667	-74.658	-2.56	0.19	2.13	0.14	1.9	0.6		-0.13	0.00	-0.38
GRMS	1	CBN	56.364	-117.669	-0.1	0.17	3.04	0.12	1.63	0.49		0.01	0.05	0.23

					Velocities (mm/yr) and Uncertainties (1σ , mm/yr)						Outlier rationale	Residuals (mm/yr)		
Site	Solution	Type	Latitude	Longitude	v_{North}	σ_{North}	v_{East}	σ_{East}	v_{Up}	σ_{Up}		$\text{res}_{\text{North}}$	res_{East}	res_{Up}
GRNB	1	ACS	53.847	-129.958	0.59	0.17	0.45	0.12	0.64	0.46	NED	-4.39	-1.16	1.06
GRNX	1	CORS	63.836	-148.978	0.51	0.06	0.5	0.05	1.79	0.1		-0.17	-0.04	-0.26
GSBY	1	CBN	53.296	-60.538	-1.56	0.17	2.15	0.11	4.73	0.48				
GUS1	1	CORS	58.418	-135.697	3.52	0.16	2.39	0.11	20.23	0.46	DC	-1.28	1.28	0.49
GUS2	1	CORS	58.418	-135.697	3.8	0.07	2.24	0.05	19.31	0.17	DC	-0.99	1.13	-0.44
GUSS	1	CORS	58.418	-135.697	2.72	0.09	1.53	0.06	20.56	0.22	DC	-2.07	0.42	0.81
GUST	1	CORS	41.463	-80.716	-1.02	0.05	1.89	0.03	-2.49	0.1		0.00	-0.01	0.01
GUYS	1	ACS	45.387	-61.504	-0.89	0.24	1.26	0.18	-1.77	0.67		0.23	-0.06	-0.25
HAH2	1	CAMP	47.802	-70.743	-0.78	1.09	1.87	1.05	6.84	4.83	NED	1.43	-0.54	3.94
HAHA	1	CAMP	47.997	-70.778	-2.86	0.99	2.33	0.79	-0.58	3.55	NED	-0.57	-0.11	-3.82
HAHD	1	CORS	47.291	-121.788	4.42	0.11	5.18	0.08	-2.66	0.3		0.06	-0.05	0.11
HALI	1	ACS	44.657	-63.665	-2.05	0.23	1.73	0.17	-1	0.64		-0.21	0.05	0.58
HAMG	1	CORS	43.963	-112.167	-3.64	0.55	11.04	0.42	-14.33	1.85	NED	-5.02	7.70	-12.92
HARR	1	CORS	44.661	-83.286	-2.08	0.51	1.25	0.38	2.82	1.68	NNC	-0.62	-0.51	3.92
HAST	1	CORS	42.609	-85.265	-0.68	0.05	1.65	0.03	-2.67	0.12		-0.03	0.07	0.19
HBCH	1	CORS	43.846	-82.643	-1.04	0.05	2.23	0.03	-1.93	0.09		0.13	0.13	-0.10
HDBY	1	CBN	52.842	-102.384	-1.23	0.13	2.67	0.09	0.3	0.39		0.01	0.03	0.26
HEBB	1	ACS	44.321	-64.561	-1.69	0.1	1.74	0.07	-1.05	0.26		-0.02	0.07	0.03
HEM2	1	CAMP	45.098	-73.516	-3.1	0.39	2.38	0.32	2.93	1.36		-0.60	0.39	1.02
HERV	1	CAMP	46.869	-72.442	-2.14	0.37	1.64	0.28	3.88	1.24		0.12	-0.31	0.59
HJOR	1	CORS	63.418	-41.148	-2.13	0.07	0.31	0.05	4.5	0.17		-0.04	0.01	-0.18
HLAG	1	CBN	45.390	-74.703	-2.25	0.11	1.76	0.08	2.23	0.32		0.05	-0.21	0.07
HLFX	1	ACS	44.684	-63.611	-1.74	0.05	1.65	0.03	-1.79	0.08		0.07	-0.04	-0.16
HTLV	1	CBN	46.516	-66.483	-1.85	0.12	1.76	0.09	-0.3	0.35		0.00	0.01	0.31
HMLK	1	CORS	43.411	-84.237	-0.98	0.05	1.16	0.04	-2.47	0.13		0.10	-0.35	-0.01
HNTN	1	CBN	53.319	-117.720	0.02	0.17	3.27	0.12	0.56	0.49		-0.02	0.02	0.10
HOLB	1	ACS	50.640	-128.135	4.17	0.1	2.9	0.07	0.91	0.27		0.05	-0.30	0.18
HOLL	1	CORS	42.761	-86.195	-0.53	0.4	2.21	0.32	-2.51	1.33		0.14	0.25	0.68
HOLM	1	ACS	70.736	-117.761	-0.39	0.04	2.89	0.04	1.12	0.08		0.00	0.00	0.00
HRB2	1	CORS	43.844	-82.650	-1.34	0.19	1.94	0.15	-1.96	0.66		-0.17	-0.15	-0.12
HRB3	1	CORS	43.877	-82.675	-1.4	0.34	2.17	0.24	-1.09	1.17		-0.21	0.07	0.72
HRDG	1	CORS	81.880	-44.517	-2.68	0.06	0.07	0.05	5.62	0.2		-0.06	-0.01	-0.31
HRN1	1	CORS	40.878	-78.181	-1.55	0.17	2.97	0.13	-1.96	0.54	DC			
HRN2	1	CORS	40.878	-78.181	-1.78	0.13	2.14	0.1	-2.03	0.4	DC			
HRN5	1	CORS	40.878	-78.181	-0.8	0.51	1.5	0.4	-1.35	1.65	DC			
HRN6	1	CORS	40.878	-78.181	-1.27	0.06	1.99	0.05	-2.16	0.17	DC			
HRST	1	ACS	49.667	-83.511	-1.59	0.05	1.95	0.03	5.83	0.12		0.03	0.00	-0.01
HRUF	1	CORS	42.285	-83.340	-0.56	0.05	1.34	0.03	-2.2	0.11		0.12	-0.27	0.35
HSTP	1	ACS	50.243	-63.606	-2.64	0.05	1.79	0.03	2.52	0.1		-0.07	-0.10	0.04
HTSP	1	ACS	52.576	-131.444	-1.98	0.16	-1.44	0.11	-6.59	0.45	PS	-10.90	-2.50	-5.41
HUDS	1	CAMP	45.459	-74.122	-2.43	0.16	2.74	0.13	3.13	0.61		0.02	0.45	1.13
HULL	1	ACS	45.427	-75.711	-1.05	0.08	1.2	0.05	0.92	0.22		0.86	-0.74	-1.13
HVRP	1	CBN	50.303	-63.826	-2.42	0.13	2.18	0.09	2.65	0.37		0.12	0.09	-0.08
HWKB	1	ACS	53.599	-129.155	-0.05	0.26	-1.1	0.18	2.99	0.68	NED	-4.03	-2.64	2.72
IANA	1	CORS	43.497	-91.291	-0.08	0.09	1.82	0.07	-3.73	0.28		0.05	-0.03	-0.08
IGLO	1	CBN	69.376	-81.810	-2.04	0.52	2.03	0.37	9.49	1.81		-0.03	-0.01	-0.14
IGNC	1	CBN	49.292	-91.459	-1.5	0.11	2.22	0.09	0.26	0.39		0.01	0.03	-0.03
ILCH	1	CORS	41.730	-87.538	-0.4	0.24	1.75	0.21	-3.8	0.94	DC	-0.08	-0.20	-0.54
ILUL	1	CORS	69.240	-51.061	-2.79	0.05	-0.59	0.04	9.25	0.12		0.03	0.00	-0.07
INBR	1	CORS	41.458	-86.193	-0.3	0.06	1.92	0.05	-2.94	0.17		-0.04	-0.15	-0.07
INFW	1	CORS	41.128	-85.178	-1.35	0.1	2.05	0.08	-2.05	0.31		-0.44	0.09	0.41
INGY	1	CORS	41.595	-87.247	0.02	0.06	2.08	0.05	-3.31	0.18		0.15	0.04	-0.21
INJK	1	CBN	58.458	-78.106	-0.52	0.18	2.31	0.12	10.23	0.51		0.02	0.00	-0.36
INLP	1	CORS	41.585	-86.693	-0.37	0.07	1.95	0.05	-2.87	0.18		-0.09	-0.12	0.04
INLW	1	CORS	41.290	-87.316	-0.22	0.06	2.01	0.05	-2.99	0.17		-0.07	0.04	-0.12
INMO	1	CORS	40.726	-86.753	-0.34	0.1	1.92	0.08	-2.52	0.31				
INNC	1	CORS	41.383	-85.423	-0.4	0.07	1.63	0.05	-2.68	0.2		0.16	-0.14	-0.15
INRN	1	CORS	40.946	-87.140	0.12	0.06	1.57	0.05	-2.63	0.17				
INVK	1	ACS	68.306	-133.527	0.43	0.05	3.34	0.04	-2.87	0.08		0.06	-0.10	-0.02
INWB	1	CORS	40.825	-85.803	-0.45	0.06	1.97	0.05	-2.6	0.17				
INWN	1	CORS	41.079	-86.604	0.09	0.06	2	0.05	-2.3	0.17		0.12	0.07	0.18
INWR	1	CORS	41.270	-85.895	-0.19	0.07	1.91	0.05	-2.52	0.18		0.07	0.00	0.07
IQAL	1	ACS	63.756	-68.511	-2.13	0.06	2.73	0.04	3.3	0.13		0.01	0.00	0.02

			Velocities (mm/yr) and Uncertainties (1σ , mm/yr)						Outlier rationale	Residuals (mm/yr)				
Site	Solution	Type	Latitude	Longitude	v_{North}	σ_{North}	v_{East}	σ_{East}	v_{Up}	σ_{Up}	$\text{res}_{\text{North}}$	res_{East}	res_{Up}	
IQLU	1	CBN	63.747	-68.547	-2.46	0.44	2.78	0.31	2.07	1.37		-0.31	0.04	-1.23
ISMD	1	CBN	47.409	-61.823	-1.83	0.13	1.62	0.09	-1.41	0.39		-0.09	0.00	0.25
JEDW	1	ACS	52.293	-131.198	-1.71	0.29	0.56	0.19	-9.11	0.75	PS	-9.89	-0.66	-7.86
JEDY	1	ACS	52.293	-131.198	3.92	0.63	-0.92	0.42	-2.74	1.7	PS	-4.26	-2.13	-1.49
JFWS	1	CORS	42.914	-90.248	-0.27	0.08	2.45	0.06	-4.72	0.26		0.01	0.10	-0.60
JOLN	1	CAMP	45.992	-73.460	-1.47	0.44	2.34	0.35	2.63	1.49		0.16	0.24	0.36
JWLF	1	CORS	83.112	-45.120	-1.51	0.06	-0.11	0.05	4.13	0.2		0.06	-0.02	0.18
KA10	1	CORS	41.598	-87.847	-0.37	0.06	1.8	0.04	-2.51	0.16		-0.22	-0.22	0.17
KA11	1	CORS	41.655	-88.444	0.15	0.57	1.93	0.46	-3.89	1.8	NED	0.18	0.11	-1.14
KA16	1	CORS	40.449	-89.018	-0.15	0.23	1.32	0.19	-2.18	0.76				
KA18	1	CORS	41.099	-87.851	-0.36	0.07	2.01	0.06	-2.67	0.21		-0.07	0.02	-0.09
KA20	1	CORS	41.328	-89.147	-0.17	0.07	1.89	0.06	-1.78	0.22		0.04	-0.04	0.25
KA21	1	CORS	40.792	-89.196	-0.61	0.06	2.35	0.04	-1.72	0.15				
KAGA	2	CORS	69.222	-49.815	-3.41	0.14	-0.95	0.1	13.71	0.44		-0.08	-0.06	2.39
KAGZ	1	CORS	79.132	-65.853	-2.83	0.06	0.76	0.05	7.95	0.21		-0.02	-0.03	-0.10
KAR2	1	CORS	41.993	-87.865	-0.55	0.06	1.95	0.04	-2.39	0.16		-0.29	0.08	0.30
KAR3	1	CORS	42.384	-87.867	-0.93	0.41	1.4	0.33	-2.16	1.39	NED	-0.80	-0.68	1.13
KAR6	1	CORS	41.521	-88.147	-0.05	0.27	1.86	0.22	-2.93	0.91		0.05	0.00	-0.29
KAR7	1	CORS	41.876	-87.650	-0.52	0.4	0.93	0.33	-1.42	1.37		-0.22	-1.00	1.64
KASK	1	CAMP	60.761	-139.290	11.86	1.2	0.85	0.69	14.35	3.56		-1.20	0.77	1.96
KATN	1	CBN	51.209	-113.819	-0.36	0.16	3.77	0.11	-0.48	0.48		-0.01	0.10	0.12
KBUG	2	CORS	65.144	-41.158	-1.98	0.11	-1.44	0.07	1.38	0.3		0.04	-0.14	-1.14
KELY	3	CORS	66.987	-50.945	-2.61	0.06	0.55	0.05	5.13	0.15		0.00	0.02	-0.05
KEN1	2	CORS	60.675	-151.350	-6.16	0.13	2.25	0.09	11.6	0.37	DC			
KEN5	1	CORS	60.675	-151.350	-4.96	0.07	1.88	0.05	7.08	0.14	DC			
KEW1	1	CORS	47.227	-88.624	-2.43	0.07	2.91	0.04	0.1	0.18	DC	-0.57	0.87	0.57
KEW2	1	CORS	47.227	-88.624	-1.77	0.12	2.19	0.08	-0.06	0.37	DC	0.09	0.15	0.42
KEW5	1	CORS	47.227	-88.624	-2.24	0.09	2.45	0.06	-1.29	0.24	DC	-0.37	0.42	-0.81
KEW6	1	CORS	47.227	-88.624	-1.66	0.06	1.87	0.04	-1.97	0.16	DC	0.21	-0.17	-1.49
KEWA	1	CORS	44.464	-87.502	-1.4	0.31	1.35	0.24	-2.95	1.04		-0.06	-0.24	0.15
KGLK	1	ACS	67.818	-115.135	-0.51	0.1	3.27	0.07	2.88	0.3		-0.01	0.17	-0.29
KINF	1	CAMP	45.851	-72.083	-3.11	0.32	1.07	0.26	2.18	1.09		-0.44	-0.56	0.19
KLRS	1	ACS	61.028	-138.410	7.66	0.17	3.4	0.12	7.9	0.5		-0.08	-0.75	0.28
KMOR	1	CORS	81.253	-63.527	-2.22	0.05	1.07	0.05	6.14	0.17		0.00	0.00	0.00
KNDL	1	CBN	51.504	-109.164	-0.84	0.15	3.07	0.11	-1.16	0.44		-0.03	0.01	0.06
KNGS	1	ACS	44.219	-76.517	-1.92	0.05	2.08	0.03	-0.12	0.09	EP	-0.06	0.19	-0.98
KNGV	1	ACS	42.027	-82.735	-0.88	0.09	2.03	0.07	-3.54	0.27		0.03	0.04	-0.40
KNRA	1	CBN	49.716	-94.756	-1.37	0.1	2.12	0.07	-0.47	0.32		0.00	0.01	0.03
KNTN	1	CORS	40.631	-83.615	-0.81	0.08	1.83	0.06	-2.57	0.22				
KNTN	2	CORS	40.631	-83.615	-0.7	0.08	1.8	0.06	0.82	0.23	NNC			
KTCK	1	ACS	45.182	-63.718	-2.13	0.26	1.83	0.19	-0.94	0.72		-0.09	0.07	0.37
KTMT	1	ACS	54.086	-128.598	-0.36	0.35	2	0.25	2.19	1.07	NED	-3.63	-0.11	1.50
KUGL	1	CBN	67.818	-115.132	-0.45	0.15	2.83	0.1	3.65	0.48		0.05	-0.27	0.48
KUJQ	1	CBN	58.111	-68.414	-0.48	0.16	2.59	0.11	7.69	0.48		0.02	0.00	-0.27
KULL	1	CORS	74.581	-57.227	-3.5	0.06	-0.31	0.05	9.09	0.16		-0.08	0.02	-0.43
KUSA	1	CAMP	60.601	-136.137	6.54	0.93	7.87	0.64	2.25	2.86		0.92	2.55	-3.63
KUUJ	1	ACS	55.278	-77.745	-1.05	0.06	2.1	0.04	13.21	0.13		0.01	0.00	0.04
LADU	1	CAMP	46.843	-70.840	-2.43	0.27	1.65	0.21	1.65	0.91		-0.15	-0.14	-0.10
LAKE	1	CORS	43.140	-82.495	-1.78	0.3	1.94	0.26	-0.94	1.08		-0.74	0.30	1.05
LANG	1	CAMP	54.256	-133.060	14.09	2.02	-0.2	1.3	-2.26	6.32		3.28	-0.81	-0.06
LANS	1	CORS	42.674	-84.663	-0.79	0.05	1.96	0.03	-2.36	0.1		-0.04	0.09	0.15
LATU	1	ACS	47.436	-72.778	-2.82	0.05	2.25	0.03	4.62	0.1		-0.13	0.01	0.14
LAUP	1	CAMP	47.723	-71.209	-2.35	0.19	2.93	0.15	2.66	0.66		0.03	0.13	-0.50
LAUR	1	ACS	46.545	-75.479	-2.01	0.05	2.13	0.03	3.86	0.08		0.05	0.04	0.07
LAVE	1	CBN	46.782	-71.284	-0.61	0.12	0.72	0.08	2.42	0.35		1.05	-0.73	0.32
LCDT	1	CORS	42.295	-87.960	-0.15	0.04	2.02	0.03	-3.33	0.07		-0.03	0.03	-0.16
LCUR	1	ACS	45.981	-81.925	-2.5	0.14	-1.38	0.1	2.77	0.43	LD	-0.75	-3.32	1.78
LDMN	1	CBN	53.249	-109.871	-0.74	0.13	2.97	0.09	-0.48	0.37		0.01	0.00	0.04
LETH	1	CBN	49.592	-112.601	-0.46	0.16	3.56	0.11	-1.71	0.48		-0.03	0.06	0.17
LEV1	1	CORS	56.466	-133.093	2.85	0.14	0.18	0.09	5.53	0.36	DC	-1.26	0.13	0.91
LEV5	1	CORS	56.466	-133.093	3.88	0.1	-0.01	0.07	4.26	0.26	DC	-0.23	-0.05	-0.36
LFRG	1	CBN	54.598	-71.273	-1.33	0.24	2.17	0.16	12	0.69		0.05	-0.04	-0.11
LG1G	1	ACS	53.698	-78.571	-1.4	0.08	1.93	0.06	12.97	0.22		0.02	-0.02	0.05

					Velocities (mm/yr) and Uncertainties (1σ , mm/yr)						Outlier rationale	Residuals (mm/yr)		
Site	Solution	Type	Latitude	Longitude	v_{North}	σ_{North}	v_{East}	σ_{East}	v_{Up}	σ_{Up}		$\text{res}_{\text{North}}$	res_{East}	res_{Up}
LG4G	1	ACS	53.833	-73.514	-2.88	1.02	3.05	0.69	8.82	2.66		-0.48	0.29	-3.49
LGLK	1	CBN	49.780	-86.517	-1.8	0.18	1.92	0.12	4.27	0.56		0.03	0.01	-0.05
LINH	1	CORS	47.000	-120.539	2.55	0.06	3.8	0.04	-2.89	0.09		-0.03	0.06	-0.03
LITT	1	CORS	46.486	-84.301	-1.56	0.68	2.12	0.52	-0.53	2.45	NNC	0.25	0.48	-0.96
LNLK	1	CBN	56.862	-101.067	-1.31	0.12	2.59	0.08	5.58	0.33		0.02	0.00	0.05
LOCN	1	CBN	56.896	-108.980	-1.41	0.17	2.72	0.12	3.26	0.51		-0.02	-0.02	0.27
LOLO	1	CORS	46.763	-114.097	0.31	0.08	2.76	0.06	-1.32	0.22		-0.03	-0.07	0.13
LON1	1	CBN	42.883	-81.251	-1.47	0.15	2.05	0.12	-1.18	0.49		-0.01	0.08	0.53
LONG	1	ACS	45.542	-73.493	-2.04	0.28	1.78	0.22	2.9	0.94		0.26	-0.02	0.82
LORB	1	CBN	51.227	-106.612	-0.5	0.11	2.77	0.08	-2.01	0.32		0.05	-0.02	-0.09
LOUI	1	CAMP	47.978	-69.867	-1.99	0.31	1.99	0.25	3.2	1.1		0.22	-0.11	0.83
LOUP	1	ACS	47.827	-69.557	-1.82	0.06	2.18	0.04	-0.36	0.15	NNC	0.46	0.14	-2.21
LOZ1	1	CORS	44.620	-74.583	-2.69	0.17	1.98	0.14	7.07	0.77	LD	-0.55	0.11	5.56
LPOC	1	ACS	47.341	-70.009	-2.26	0.05	2.13	0.03	1.89	0.07		0.18	0.07	0.14
LRNG	1	CBN	55.162	-105.300	-1.48	0.15	2.54	0.1	1.04	0.44		-0.01	0.00	-0.20
LSAR	1	CBN	48.781	-79.162	-2.36	0.17	1.69	0.12	7.26	0.53		-0.03	0.01	0.01
LSBG	1	ACS	45.922	-59.972	-2.45	0.23	2.67	0.17	-4.29	0.67		-0.12	0.30	-1.05
LSBN	1	CORS	40.769	-80.810	-1.08	0.06	1.78	0.05	-3.05	0.17				
LTUQ	1	CBN	47.419	-72.790	-2.44	0.1	2.27	0.08	4.11	0.32		0.21	0.05	-0.34
LTWN	1	ACS	44.885	-65.168	-1.7	0.1	1.63	0.07	-1.11	0.28		0.06	-0.04	-0.16
LUDI	1	CORS	43.947	-86.442	-1.34	0.41	3.01	0.31	-2.77	1.39		-0.34	0.72	-0.73
LUSE	1	CBN	50.503	-77.431	-1.96	0.17	1.69	0.12	9.31	0.52		0.02	-0.02	-0.29
LVPL	1	ACS	44.033	-64.706	-1.48	0.1	1.44	0.07	-1.3	0.26		0.06	-0.03	-0.09
LYCO	1	CORS	41.241	-77.002	-1.12	0.05	1.2	0.03	-3.1	0.1		0.01	-0.01	-0.09
LYNS	1	CORS	64.431	-40.198	-2.55	0.07	-0.05	0.05	4.98	0.17		-0.06	0.07	0.38
MABU	1	ACS	46.061	-61.408	-1.72	0.16	1.18	0.12	-1.84	0.45		-0.14	-0.07	-0.17
MAMI	1	CAMP	63.175	-130.201	0.21	1.14	0.3	0.75	2.87	3.55	DC	0.79	-3.16	0.36
MARG	1	CORS	77.187	-65.695	-2.33	0.05	1.08	0.05	7.52	0.15		0.02	0.05	-0.37
MARQ	1	CORS	46.547	-87.379	-1.52	0.15	2.02	0.12	-0.35	0.54		-0.21	0.18	0.17
MASK	1	CAMP	46.231	-73.018	-1.69	0.38	2.33	0.28	2.44	1.37		0.12	0.17	-0.09
MAST	1	CAMP	46.571	-73.286	-1.98	0.28	1.42	0.22	2.96	0.93		0.08	-0.32	-0.17
MAWY	1	CORS	44.973	-110.689	0.91	0.05	3.05	0.04	-1.56	0.12		0.02	-0.01	0.00
MBRV	1	CORS	42.974	-82.419	-0.41	0.66	2.32	0.54	-3.72	2.48		0.28	0.90	-1.70
MCGT	1	CBN	44.528	-63.859	-1.87	0.11	1.66	0.08	-1.37	0.32		-0.03	0.00	0.03
MCHN	2	ACS	47.961	-84.901	-7.36	0.21	6.01	0.14	0.16	0.51	LD	-5.54	3.87	-2.47
MCTN	1	ACS	46.096	-64.834	-1.74	0.06	1.41	0.04	-0.72	0.14		0.04	-0.18	0.12
MDFC	1	ACS	60.122	-136.958	9.32	0.08	3.69	0.06	17.22	0.2		0.42	-0.40	0.68
MDLK	1	CBN	54.093	-108.478	-1.08	0.16	2.98	0.11	0.21	0.47		-0.01	0.02	0.10
MDR5	2	CORS	46.905	-103.275	2.67	0.13	4.75	0.1	-2.55	0.41	NNC	2.64	2.11	1.63
MECC	1	CORS	44.826	-68.744	-1.38	0.22	1.12	0.16	-2.03	0.63	NNC	0.22	-0.72	-2.78
MEDX	1	CORS	45.026	-69.297	-1.91	0.09	1.67	0.06	1.15	0.23		-0.04	-0.04	0.13
MEFR	1	CORS	44.675	-70.132	-1.67	0.09	1.56	0.06	1.56	0.23		0.15	-0.02	0.39
MEGR	1	CORS	45.464	-69.594	-2.06	0.18	1.98	0.14	0.18	0.53		-0.06	0.04	-0.62
MEJD	1	CORS	44.608	-69.600	-1.8	0.1	1.92	0.07	0.17	0.27		0.01	0.10	-0.37
MELI	1	CORS	45.364	-68.507	-1.06	0.09	1.78	0.06	1.88	0.23		0.20	-0.02	0.53
MEMA	1	CORS	44.710	-67.458	-2.6	0.09	2.07	0.07	0.64	0.24		-0.14	0.03	0.40
MENO	1	CORS	45.096	-87.590	-1.41	0.56	2.63	0.44	-5.3	2.01	LD	0.25	0.66	-2.91
MEPI	1	CORS	46.671	-68.017	-1.86	0.09	1.8	0.07	0.55	0.24		0.03	-0.03	0.28
MERA	1	CORS	44.974	-70.653	-1.99	0.1	1.62	0.07	1	0.27		0.00	-0.01	-0.10
MESP	1	CORS	44.218	-70.513	-2.88	0.09	1.04	0.06	1.56	0.24		-0.10	-0.11	0.48
METR	1	CORS	42.685	-83.243	-0.61	0.05	1.85	0.03	-2.25	0.09		0.13	0.09	0.06
MFLD	1	CORS	44.637	-90.135	-3.05	0.07	3.07	0.05	-2.13	0.19	EP	-2.17	0.75	2.25
MIAL	1	CORS	45.063	-83.429	-1.67	0.06	1.62	0.04	-0.85	0.16		-0.02	0.01	-0.07
MIAR	1	CORS	43.983	-83.980	-1.29	0.06	1.65	0.05	-2.02	0.18		-0.01	-0.04	0.00
MIBC	1	CORS	42.322	-85.203	-0.5	0.05	0.93	0.03	-3.41	0.12		0.09	-0.35	-0.30
MIBH	1	CORS	42.088	-86.390	0.93	0.06	1.73	0.05	-3.17	0.17	LD	1.27	-0.78	-0.09
MIBO	1	CORS	45.206	-84.996	-1.16	0.06	1.52	0.04	-2.5	0.14		0.05	0.04	-0.38
MIBX	1	CORS	46.764	-88.513	-1.6	0.06	1.93	0.04	-0.93	0.17		-0.02	0.02	-0.03
MIBY	1	CORS	43.623	-83.947	-0.99	0.06	1.76	0.05	-2.12	0.17		0.15	-0.01	0.07
MICA	1	CORS	43.428	-82.668	-0.96	0.1	1.86	0.08	-1.94	0.31		0.15	-0.02	0.05
MICC	1	CORS	43.607	-83.172	-0.86	0.1	1.95	0.08	-2.6	0.3		0.21	0.10	-0.56
MICO	1	CORS	43.060	-85.946	-0.58	0.05	1.84	0.03	-2.92	0.12		0.07	0.06	-0.19
MICV	1	CORS	41.923	-85.516	-0.7	0.06	1.48	0.04	-2.65	0.15		-0.07	-0.11	0.15

			Velocities (mm/yr) and Uncertainties (1σ , mm/yr)						Outlier rationale	Residuals (mm/yr)				
Site	Solution	Type	Latitude	Longitude	v_{North}	σ_{North}	v_{East}	σ_{East}	v_{Up}	σ_{Up}	$\text{res}_{\text{North}}$	res_{East}	res_{Up}	
MICW	1	CORS	41.940	-84.980	-0.8	0.05	1.85	0.04	-2.8	0.12		-0.08	0.15	0.01
MICX	1	CORS	45.310	-85.263	-1.07	0.05	1.3	0.03	-1.21	0.11		0.05	-0.09	0.25
MIDA	1	ACS	52.938	-132.123	-4.02	0.29	-10.34	0.2	-12.71	0.82	PS	-14.60	-11.26	-11.38
MIDD	1	CORS	41.956	-83.649	-0.82	0.05	2.09	0.03	-2.55	0.12		-0.04	0.15	-0.03
MIDS	1	CORS	43.050	-83.520	-1.27	0.05	1.11	0.04	-2.37	0.13		-0.14	-0.21	-0.03
MIDT	1	CORS	42.444	-83.006	-0.86	0.05	1.6	0.04	-2.17	0.13		0.11	-0.07	0.23
MIGD	1	CORS	45.027	-84.645	-1.35	0.07	1.61	0.05	-2.03	0.18		-0.05	0.02	-0.06
MIGH	1	CORS	43.008	-86.209	-0.66	0.05	1.75	0.03	-3.16	0.11		0.03	-0.04	-0.05
MIGL	1	CORS	44.656	-84.704	-0.84	0.05	1.49	0.03	-1.26	0.1		0.10	0.01	0.24
MIHA	1	CORS	44.019	-84.812	-0.91	0.06	2.14	0.05	-2.6	0.17		0.02	0.11	-0.21
MIHD	1	CORS	41.889	-84.616	-0.61	0.07	1.84	0.05	-2.44	0.19		0.03	0.14	0.25
MIHL	1	CORS	44.333	-84.795	-1.26	0.05	1.46	0.03	-2.19	0.13		-0.13	-0.11	-0.18
MIHO	1	CORS	42.814	-86.084	-0.9	0.05	1.81	0.04	-3.35	0.13		-0.15	-0.03	-0.21
MIHT	1	CORS	43.688	-86.365	-0.44	0.05	1.51	0.03	-1.89	0.1		0.19	-0.26	0.13
MIHV	1	CORS	42.887	-85.859	-0.67	0.05	1.8	0.04	-2.69	0.12		0.02	0.01	0.17
MIIR	1	CORS	46.080	-88.633	-1.01	0.05	1.61	0.03	-0.97	0.09		0.09	-0.14	0.37
MIIT	1	CORS	43.289	-84.592	-0.87	0.05	1.77	0.03	-2.55	0.1		0.05	-0.06	0.00
MIIW	1	CORS	46.470	-90.166	-1.16	0.05	2.03	0.04	-2.54	0.12		0.05	-0.03	-0.02
MIKK	1	CORS	44.742	-85.185	-0.97	0.05	1.09	0.04	-1.05	0.12		0.00	-0.15	0.27
MIKS	1	CORS	41.851	-84.351	-0.72	0.05	1.93	0.04	-2.47	0.12		-0.04	0.09	0.02
MIL1	1	CORS	43.003	-87.888	-0.37	0.07	3.39	0.05	-4.69	0.2	DC	-0.14	0.55	-1.08
MIL2	1	CORS	43.002	-87.888	0.15	0.24	3.64	0.18	-0.89	0.78		0.38	0.81	2.71
MILI	1	CORS	42.435	-83.415	-0.6	0.08	1.89	0.06	-2.6	0.22		0.05	0.10	-0.13
MILS	1	CORS	46.487	-84.364	-1.76	0.1	1.72	0.07	0.17	0.28		0.04	0.07	-0.28
MILT	1	CORS	43.947	-86.442	-1.9	0.11	2.18	0.08	-2.16	0.33	NED	-0.89	-0.10	-0.12
MILW	1	CORS	43.003	-87.889	0.39	0.23	2.52	0.18	-3.51	0.77		0.62	-0.32	0.09
MIMA	1	CORS	42.564	-84.452	-0.8	0.05	1.66	0.03	-2.53	0.11		-0.01	-0.14	-0.04
MIMC	1	CORS	45.777	-84.721	-1.38	0.12	1.86	0.09	-1.48	0.34		0.07	-0.08	-0.52
MIMK	1	CORS	43.203	-86.249	-0.99	0.06	1.84	0.04	-2.91	0.14		-0.14	0.02	-0.11
MIMN	1	CORS	44.373	-86.163	-0.86	0.05	1.69	0.03	-2.03	0.12		0.09	-0.12	-0.07
MIMO	1	CORS	41.925	-83.465	-0.53	0.05	1.97	0.03	-2.35	0.12		0.23	0.07	0.18
MIMQ	1	CORS	46.546	-87.379	-1.28	0.05	1.84	0.03	-0.51	0.12		0.03	0.00	0.01
MIMR	1	CORS	42.153	-84.039	-0.66	0.05	2.35	0.04	-2.37	0.12		0.03	0.28	0.11
MIMU	1	CORS	46.377	-86.639	-1.47	0.07	2.07	0.05	-0.7	0.18		0.05	0.02	-0.02
MINB	1	CORS	46.285	-84.210	-1.46	0.08	1.5	0.06	0.03	0.21		0.07	-0.10	-0.09
MIND	1	CORS	45.385	-84.630	-2.25	0.06	1.44	0.04	-1.99	0.14		-0.38	-0.09	-0.22
MINH	1	CORS	42.729	-82.797	-1.82	0.05	1.65	0.04	-2.11	0.12		-0.42	0.00	0.06
MINI	1	CORS	41.809	-86.224	-0.14	0.08	3.5	0.06	-3.35	0.23		0.09	0.50	-0.22
MINT	1	CAMP	62.576	-136.794	2.59	0.92	5.59	0.6	-1.84	2.71		0.69	-0.50	0.58
MINW	1	CORS	45.790	-87.918	-0.17	0.05	0.55	0.03	-2.07	0.12		0.35	-0.35	-0.20
MIO1	1	CORS	44.651	-84.134	-1.47	0.1	1.68	0.07	-1.25	0.29		-0.29	0.05	-0.06
MIO2	1	CORS	44.647	-84.149	-0.84	0.05	1.56	0.03	-0.77	0.12		0.31	-0.07	0.43
MIOG	1	CORS	44.302	-84.127	-1.22	0.07	1.81	0.05	-1.79	0.18		-0.05	0.07	-0.08
MION	1	CORS	42.996	-85.074	-0.66	0.05	1.98	0.03	-2.95	0.11		0.04	0.03	-0.15
MIOT	1	CORS	46.864	-89.300	-1.1	0.09	1.51	0.07	-1.36	0.25		0.16	-0.21	-0.03
MIPP	1	CORS	42.219	-85.877	-0.58	0.05	1.46	0.03	-3.07	0.12		-0.02	-0.22	-0.04
MIPV	1	CORS	42.692	-83.762	-0.99	0.06	1.71	0.04	-2.31	0.14		-0.09	-0.05	0.03
MIPW	1	CORS	42.463	-85.657	-0.59	0.06	1.9	0.04	-3.12	0.17		0.02	0.11	-0.06
MIQE	1	CORS	45.967	-86.236	-1.42	0.08	2.13	0.06	-1.38	0.24		0.03	0.05	-0.16
MIRA	1	ACS	46.992	-65.568	-1.74	0.06	1.34	0.04	-2.26	0.15		0.06	-0.07	-0.33
MISC	1	CORS	42.968	-83.835	-0.84	0.05	1.78	0.03	-2.22	0.1		0.16	0.04	0.10
MISH	1	CORS	42.384	-86.265	-0.54	0.06	1.82	0.04	-2.74	0.16		-0.01	-0.13	0.24
MISI	1	CORS	45.854	-84.703	-1.24	0.08	2.68	0.06	-0.32	0.21		0.23	0.59	0.43
MISJ	1	CORS	42.965	-84.544	-0.72	0.06	1.94	0.04	-2.46	0.14		0.09	0.01	0.04
MIST	1	CORS	45.422	-87.600	-1.96	0.05	1.66	0.03	-1.42	0.11		-0.31	0.01	0.31
MITC	1	CORS	44.713	-85.606	-1.05	0.07	2.02	0.05	-2.2	0.21		-0.02	0.20	-0.37
MITO	1	CORS	41.800	-86.604	-1.28	0.06	0.81	0.05	-2.82	0.17	EP	-1.00	-1.69	0.26
MITS	1	CORS	43.301	-85.087	-1.05	0.06	2.14	0.04	-2.58	0.13		-0.14	0.12	-0.08
MITU	1	CORS	47.111	-88.552	-1.5	0.05	4.49	0.04	-1.73	0.13	NNC	0.30	2.48	-1.17
MITW	1	CORS	44.280	-83.584	-1.19	0.08	1.78	0.06	-1.57	0.21		0.04	-0.01	-0.01
MIVA	1	CORS	43.379	-83.585	-0.97	0.09	1.82	0.07	-2.11	0.26		0.14	0.07	0.09
MIWA	1	CORS	42.783	-83.006	-1.18	0.05	1.77	0.03	-2.25	0.11		-0.01	0.04	0.02
MIWB	1	CORS	42.677	-84.218	-1.46	0.05	1.18	0.03	-2.64	0.11	NNC	-0.61	-0.69	-0.22

					Velocities (mm/yr) and Uncertainties (1σ , mm/yr)						Outlier rationale	Residuals (mm/yr)		
Site	Solution	Type	Latitude	Longitude	v_{North}	σ_{North}	v_{East}	σ_{East}	v_{Up}	σ_{Up}		$\text{res}_{\text{North}}$	res_{East}	res_{Up}
MIWC	1	CORS	43.569	-85.778	-0.44	0.05	1.44	0.03	-1.49	0.1		0.09	-0.07	0.16
MILTN	1	CBN	44.472	-75.868	-2.05	0.11	1.82	0.08	1.46	0.34		0.28	-0.29	0.09
MMEP	1	ACS	63.175	-130.201	-0.75	0.44	2.43	0.3	4	1.37	DC	-0.17	-1.03	1.50
MMSQ	1	ACS	45.052	-63.134	-1.78	0.27	3.97	0.2	-1.4	0.76	NED	-0.09	2.14	0.17
MNAS	1	CORS	48.294	-92.970	-1.59	0.06	2.05	0.04	-1.93	0.16		-0.04	0.01	-0.05
MNBDF	1	CORS	48.628	-94.067	-0.9	0.07	1.9	0.05	-1.18	0.17		0.05	0.01	0.29
MNBE	1	CORS	43.663	-94.122	-0.09	0.07	2.25	0.05	-3.36	0.17		-0.01	-0.05	-0.11
MNBJ	1	CORS	47.501	-94.938	-1.18	0.07	2.19	0.05	-2.45	0.17		-0.05	-0.01	0.06
MNC5	1	CBN	51.249	-68.197	-2.65	0.17	2.21	0.11	6.78	0.5		0.01	-0.02	-0.44
MNCA	1	CORS	43.633	-91.496	-0.3	0.07	1.89	0.05	-3.6	0.18		-0.05	-0.03	0.01
MNDN	1	CORS	48.572	-96.915	-0.94	0.07	2.09	0.04	-2.11	0.16		0.05	-0.15	-0.11
MNDR	1	CBN	53.565	-112.410	-0.78	0.19	3.09	0.13	-0.2	0.54		-0.04	-0.02	-0.11
MNDT	1	CORS	46.823	-95.860	-0.85	0.09	2.44	0.06	-3.07	0.24		0.00	-0.02	-0.12
MNEM	1	CORS	46.688	-93.955	-0.84	0.05	2.26	0.03	-2.76	0.1		0.02	-0.05	0.07
MNEY	2	CORS	43.956	-92.205	-1.06	0.14	2.11	0.11	-3.17	0.41		-0.18	0.00	0.25
MNGP	1	CORS	47.224	-93.484	-1.14	0.06	2.02	0.04	-2.58	0.12		-0.01	-0.03	0.00
MNHK	1	CORS	48.772	-96.949	-1.16	0.08	2.63	0.05	-1.79	0.2		-0.13	0.18	0.12
MNHN	1	CORS	45.985	-92.948	-1.17	0.07	2.41	0.04	-3.24	0.17		0.01	-0.02	0.18
MNHY	1	CORS	47.949	-95.626	-0.98	0.15	2.52	0.1	-2.15	0.39		0.01	0.09	0.04
MNJJC	1	CORS	46.978	-93.274	-0.97	0.05	2.4	0.03	-2.43	0.1		0.02	0.02	0.05
MNLCC	1	CORS	44.478	-93.292	-0.36	0.06	2.28	0.04	-3.71	0.14		0.00	0.02	-0.15
MNLS	1	CORS	44.441	-93.907	-0.2	0.07	1.96	0.05	-6.47	0.17	NNC	0.09	-0.32	-3.07
MNMA	1	CORS	45.876	-93.664	0.51	0.09	3.08	0.07	-2.21	0.25	NNC	1.38	0.61	1.03
MNMGM	1	CORS	48.135	-93.879	-1.04	0.08	1.78	0.06	-2.95	0.21		-0.04	-0.06	-0.42
MNPL	1	CORS	46.340	-93.262	-1.1	0.05	3	0.03	-2.72	0.12		-0.02	0.16	0.11
MNRE	1	CORS	47.059	-93.907	-0.98	0.06	2.24	0.04	-3.18	0.16		-0.01	0.02	-0.27
MNRV	1	CORS	48.789	-95.051	-1.06	0.07	1.81	0.05	-1.53	0.17		-0.02	-0.04	0.02
MNSC	1	CORS	45.713	-94.931	-0.55	0.08	2.31	0.06	-3.64	0.21		0.01	-0.01	-0.16
MNSQ	1	CORS	47.604	-94.127	-0.96	0.08	1.99	0.06	-2.17	0.21		0.00	-0.01	0.36
MNTF	1	CORS	48.119	-96.207	-1.06	0.06	2.24	0.04	-1.96	0.14		-0.01	-0.03	0.06
MNTL	1	CORS	43.508	-93.354	-0.05	0.06	2.36	0.04	-3.11	0.14		0.04	0.01	0.04
MNTN	1	CBN	46.132	-64.959	-2	0.12	1.84	0.08	-1.25	0.35		-0.13	0.17	-0.32
MNVI	1	CORS	47.523	-92.562	-1.42	0.05	2.17	0.03	-1.94	0.1		-0.02	0.02	0.06
MNVN	1	CORS	46.413	-95.055	-0.85	0.05	2.26	0.03	-2.7	0.09		-0.04	-0.02	0.15
MNVT	1	CORS	48.971	-97.202	-0.33	0.18	1.87	0.12	-2.36	0.48		0.19	-0.13	-0.38
MNWH	1	CORS	48.150	-94.512	-0.44	0.1	1.98	0.07	-2.81	0.25		0.15	0.01	-0.33
MNWNN	1	CORS	44.065	-91.713	-0.11	0.06	2.18	0.04	-3.69	0.15		0.10	0.05	0.01
MONT	1	ACS	45.546	-73.639	-1.76	0.05	2.15	0.03	1.7	0.11		0.48	0.31	-0.22
MORE	1	CAMP	53.020	-132.087	-31.82	0.23	-24.93	0.16	-8.44	0.74	PS	-42.42	-25.84	-7.13
MORH	1	CORS	46.884	-96.764	-0.56	0.06	2.32	0.04	-4.98	0.12	NNC	0.23	-0.49	-2.09
MOSN	1	CBN	51.288	-80.613	-2.14	0.15	1.94	0.1	9.93	0.42		-0.02	0.01	0.06
MOTD	1	CAMP	60.958	-138.040	6.95	0.3	4.63	0.2	7.04	0.9		-0.08	0.37	-0.33
MPCK	1	CBN	49.990	-109.468	-0.24	0.16	3.07	0.11	-2.42	0.48		0.02	0.01	-0.22
MPL	1	CORS	43.615	-84.762	-0.63	0.05	2.11	0.03	-2.44	0.09		0.11	0.10	0.00
MRLK	1	CBN	55.945	-112.029	-0.9	0.17	3.24	0.12	0.91	0.49		-0.01	0.01	-0.39
MRML	1	CBN	45.308	-67.248	-2.19	0.12	1.8	0.09	-0.29	0.36		-0.05	-0.01	0.03
MSKY	1	CORS	43.238	-86.055	-0.59	0.05	1.85	0.03	-2.4	0.09		0.06	0.04	0.07
MSOL	1	CORS	46.929	-114.109	0.4	0.05	3.28	0.03	-1.48	0.09		0.06	0.20	0.01
MTCV	1	CAMP	46.920	-71.341	-2.11	0.25	2.53	0.21	2.88	0.9		-0.13	0.51	0.54
MTDT	1	CORS	46.589	-111.994	-0.25	0.07	3.3	0.05	-2.42	0.15		-0.05	0.05	-0.06
MTFV	1	CORS	48.228	-114.327	0.15	0.05	2.88	0.03	-1.68	0.09		0.02	-0.06	-0.03
MTGN	1	ACS	44.226	-66.132	-1.88	0.11	1.84	0.08	-0.54	0.29		0.08	0.01	0.09
MTJL	1	CBN	48.521	-67.984	-2.36	0.12	2.29	0.09	1.65	0.37		0.00	0.01	0.04
MTLW	1	CORS	47.054	-109.443	-0.14	0.08	2.86	0.05	-2.3	0.18		-0.01	0.02	0.08
MTMG	1	CAMP	46.972	-70.578	-2.36	0.24	1.69	0.19	2.54	0.81		-0.09	-0.12	0.78
MTMS	1	CORS	48.541	-109.687	-0.73	0.05	2.27	0.03	-2.82	0.1		-0.06	-0.07	0.01
MTUM	1	CORS	46.950	-113.472	0.2	0.12	2.42	0.09	-2.52	0.33		0.04	-0.22	-0.60
MTVR	1	CORS	40.382	-82.511	-0.75	0.05	2.04	0.03	-2.23	0.1				
MURR	1	CAMP	47.757	-70.042	-1.43	0.27	1.79	0.22	0.73	1.01	NNC	0.87	-0.40	-1.45
MVCC	1	CORS	43.078	-75.219	-0.38	0.3	1.94	0.24	-0.89	1.02	NED	1.65	0.41	-0.58
MWRD	1	CORS	41.668	-87.598	-0.47	0.07	1.74	0.05	-2.73	0.2		-0.20	-0.17	0.30
MYRA	1	ACS	49.551	-125.571	5.84	0.08	8.95	0.06	3.35	0.22		-0.05	0.02	0.64
NAIN	1	ACS	56.537	-61.689	-0.6	0.05	2.95	0.03	3.62	0.08		0.02	0.02	0.11

Site	Solution	Type	Latitude	Longitude	Velocities (mm/yr) and Uncertainties (1σ , mm/yr)						Outlier rationale	Residuals (mm/yr)		
					v_{North}	σ_{North}	v_{East}	σ_{East}	v_{Up}	σ_{Up}		$\text{res}_{\text{North}}$	res_{East}	res_{Up}
NANO	1	ACS	49.295	-124.087	5.38	0.07	7.75	0.05	0.14	0.14		0.07	0.11	-0.23
NBTF	1	CBN	52.741	-108.230	-1.1	0.16	2.77	0.11	-0.55	0.47		-0.01	-0.01	0.25
NCRS	2	CAMP	53.144	-131.960	-2.2	0.4	-7.54	0.27	-6.36	1.14	PS	-12.68	-8.51	-5.10
NDCO	1	CORS	47.448	-98.118	-2.48	0.26	2.15	0.19	0.03	0.79	NED	-1.71	-0.24	2.76
NDDI	1	CORS	46.885	-102.744	0.21	1.25	2.76	0.93	-1.76	3.58		0.14	0.15	2.44
NDFA	1	CORS	46.829	-96.838	-0.69	0.3	2.98	0.21	-3.55	0.84		0.05	0.15	-0.64
NDGR	1	CORS	48.621	-103.933	-0.5	1.16	-0.17	0.81	1.57	3.06	NED	-0.08	-2.82	5.60
NDHI	1	CORS	47.405	-97.054	-1.22	0.34	2.35	0.24	-1.74	0.97		-0.12	-0.07	0.74
NDMB	1	CORS	48.416	-101.330	-0.62	0.06	2.12	0.05	-3.37	0.17		-0.03	-0.03	0.12
NDMU	1	CORS	48.667	-98.836	-0.71	0.73	0.88	0.51	7.67	2.08	NED	0.02	-1.28	10.22
NDST	1	CORS	46.850	-99.916	-0.36	0.24	2.58	0.18	0.55	0.72	NED	-0.18	0.19	4.23
NEAH	2	CORS	48.298	-124.625	8.8	0.05	13.1	0.04	1.27	0.08		0.29	0.26	0.15
NGLW	1	ACS	45.567	-62.634	-1.88	0.26	1.02	0.19	-1.58	0.72		-0.24	-0.26	0.02
NHBR	1	ACS	46.825	-60.359	-0.79	0.17	1.07	0.12	-1.78	0.49		0.28	-0.18	0.27
NLIB	1	CORS	41.772	-91.575	-0.02	0.05	2.01	0.03	-3.29	0.12		0.01	-0.03	-0.02
NNVN	1	CORS	61.632	-44.901	-1.7	0.06	0.02	0.04	5.48	0.12		0.06	-0.04	-0.34
NOR1	1	CORS	44.256	-85.437	-1.04	0.05	1.62	0.03	-1.51	0.12		-0.02	-0.01	0.10
NOR2	1	CORS	44.989	-84.683	-1.13	0.12	1.69	0.09	-2.87	0.38		0.06	0.08	-0.88
NOR3	1	CORS	45.069	-83.569	-1.64	0.04	1.48	0.02	-0.74	0.07		0.01	-0.08	0.10
NRC1	1	ACS	45.454	-75.624	-1.88	0.04	1.95	0.03	2.54	0.07		0.10	-0.04	0.36
NRDG	1	CBN	52.480	-116.123	0.22	0.18	3.63	0.12	0.27	0.51		0.04	0.01	-0.04
NSLM	1	CAMP	60.993	-138.496	8.47	0.22	4.47	0.14	9.11	0.75		0.14	0.39	0.81
NTKA	2	ACS	49.592	-126.617	6.66	0.09	11.72	0.06	2.62	0.22		0.14	0.69	0.85
NUVB	1	CAMP	46.735	-71.569	-1.49	0.27	2.61	0.21	1.5	0.94		0.23	0.35	-0.77
NYBT	1	CORS	42.988	-78.122	-1.46	0.05	1.57	0.04	-1.04	0.12		0.03	-0.02	0.02
NYCL	1	CORS	42.584	-76.211	-1.66	0.05	1.36	0.04	-0.71	0.12		0.05	-0.06	-0.02
NYCP	1	CORS	42.188	-77.143	-1.5	0.05	1.5	0.04	-1.01	0.13		0.05	-0.06	0.14
NYDV	1	CORS	42.549	-77.698	-1.56	0.05	1.48	0.04	-1.49	0.13		-0.02	-0.07	-0.04
NYET	1	CORS	44.210	-73.541	-1.93	0.05	1.75	0.04	0.92	0.13		-0.02	0.01	-0.02
NYFD	1	CORS	42.428	-79.340	-1.18	0.05	1.45	0.04	-1.8	0.13		0.02	-0.10	-0.03
NYFS	1	CORS	42.205	-78.144	-1.46	0.05	1.8	0.04	-1.67	0.12		-0.01	0.01	-0.01
NYHB	1	CORS	42.717	-78.847	-1.35	0.05	2.1	0.04	-1.35	0.13		0.01	0.24	0.01
NYHL	1	CORS	44.309	-75.449	-1.89	0.05	1.92	0.03	1.17	0.11		0.19	-0.04	-0.01
NYHM	1	CORS	43.018	-74.996	-2.25	0.06	1.5	0.05	-0.53	0.17		-0.03	0.00	-0.05
NYIL	1	CORS	43.783	-74.278	-1.85	0.05	1.48	0.04	0.67	0.12		0.01	-0.04	0.05
NYLP	1	CORS	43.165	-78.754	-1.66	0.05	1.57	0.04	-1.06	0.12		-0.06	-0.13	0.04
NYLV	1	CORS	43.797	-75.485	-1.82	0.05	1.91	0.04	0.45	0.11		-0.02	0.07	-0.03
NYMC	1	CORS	43.112	-77.614	-1.65	0.09	1.58	0.07	-1.53	0.26		-0.02	-0.06	-0.81
NYML	1	CORS	44.871	-74.288	-1.96	0.05	1.94	0.03	1.72	0.1		0.07	-0.04	0.00
NYMP	1	CAMP	46.415	-73.509	-2.12	0.33	2.34	0.26	3.83	1.14		-0.21	0.33	0.88
NYMX	1	CORS	43.470	-76.232	-1.65	0.05	1.43	0.03	0.17	0.1		0.04	-0.04	-0.01
NYNS	1	CORS	43.119	-76.142	-1.9	0.06	1.54	0.04	0.06	0.14		-0.13	0.04	0.16
NYPB	1	CORS	44.681	-73.454	-1.94	0.05	1.92	0.03	1.57	0.09		0.08	0.04	0.01
NYPD	1	CORS	44.653	-75.042	-2.4	0.05	1.57	0.03	1.65	0.08		0.01	-0.20	0.03
NYPF	1	CORS	43.093	-77.525	-1.69	0.06	1.71	0.04	-0.38	0.14		-0.03	0.05	0.28
NYRB	1	CORS	44.304	-74.078	-2.04	0.06	1.87	0.04	1.06	0.14		-0.03	0.04	-0.04
NYRM	1	CORS	43.178	-75.487	-1.79	0.05	1.57	0.04	-0.05	0.12		0.03	0.01	0.05
NYSB	1	CORS	42.679	-75.513	-0.13	0.05	3.04	0.04	-1.14	0.12	LD	1.74	1.62	-0.48
NYSM	1	CORS	42.192	-78.747	-1.39	0.05	1.81	0.04	-1.52	0.13		-0.01	0.01	0.05
NYSP	1	CORS	42.692	-79.047	-1.32	0.48	1.46	0.38	-1.98	1.73		0.00	-0.25	-0.51
NYWG	1	CORS	42.351	-76.876	-1.75	0.05	1.81	0.04	-0.83	0.11		-0.04	0.12	0.07
NYWL	1	CORS	42.899	-76.852	-1.68	0.05	1.83	0.04	-0.56	0.12		0.03	0.06	-0.05
NYWT	1	CORS	44.028	-75.921	-1.67	0.05	1.46	0.03	0.74	0.08		0.04	-0.12	-0.01
NYWV	1	CORS	42.012	-76.522	-1.83	0.05	1.47	0.04	-0.94	0.12		-0.02	0.00	0.07
OGDB	1	CORS	44.699	-75.494	-1.07	0.56	1.68	0.46	-0.86	2.07	NNC	1.86	-0.58	-2.53
OGDE	1	CORS	44.701	-75.495	-2.2	0.56	3.38	0.46	0.03	2.06	NNC	0.73	1.11	-1.63
OHAL	1	CORS	40.769	-84.107	-0.73	0.05	1.94	0.03	-2.39	0.09				
OHAS	1	CORS	41.925	-80.551	-0.72	0.06	1.92	0.04	-2.43	0.15		0.10	0.01	-0.01
OHCD	1	CORS	41.541	-81.635	-0.82	0.05	1.68	0.03	-2.67	0.09		0.14	-0.21	0.39
OHCO	1	CORS	40.297	-81.842	-0.62	0.06	1.89	0.04	-2.77	0.14				
OHFH	1	CORS	41.760	-81.281	-1.11	0.23	0.89	0.18	-0.36	0.71	NNC	-0.14	-1.12	2.65
OHFN	1	CORS	41.558	-84.135	-0.74	0.06	1.99	0.04	-1.88	0.16		-0.14	0.18	0.38
OHHA	1	CORS	41.041	-83.676	-0.81	0.05	1.89	0.04	-2.37	0.13		-0.06	-0.02	-0.11

					Velocities (mm/yr) and Uncertainties (1σ , mm/yr)						Outlier rationale	Residuals (mm/yr)		
Site	Solution	Type	Latitude	Longitude	v_{North}	σ_{North}	v_{East}	σ_{East}	v_{Up}	σ_{Up}		$\text{res}_{\text{North}}$	res_{East}	res_{Up}
OHHU	1	CORS	41.177	-82.561	-0.53	0.05	2.14	0.04	-2.62	0.12		0.20	0.07	-0.18
OHJE	1	CORS	40.375	-80.730	-1.36	0.1	1.48	0.08	-2.02	0.31				
OHLA	1	CORS	41.727	-81.286	-0.98	0.05	2.04	0.03	-3.12	0.11		-0.01	0.03	-0.11
OHLO	1	CORS	41.294	-82.233	-1.15	0.05	1.74	0.04	-2.14	0.12		-0.15	-0.08	0.29
OHLU	2	CORS	41.721	-83.526	6.56	0.38	20.33	0.31	-6.13	1.35	NNC	7.45	18.56	-3.73
OHMH	1	CORS	41.544	-82.731	-0.96	0.05	1.88	0.03	-2.4	0.09		-0.02	-0.05	0.15
OHMN	1	CORS	41.024	-80.773	-1.1	0.05	1.9	0.03	-2.17	0.09		0.01	0.01	0.10
OHMR	1	CORS	40.546	-84.631	-0.4	0.07	1.82	0.05	-3.08	0.2				
OHPO	1	CORS	41.106	-81.245	-1.11	0.08	2.02	0.06	-1.91	0.25		-0.03	-0.05	0.55
OHRI	1	CORS	40.768	-82.561	-0.84	0.05	2.03	0.03	-2.16	0.1				
OHSB	1	CORS	41.636	-82.830	-1.07	0.08	2.04	0.06	-3.17	0.22		-0.09	0.08	-0.46
OHTU	1	CORS	40.457	-81.408	-0.06	0.12	3.23	0.1	-1.2	0.37				
OHUN	1	CORS	40.233	-83.361	-0.97	0.05	1.44	0.03	-2.43	0.11				
OHVW	1	CORS	40.856	-84.624	-0.65	0.05	2.19	0.03	-3.23	0.09				
OHWI	1	CORS	41.582	-84.558	-0.34	0.05	0.86	0.03	-3.34	0.09		0.03	-0.46	-0.38
OKEE	2	CORS	42.914	-82.595	0.41	0.05	0.89	0.03	-2.31	0.12		1.14	-0.64	-0.15
OLCO	1	CORS	43.334	-78.719	-1.57	0.21	1.97	0.15	-0.86	0.7		0.01	0.21	0.14
ONTO	1	CORS	46.850	-89.369	-1.37	0.25	1.99	0.19	-1.65	0.8		-0.11	0.25	-0.26
OSPA	1	CORS	43.465	-76.512	-1.92	0.05	1.73	0.03	0.22	0.09		-0.05	0.03	0.03
OSWE	1	CORS	43.466	-76.511	-1.9	0.14	1.95	0.1	-0.75	0.44	NNC	-0.03	0.26	-0.94
P020	1	CORS	47.002	-118.566	1.57	0.05	3	0.03	-1.76	0.08		0.00	-0.02	0.03
P025	1	CORS	48.731	-116.288	0.52	0.06	3.32	0.04	-0.55	0.14		0.00	0.01	0.06
P046	1	CORS	47.030	-113.332	0.02	0.05	2.94	0.03	-1.77	0.09		-0.03	0.09	0.10
P049	1	CORS	47.350	-110.906	-0.12	0.05	2.82	0.03	-2.6	0.08		0.03	-0.02	-0.03
P050	1	CORS	48.810	-111.248	-0.15	0.05	3.08	0.03	-2.53	0.09		0.03	0.01	0.00
P052	1	CORS	47.375	-107.019	0.01	0.05	2.65	0.03	-3.54	0.08		0.02	-0.01	-0.03
P053	1	CORS	48.726	-107.725	-0.25	0.06	2.83	0.04	-3.03	0.13		0.02	0.00	0.02
P055	1	CORS	47.117	-104.685	-0.13	0.06	2.7	0.04	-3.97	0.15		-0.02	0.00	0.00
P422	1	CORS	46.798	-116.980	0.93	0.07	2.94	0.04	-1.5	0.14		-0.03	-0.02	0.00
P451	1	CORS	46.793	-119.041	1.87	0.05	3.24	0.04	-2.11	0.08		-0.01	-0.01	0.00
P775	1	CORS	40.475	-86.992	-0.69	0.07	2.98	0.05	-2.1	0.19				
P803	1	CORS	46.326	-90.684	-1.48	0.09	2.32	0.07	-2.82	0.3		-0.07	0.06	0.14
PABW	2	CORS	47.213	-124.205	12.24	0.08	16.27	0.06	-1.07	0.21		0.31	0.38	0.01
PACP	1	CORS	41.764	-78.024	-0.53	0.51	2.01	0.38	-2.12	1.7	NED	1.02	0.21	-0.58
PACS	1	CORS	41.239	-79.429	-1.22	0.06	1.5	0.04	-2.12	0.13		0.01	-0.06	0.00
PAII	1	CORS	40.606	-79.186	-1.41	0.08	1.74	0.06	-1.59	0.21				
PAMM	1	CORS	41.230	-80.245	-1.25	0.06	1.89	0.04	-2.06	0.16		-0.02	0.01	0.07
PAPC	1	CORS	41.764	-78.023	-1.57	0.06	1.81	0.04	-1.45	0.14		-0.02	0.01	0.09
PAPT	1	CORS	40.445	-79.959	-1.17	0.07	2.15	0.05	-1.67	0.22				
PARS	1	CBN	45.365	-80.023	-1.7	0.16	1.79	0.12	0.8	0.5		0.16	0.10	0.21
PARY	1	ACS	45.339	-80.036	-1.9	0.04	1.64	0.02	0.51	0.06		-0.03	-0.03	-0.04
PAWG	1	CORS	40.305	-79.506	-0.97	0.05	1.79	0.04	-1.69	0.11				
PBRO	1	ACS	45.405	-64.329	-1.15	0.27	1.41	0.2	-1	0.79		0.29	-0.14	-0.03
PCK1	2	CORS	46.065	-84.362	-1.52	0.2	2.17	0.15	0.8	0.62	NED	-0.03	0.23	0.99
PCK2	1	CORS	46.065	-84.362	-0.93	0.17	2.66	0.13	0.49	0.53	NED	0.56	0.73	0.68
PCK5	2	CORS	46.065	-84.362	-2.23	0.15	1.71	0.12	-2.51	0.45	NED	-0.74	-0.23	-2.32
PCK6	2	CORS	46.065	-84.362	-2.45	0.16	1.69	0.12	-2.48	0.47	NED	-0.95	-0.25	-2.29
PCRT	1	CBN	50.050	-66.778	-2.76	0.13	2.24	0.09	3.65	0.39		0.19	-0.17	-0.01
PEAW	1	CBN	55.013	-85.409	-1.43	0.16	1.84	0.1	11.16	0.45		0.00	-0.01	0.37
PEMB	1	CBN	45.837	-77.245	-1.97	0.17	1.91	0.13	1.34	0.6		0.08	0.02	-0.66
PGC5	1	ACS	48.649	-123.451	5.26	0.07	7.81	0.05	-0.76	0.14	DC	0.16	-0.24	0.27
PICL	1	ACS	51.480	-90.162	-1.63	0.04	1.78	0.03	4.88	0.09		0.00	-0.02	0.09
PIDG	1	CAMP	46.174	-71.681	-2.25	1.01	1.85	0.8	4.5	3.49		-0.14	-0.08	2.64
PIER	1	ACS	45.496	-73.848	-2.27	0.12	1.59	0.09	1.44	0.36		0.03	-0.33	-0.37
PILO	1	CAMP	47.869	-69.521	-2.21	0.25	1.62	0.19	1.04	0.77		0.13	-0.42	-0.86
PIPR	1	CBN	52.329	-90.785	-1.64	0.16	2.05	0.1	4.71	0.47		0.00	0.02	0.00
PIT1	1	CORS	40.551	-79.697	-0.89	0.07	1.84	0.05	-3.16	0.19				
PJCA	1	CAMP	47.461	-71.521	-2.79	0.28	2.51	0.23	3.03	1.01		-0.14	-0.06	-0.13
PLS6	1	CORS	47.664	-114.114	-0.02	0.07	3.38	0.05	-1.52	0.17		-0.05	0.09	0.05
PMTL	1	ACS	45.557	-73.520	-2.95	0.05	1.9	0.04	2.27	0.12		-0.65	0.08	0.21
PNR1	1	CORS	46.864	-94.722	0.36	0.09	1.89	0.07	-3.31	0.27	NED	1.15	-0.34	-0.49
PNR2	1	CORS	46.864	-94.723	-0.28	0.21	2.81	0.15	-2.52	0.63	NED	0.51	0.59	0.29
PNR5	1	CORS	46.864	-94.722	-0.51	0.06	2.11	0.04	-2.87	0.14	DC	0.28	-0.12	-0.05

					Velocities (mm/yr) and Uncertainties (1σ , mm/yr)						Outlier rationale	Residuals (mm/yr)		
Site	Solution	Type	Latitude	Longitude	v_{North}	σ_{North}	v_{East}	σ_{East}	v_{Up}	σ_{Up}		$\text{res}_{\text{North}}$	res_{East}	res_{Up}
PNR6	1	CORS	46.864	-94.723	-0.9	0.06	2.35	0.04	-2.81	0.16	DC	-0.11	0.12	0.00
PNTN	1	CBN	54.695	-99.010	-1.7	0.11	2.35	0.07	3.61	0.31		-0.01	0.00	0.04
POA2	1	ACS	45.668	-73.495	-2.34	0.09	1.37	0.06	1.85	0.24		-0.17	-0.31	-0.13
POAT	1	ACS	45.668	-73.495	-2.25	0.29	1.3	0.23	1.85	0.96		-0.09	-0.38	-0.13
POIN	1	CORS	46.484	-84.632	-0.48	0.18	1.79	0.13	-0.77	0.58	NNC	1.35	0.06	-1.25
PORT	1	CORS	45.973	-85.873	-1.61	0.39	1.45	0.31	-0.84	1.36		0.10	-0.30	0.24
POT3	2	CORS	61.056	-146.697	24.76	0.14	-12.14	0.1	8.63	0.41	DC			
POTS	1	CORS	61.056	-146.697	24.37	0.09	-11.79	0.06	6.35	0.22	DC			
PPER	1	ACS	48.517	-68.469	-2.31	0.07	2.34	0.05	2.33	0.18		0.16	0.04	0.13
PRAL	1	ACS	53.213	-105.931	-1.1	0.08	2.47	0.06	-0.64	0.24		0.01	-0.02	0.07
PRDS	1	ACS	50.871	-114.294	-0.11	0.06	3.1	0.04	-0.56	0.11		0.08	-0.15	0.02
PRDU	1	CORS	40.428	-86.911	-0.27	0.07	1.82	0.05	-2.81	0.2				
PRG6	1	CBN	53.910	-122.340	0.64	0.26	2.03	0.18	1.36	0.75		0.00	0.01	-0.29
PRNT	1	CBN	47.922	-74.624	-2.59	0.13	2.02	0.1	5.68	0.44		-0.02	0.00	0.00
PSAG	1	CAMP	48.201	-70.102	-2.35	0.27	2.29	0.19	2.21	0.82		-0.05	0.04	-0.61
PSC1	1	CORS	44.435	-74.250	-2.02	0.06	1.88	0.04	1.25	0.16		0.00	0.02	-0.01
PSTA	1	ACS	42.659	-81.213	-1.52	0.24	1.89	0.18	-2.19	0.8		-0.11	-0.05	-0.21
PSU1	1	CORS	40.807	-77.850	-0.84	0.05	1.69	0.03	-1.8	0.08				
PTAA	1	CORS	48.117	-123.494	5.82	0.09	8.86	0.06	-0.16	0.21		-0.15	-0.18	0.38
PTAL	1	ACS	49.256	-124.861	6.05	0.05	8.36	0.04	1.68	0.08		-0.03	-0.18	0.09
PTEG	1	CBN	44.445	-81.397	-1.69	0.18	1.75	0.13	-0.97	0.57		0.00	0.00	-0.06
PTER	1	CBN	44.311	-78.303	-1.66	0.14	1.86	0.1	0.59	0.45		-0.04	0.10	0.14
PTHK	1	ACS	45.622	-61.342	-2.89	0.18	2.1	0.14	-4.33	0.52	NNK	-1.55	0.75	-2.79
PTIR	1	CORS	46.485	-84.631	-1.76	0.05	1.72	0.03	0.65	0.11		0.07	-0.01	0.17
PTRF	1	ACS	48.544	-124.413	6.17	0.07	10.81	0.05	1.9	0.15		-0.30	-0.03	0.55
PUGW	1	ACS	45.855	-63.658	-1.2	0.27	2.03	0.2	-0.92	0.79		0.00	0.23	0.16
PWEL	1	ACS	43.237	-79.220	-1.31	0.04	1.84	0.03	-1.62	0.07		0.05	0.03	-0.07
QAAR	1	CORS	70.740	-52.688	-2.02	0.06	0.28	0.05	7.44	0.15		-0.01	-0.03	-0.07
QAQ1	3	CORS	60.715	-46.048	-2.84	0.09	0.6	0.06	4.53	0.24		-0.02	0.04	-0.41
QIKI	1	ACS	67.559	-64.034	-1.62	0.04	2.67	0.04	2.77	0.08		0.02	0.04	-0.04
QUAD	1	ACS	50.133	-125.331	5.03	0.07	5.76	0.05	3.25	0.17		0.00	-0.09	0.11
QUIC	1	CORS	58.909	-136.587	6.86	0.07	1.8	0.05	29.15	0.15		-0.73	0.54	0.95
RCMI	1	CORS	46.265	-84.191	-0.92	0.37	1.49	0.28	-1.11	1.2	NNC	0.58	-0.11	-1.21
REG8	1	CBN	50.309	-104.206	-0.73	0.15	2.92	0.1	-2.37	0.43		0.04	0.02	-0.13
REPL	1	ACS	66.524	-86.231	-1.07	0.11	2.06	0.08	6.48	0.32		0.01	-0.01	-0.07
RESO	1	ACS	74.691	-94.894	-1.95	0.04	3.26	0.04	4.34	0.1		0.00	0.03	0.03
RG12	1	CBN	49.799	-104.265	-0.7	0.3	3.02	0.22	-1.93	0.88		-0.01	0.05	0.73
RG14	1	CBN	50.339	-103.613	-1.05	0.29	2.64	0.21	-2.36	0.84		-0.10	-0.03	-0.16
RICH	1	CAMP	67.098	-136.126	0.59	0.6	4.3	0.4	-2.71	1.96		0.02	0.00	0.18
RIMO	1	ACS	48.443	-68.521	-2.44	0.06	2.27	0.04	2.1	0.13		0.01	-0.03	-0.01
RINK	1	CORS	71.849	-50.994	-0.4	0.06	3.12	0.05	8.81	0.14		0.21	0.32	-0.47
RIS1	1	CORS	42.012	-90.226	0.61	0.08	1.81	0.06	-3.76	0.24	DC	0.81	-0.07	-0.52
RIS2	1	CORS	42.012	-90.225	1.04	0.25	2.38	0.18	-2.26	0.8	NED	1.24	0.50	0.99
RIS5	1	CORS	42.012	-90.226	-0.72	0.08	1.25	0.06	-5.62	0.23	DC	-0.53	-0.62	-2.37
RIS6	1	CORS	42.012	-90.225	-0.62	0.08	2.19	0.06	-0.79	0.23	DC	-0.42	0.31	2.45
RKD1	1	CORS	48.964	-119.413	1.64	0.09	3.71	0.06	-1.04	0.23		0.01	0.02	0.01
RNKN	1	ACS	62.814	-92.090	-1.43	0.1	3.23	0.07	9.4	0.28		-0.01	0.01	0.04
ROBV	1	CAMP	46.180	-71.161	-2.1	0.24	1.48	0.19	0.61	0.83		0.11	-0.23	-0.58
ROCH	1	CORS	43.269	-77.628	-2.3	0.24	1.63	0.19	-0.09	0.83	NNC	-0.69	0.01	0.51
ROSR	1	CAMP	61.969	-132.488	0.73	2.89	3.57	1.72	-3.55	8.48		0.03	-0.86	-2.42
ROSS	1	ACS	48.834	-87.520	-3.03	0.05	1.62	0.03	1.92	0.12		-0.13	-0.04	-0.08
ROUY	1	ACS	48.241	-79.029	-2.13	0.04	1.52	0.03	6.73	0.09		0.01	-0.02	0.04
RPOR	1	CAMP	47.042	-72.210	-2.35	0.31	2.48	0.28	3.39	1.25		-0.02	0.20	0.04
RPT6	1	CORS	47.387	-122.375	4.82	0.07	6.72	0.05	-3.46	0.15		-0.16	0.01	-0.67
RRW1	1	CORS	42.351	-89.058	-0.08	0.08	1.98	0.06	-3.27	0.25		0.00	0.04	-0.03
SABL	1	ACS	43.933	-60.006	-1.15	0.23	1.39	0.17	-2.16	0.67		0.02	-0.05	0.13
SACH	1	ACS	71.990	-125.250	0.29	0.22	2.87	0.15	-2.27	0.78		0.01	-0.01	0.53
SAG1	1	CORS	43.629	-83.838	-2.23	0.06	0.78	0.04	-3.59	0.16	NNC	-1.01	-1.10	-1.46
SAG2	1	CORS	43.628	-83.838	-1.92	0.14	2.31	0.1	-4.82	0.44	NNC	-0.69	0.43	-2.68
SAG5	1	CORS	43.629	-83.838	-1.87	0.1	0.93	0.07	-3.91	0.3	NNC	-0.64	-0.95	-1.77
SAG6	1	CORS	43.628	-83.838	-1.43	0.09	2.06	0.07	-4.38	0.27	NNC	-0.20	0.18	-2.25
SAGA	1	CAMP	46.544	-71.449	-2.8	0.26	2.66	0.21	1.73	0.89		-0.51	0.35	-0.16
SAHC	1	CAMP	53.216	-131.983	10.46	0.6	1.21	0.4	0.62	1.87	NED	-0.11	0.22	1.89

					Velocities (mm/yr) and Uncertainties (1σ , mm/yr)						Outlier rationale	Residuals (mm/yr)		
Site	Solution	Type	Latitude	Longitude	v_{North}	σ_{North}	v_{East}	σ_{East}	v_{Up}	σ_{Up}		$\text{res}_{\text{North}}$	res_{East}	res_{Up}
SAK4	1	CBN	52.045	-106.480	-1.05	0.13	2.78	0.09	-5.7	0.38	NNC	-0.08	-0.03	-3.95
SALB	1	CAMP	46.701	-72.074	-2.31	0.32	1.79	0.25	1.74	1.08		-0.20	-0.27	-0.99
SALL	1	CBN	62.188	-75.669	-1.19	0.19	2.78	0.12	6.05	0.57		0.00	0.01	-0.09
SAPO	1	CAMP	46.809	-70.200	-1.89	0.24	1.83	0.2	0.41	0.88		0.19	-0.25	-0.78
SASK	1	ACS	52.196	-106.398	-1.05	0.05	2.82	0.03	-1.67	0.1		-0.01	0.02	0.00
SBE2	1	CAMP	45.742	-73.108	-2.45	0.39	0.7	0.31	7.86	1.31	NNC	-0.56	-0.93	5.70
SBON	1	CAMP	46.472	-72.859	-2.56	0.32	1.88	0.26	2.22	1.07		-0.27	-0.03	-0.57
SC00	2	CORS	46.951	-120.725	2.86	0.06	3.45	0.04	-2.84	0.11		-0.04	-0.19	-0.01
SC04	1	ACS	48.923	-123.704	5.13	0.05	7.94	0.04	-0.34	0.08		0.01	0.05	0.05
SCBY	1	CORS	80.260	-59.594	-2.9	0.06	1.14	0.05	7.29	0.2		-0.01	0.01	0.00
SCH2	1	ACS	54.832	-66.833	-1.18	0.04	2.44	0.03	10.15	0.08		0.01	0.00	-0.02
SCOM	1	CAMP	46.270	-73.778	-1.54	0.22	1.91	0.16	2.98	0.73		0.09	-0.08	0.23
SCSH	1	CORS	42.474	-82.882	-1.48	0.34	2.01	0.33	-0.95	1.44		-0.35	0.27	1.40
SDBY	1	CBN	46.450	-81.195	-1.8	0.16	2.06	0.12	2.16	0.5		0.01	0.02	0.09
SDNY	1	ACS	46.161	-60.189	-2.31	0.19	1.69	0.14	-4.54	0.52		-0.11	-0.18	-1.50
SDPT	1	CBN	53.259	-131.824	10.46	0.17	1.33	0.12	-0.92	0.51		0.13	0.44	0.28
SEAT	1	CORS	47.654	-122.310	4.28	0.06	6.35	0.04	-2.31	0.09		-0.08	0.09	-0.01
SED2	1	CAMP	45.154	-73.928	0.17	1.01	1.87	0.82	1.29	3.49	NED	2.39	-0.16	-0.63
SEDB	1	CAMP	45.242	-73.922	-2.14	0.22	1.97	0.17	2.39	0.75		0.05	0.04	0.43
SEDR	2	CORS	48.522	-122.224	3.69	0.06	5.94	0.04	-1.69	0.12		0.00	0.02	-0.02
SELD	2	CORS	59.446	-151.707	-5.06	0.07	1.96	0.06	5.01	0.16				
SENU	1	CORS	61.070	-47.141	-2.94	0.07	-0.01	0.05	7.43	0.17		-0.06	-0.06	0.56
SEPT	1	ACS	50.205	-66.387	-4.35	0.05	3.54	0.03	3.72	0.1		-0.33	0.25	-0.05
SG27	1	CORS	71.323	-156.610	0.27	0.06	2.72	0.05	-3.8	0.09				
SGER	1	CAMP	46.005	-72.839	-1.63	0.32	1.77	0.24	2.71	1.06		0.17	-0.21	0.36
SGTN	1	CBN	49.679	-102.977	-0.43	0.12	2.33	0.09	-3.44	0.36		0.05	-0.04	-0.30
SHBK	1	ACS	45.151	-61.974	-1.32	0.24	1.4	0.18	-1.41	0.7		-0.01	0.04	0.13
SHBR	1	ACS	44.919	-62.519	-1.17	0.29	1.72	0.22	-1.03	0.86		0.12	0.03	0.55
SHE2	1	ACS	46.221	-64.552	-2.01	0.06	1.57	0.04	-0.55	0.15		-0.09	-0.01	0.15
SHEL	1	ACS	43.772	-65.302	-2	0.12	1.35	0.09	-0.92	0.35		-0.09	-0.08	0.13
SHER	1	ACS	45.401	-71.898	-2.14	0.06	1.63	0.04	1.69	0.14		0.09	-0.05	0.05
SIBY	1	CORS	42.170	-83.241	-0.73	0.05	1.88	0.03	-2.76	0.1		0.04	0.16	-0.11
SIDN	1	CORS	40.310	-84.171	-0.54	0.05	1.96	0.03	-2.86	0.11				
SIMP	1	CAMP	60.735	-129.203	0.55	2.74	2.32	2.01	-1.99	10.21		-0.06	-1.06	-1.38
SIW2	1	CORS	42.868	-87.983	-0.2	0.08	2.03	0.06	-3.3	0.22		-0.02	-0.34	0.20
SIWI	1	CORS	42.868	-87.983	-0.27	0.21	1.72	0.17	1.16	0.67	NNC	-0.09	-0.65	4.65
SJPA	1	ACS	45.258	-66.064	-1.81	0.05	2.11	0.03	-1.36	0.08		-0.02	0.12	-0.10
SLAI	1	CORS	41.901	-93.699	-0.02	0.05	3.19	0.04	-3.01	0.12		-0.01	0.07	-0.01
SLDT	1	CAMP	45.715	-73.708	-2.08	0.17	1.94	0.13	1.76	0.55		0.13	-0.01	-0.14
SLVL	1	CBN	55.544	-114.833	-0.35	0.19	3.2	0.12	1.25	0.54		0.00	0.00	-0.08
SMAI	1	CORS	47.524	-122.345	4.58	0.08	6.05	0.06	-2.18	0.2		-0.04	-0.27	0.38
SMDB	1	CAMP	45.585	-73.284	-1.89	0.17	1.7	0.13	1.72	0.54		0.20	0.00	-0.39
SMTH	1	ACS	54.824	-127.187	1.21	0.1	1.5	0.07	1.28	0.27		-0.08	-0.08	-0.06
SNAR	1	CAMP	46.563	-72.474	-2.23	0.32	2.27	0.25	4.07	1.07		0.05	0.23	1.21
SODI	1	CAMP	46.379	-70.623	-2.25	0.27	1.6	0.21	1.16	0.93		0.08	-0.02	0.26
SOOL	1	CORS	46.504	-84.355	-2.1	0.24	1.82	0.18	0.55	0.78		-0.28	0.17	0.08
SOWR	1	CORS	42.226	-85.534	-0.58	0.06	1.74	0.04	-3.11	0.13		0.01	0.10	-0.02
SPAC	1	CAMP	47.410	-69.919	-2.95	0.22	1.45	0.17	1.01	0.68		-0.47	-0.60	-0.68
SPAM	1	CAMP	46.947	-69.769	-2.36	0.24	4.14	0.19	0.85	0.77		-0.09	0.75	-0.25
SPER	1	CAMP	46.079	-72.467	-2.78	0.3	2.97	0.23	3.23	0.99		-0.35	0.69	0.89
SPLK	1	CBN	56.389	-95.899	-1.3	0.11	2.41	0.07	7.2	0.32		0.03	-0.01	-0.03
SPN6	1	CORS	47.518	-117.423	1.14	0.12	3.07	0.08	-1.34	0.33		0.02	0.01	0.07
SRBK	1	CBN	45.408	-71.986	-2.32	0.1	1.81	0.08	1.25	0.31		-0.06	0.12	-0.46
SRIT	1	CAMP	47.919	-68.955	-1.93	0.23	2.63	0.18	1.78	0.71		0.11	0.25	0.20
SRMP	1	CORS	72.911	-54.394	-4.03	0.05	-1.65	0.05	15.54	0.13		-0.21	-0.25	1.28
SSMG	1	CBN	46.530	-84.588	-1.75	0.16	1.69	0.11	0.62	0.48		0.10	-0.02	0.08
SSP3	1	CORS	42.816	-82.486	-1.07	0.72	2.2	0.61	-2.98	2.87		-0.24	0.60	-0.90
STAN	1	CBN	49.123	-66.538	-2.57	0.14	2.29	0.1	1.8	0.42		0.01	0.00	0.22
STB1	1	CORS	44.796	-87.314	-1.5	0.06	2.37	0.04	-1.79	0.16	DC	-0.02	0.39	0.78
STB5	2	CORS	44.796	-87.314	-0.96	0.18	2.21	0.14	-5.72	0.59	DC	0.52	0.24	-3.14
STB6	2	CORS	44.795	-87.314	-1.19	0.14	2.38	0.11	-5.95	0.45	DC	0.29	0.41	-3.37
STEE	1	CAMP	61.223	-140.210	9.05	2.52	-0.81	1.73	10.33	7.78		-2.97	-1.01	2.27
STGO	1	CBN	46.019	-70.745	-2.11	0.12	2.02	0.09	0.81	0.37		0.04	0.09	0.10

					Velocities (mm/yr) and Uncertainties (1σ , mm/yr)						Outlier rationale	Residuals (mm/yr)		
Site	Solution	Type	Latitude	Longitude	v_{North}	σ_{North}	v_{East}	σ_{East}	v_{Up}	σ_{Up}		$\text{res}_{\text{North}}$	res_{East}	res_{Up}
STJA	1	CAMP	51.937	-131.016	4.25	0.25	-1.76	0.17	-7.27	0.78	PS	-3.42	-3.24	-5.85
STJG	1	CBN	47.586	-52.721	-1.57	0.18	0.88	0.14	-1.07	0.57		-0.01	-0.04	-0.10
STJH	1	CBN	45.295	-66.112	-1.59	0.22	1.54	0.16	-0.88	0.69		0.19	-0.39	0.33
STJO	1	ACS	47.595	-52.678	-1.52	0.05	0.98	0.04	-0.96	0.08		0.03	0.05	0.03
STJV	1	CBN	46.115	-74.586	-2.11	0.1	1.97	0.07	2.79	0.31		0.00	-0.11	0.06
STKT	1	CBN	43.122	-79.227	-1.6	0.16	1.75	0.12	-0.9	0.5		-0.19	0.00	0.58
STLW	1	CBN	46.910	-55.369	-1.47	0.17	0.89	0.13	-1.02	0.55		0.02	-0.02	0.00
STP1	1	CORS	44.304	-91.903	0.18	0.07	1.92	0.05	-3.59	0.2		0.46	-0.18	0.21
STP2	1	CORS	44.304	-91.903	0.27	0.13	2.07	0.09	-2.63	0.39		0.55	-0.03	1.17
STP5	1	CORS	44.304	-91.903	-0.53	0.09	2.09	0.06	-4.17	0.24		-0.25	-0.02	-0.36
STP6	1	CORS	44.304	-91.903	-0.34	0.09	2.33	0.06	-4.12	0.24		-0.06	0.23	-0.31
SUAF	1	CORS	64.859	-147.836	-1.95	0.07	3.32	0.05	-0.95	0.14				
SUP1	1	CORS	46.749	-88.442	0.37	0.21	1.16	0.15	-2.4	0.66	NNC	1.94	-0.74	-1.54
SUP2	1	CORS	45.750	-87.074	-1.35	0.04	2.08	0.02	-1.13	0.07		-0.02	0.08	0.03
SUP3	1	CORS	46.303	-85.513	-2.94	0.06	1.86	0.04	-0.68	0.13		-0.23	0.00	-0.09
SUR6	1	CBN	49.074	-122.692	3.98	0.35	5.86	0.24	-1.71	1.07		0.07	-0.27	-0.18
SVAL	1	CAMP	45.578	-72.728	-2.63	0.2	1.27	0.15	2.53	0.64		-0.41	-0.24	0.34
SVLK	1	CBN	50.704	-90.562	-1.53	0.13	1.95	0.09	2.87	0.4		0.02	0.00	-0.16
SWCR	1	CBN	50.249	-107.769	-0.81	0.15	3	0.1	-1.7	0.43		-0.01	0.00	0.08
SWNR	1	CBN	52.067	-101.275	-1.24	0.1	2.52	0.07	-0.7	0.29		0.00	0.00	-0.11
SYCN	1	CORS	43.116	-76.093	-1.67	0.05	1.45	0.03	-0.16	0.11		0.09	-0.04	-0.05
TALB	1	CAMP	61.629	-138.641	4.26	0.99	2.44	0.65	0.18	2.89		-0.41	-2.31	-1.67
TATA	1	ACS	45.712	-63.295	-0.98	0.27	1.5	0.2	-0.8	0.79		0.16	-0.09	0.47
TATC	1	ACS	59.630	-137.738	13.28	0.07	3.08	0.05	21.98	0.16		-1.61	1.89	-1.28
TBON	1	CORS	61.180	-149.785	5.31	0.07	-5.9	0.05	3.79	0.15				
TBYG	1	CBN	48.466	-89.217	-1.72	0.1	1.91	0.08	0.81	0.33		0.03	0.01	0.03
TFNO	1	ACS	49.154	-125.908	7.9	0.1	12.76	0.08	0.11	0.3		0.17	0.34	-0.72
THMP	1	CBN	55.847	-98.023	-1.6	0.1	2.45	0.07	5.63	0.29		0.00	0.02	0.01
THU2	3	CORS	76.537	-68.825	-2.99	0.06	0.17	0.05	5.06	0.21		-0.03	-0.04	-0.13
TIFF	1	CORS	41.075	-83.150	-0.85	0.05	2.54	0.03	-2.23	0.1		-0.04	0.23	0.01
TIMM	1	CORS	62.536	-42.286	-1.78	0.06	0.94	0.04	6.57	0.12		-0.03	0.07	0.12
TIMS	1	CBN	48.523	-81.540	-2.08	0.26	1.98	0.18	6.14	0.8		-0.01	0.01	0.37
TKTO	1	ACS	62.490	-103.282	-0.9	0.23	3.33	0.16	9.85	0.66		0.01	0.01	-0.16
TLDO	1	CORS	41.613	-83.475	-0.8	0.08	1.88	0.06	-2.66	0.24		0.02	0.09	-0.36
TLKA	3	CORS	62.308	-150.420	-2.28	0.16	-1.63	0.11	0.91	0.52				
TMPG	1	CBN	55.441	-98.219	-1.69	0.11	2.31	0.07	4.94	0.31		-0.01	-0.02	-0.01
TMSC	1	CBN	46.717	-79.091	-2.22	0.12	1.88	0.09	2.43	0.43		-0.01	0.02	-0.39
TOLE	1	CORS	41.693	-83.472	-1.13	0.21	1.55	0.17	-2.35	0.73		-0.23	-0.23	0.06
TORT	1	CBN	43.727	-79.610	-1.49	0.13	1.7	0.1	-1.27	0.41		0.01	0.01	-0.11
TOWH	1	CAMP	64.189	-140.030	1.21	1.29	6.49	0.86	-0.67	3.92		0.17	-0.71	2.47
TREO	1	CORS	64.277	-41.375	-2.02	0.07	-0.36	0.05	5.29	0.17		0.02	0.00	0.14
TRIV	1	ACS	46.344	-72.539	-2.32	0.06	1.91	0.04	2.61	0.15		0.05	-0.27	0.06
TRUR	1	ACS	45.379	-63.234	-1.73	0.26	2.03	0.19	-1.64	0.73		-0.11	0.21	-0.21
TSEA	4	CORS	61.187	-149.895	9.12	0.1	-4.19	0.08	1.97	0.27				
TSKT	1	ACS	43.870	-65.963	-2.16	0.07	1.75	0.05	-1.04	0.18		-0.16	-0.04	-0.08
TSLN	1	CAMP	60.210	-132.816	3.48	2.24	5.39	1.47	0.98	6.62		0.22	0.88	1.21
TUKT	1	ACS	69.438	-132.994	-1.01	0.06	5.32	0.04	-3.33	0.12		-0.08	0.12	0.03
U346	1	CORS	47.474	-87.860	-1.75	0.27	1.89	0.2	0.37	0.86		0.07	-0.02	0.03
UCLU	1	ACS	48.926	-125.542	8.15	0.06	12.65	0.04	0.38	0.1		0.08	0.16	-0.14
UNB3	1	ACS	45.950	-66.642	-1.68	0.07	1.79	0.05	-0.93	0.15		0.17	0.02	-0.28
UNIV	1	CORS	42.286	-84.386	-0.75	0.05	2.01	0.03	-2.43	0.09		-0.02	0.03	0.05
UOFM	2	CORS	42.296	-83.840	4.52	0.08	4.87	0.06	-0.9	0.22	EP	5.24	2.96	1.59
UPTC	1	CORS	41.629	-79.664	-1.12	0.04	1.75	0.03	-2.13	0.07		0.00	0.02	0.00
UPTO	1	CAMP	60.772	-140.188	15.18	2.12	-2.73	1.5	13.8	6.43		-1.89	0.90	1.69
UPVK	1	CORS	72.788	-56.128	-3.18	0.07	-0.96	0.06	6.59	0.2		0.04	0.01	-1.01
UTMG	1	CORS	62.927	-43.306	-0.82	0.08	-0.14	0.06	6.95	0.21		0.14	-0.08	0.11
VALD	1	ACS	48.097	-77.564	-2.35	0.05	1.81	0.03	6.46	0.12		0.00	0.02	0.04
VCAP	1	CORS	44.262	-72.582	-2.12	0.05	1.3	0.03	0.21	0.07		-0.09	-0.21	-0.05
VDAV	1	CAMP	46.011	-74.232	-1.95	0.16	2.39	0.13	1.6	0.58		0.03	0.06	-0.69
VETN	1	CBN	52.043	-111.124	-0.11	0.18	2.94	0.12	-1.22	0.51		0.08	-0.03	-0.01
VODG	1	CORS	41.795	-88.004	-0.31	0.08	2.2	0.06	-3.13	0.23		-0.08	0.26	-0.35
VRN4	1	CBN	50.200	-119.318	1.53	0.23	3.44	0.17	0.62	0.72		0.05	-0.14	0.19
VRN9	1	CBN	50.215	-118.574	1.02	0.51	4.42	0.34	1.01	1.62		-0.05	0.29	0.50

Site	Solution	Type	Latitude	Longitude	Velocities (mm/yr) and Uncertainties (1σ , mm/yr)						Outlier rationale	Residuals (mm/yr)		
					v_{North}	σ_{North}	v_{East}	σ_{East}	v_{Up}	σ_{Up}		$\text{res}_{\text{North}}$	res_{East}	res_{Up}
VROY	1	CAMP	46.387	-71.875	-1.18	0.32	2.21	0.25	3.3	1.1		0.78	0.07	1.05
VTC1	1	CORS	43.939	-72.604	-1.37	0.06	2.46	0.04	-1.26	0.12		0.18	0.30	-0.55
VTD7	1	CORS	44.398	-72.026	-2.09	0.06	1.93	0.04	1.54	0.16		-0.05	-0.01	0.45
VTD9	1	CORS	44.951	-72.160	-2.03	0.07	1.92	0.05	2.65	0.19		-0.06	-0.04	0.65
VTEB	1	CORS	44.914	-72.799	-1.51	0.23	2.32	0.17	0.92	0.68		0.32	0.19	-0.77
VTHA	1	CORS	44.509	-72.366	-2.01	0.07	1.97	0.05	1.21	0.19		-0.01	0.06	0.03
VTIP	1	CORS	44.820	-71.891	-1.73	0.06	2.09	0.04	0.95	0.15		0.15	0.08	-0.46
VTMI	1	CORS	43.999	-73.153	-1.7	0.09	1.79	0.07	0.86	0.24		0.01	-0.03	0.44
VTOX	1	CORS	44.008	-72.114	-1.85	0.07	1.81	0.05	-0.21	0.16		0.01	-0.08	0.01
VTRI	1	CORS	44.413	-72.995	-1.97	0.11	1.79	0.08	0.2	0.3		-0.04	0.07	-0.62
VTSA	1	CORS	44.809	-73.083	-2.04	0.05	2.04	0.04	1.48	0.12		-0.01	0.01	-0.05
VTUV	2	CORS	44.469	-73.198	-1.9	0.08	1.47	0.06	1.65	0.22		0.01	-0.12	0.40
WARE	1	CAMP	63.657	-135.919	-0.27	1.37	5.41	0.95	-1.54	4.29		-0.65	-1.25	0.70
WARR	1	CORS	42.534	-83.020	-1.02	0.05	1.67	0.03	-2.31	0.11		-0.02	-0.01	-0.03
WATS	1	CAMP	60.083	-129.369	-1.95	2.48	-0.48	1.63	-0.04	8.16	NED	-2.99	-3.82	1.09
WAWA	1	CBN	48.074	-84.765	-1.78	0.16	2.15	0.11	2.78	0.49		0.02	0.01	-0.10
WDSR	1	ACS	44.980	-64.118	-2.75	0.18	2.52	0.13	-3.24	0.51	NNC	-0.83	0.84	-2.05
WES2	1	CORS	42.613	-71.493	-1.74	0.04	1.97	0.03	-0.66	0.07		0.01	0.01	0.04
WHIT	1	ACS	60.751	-135.222	3.9	0.06	3.61	0.04	1.41	0.11		-0.01	-0.07	0.01
WHRV	1	CAMP	61.788	-140.918	8.81	0.85	0.76	0.59	4.42	2.61		-0.47	-0.58	1.77
WHT1	1	CBN	60.673	-135.121	3.94	0.4	3.6	0.28	1.74	1.23		-0.10	-0.22	-0.30
WHTB	1	CBN	47.409	-53.539	-1.8	0.19	0.73	0.14	-0.88	0.6		-0.05	-0.03	-0.17
WIAB	1	CORS	44.791	-88.045	-1.22	0.09	2.31	0.07	-4.27	0.27		0.05	0.05	-0.47
WIBL	1	CORS	46.866	-91.086	-0.95	0.12	1.61	0.09	-2.43	0.36		0.11	-0.11	-0.07
WICR	1	CORS	45.576	-88.892	-2.52	0.12	4.01	0.09	-3.77	0.38		-0.35	0.52	-0.55
WILL	1	ACS	52.237	-122.168	1.43	0.05	2.43	0.03	0.41	0.07		0.00	-0.02	-0.17
WIM5	1	CORS	43.194	-88.060	0.41	0.07	1.03	0.05	-2.92	0.18	DC	0.48	-1.27	0.54
WIM6	1	CORS	43.194	-88.060	0.01	0.08	1.6	0.06	-3.31	0.21	DC	0.08	-0.70	0.15
WINS	1	CBN	50.182	-97.278	-1.33	0.15	2.2	0.11	-0.65	0.44		0.02	0.00	-0.11
WINA	1	CBN	49.854	-97.478	-1.43	0.1	2.21	0.07	-0.69	0.31		-0.10	0.02	0.22
WINN	1	ACS	49.901	-97.260	-5.32	0.08	-2.72	0.06	-0.4	0.22	EP	-3.99	-4.90	0.45
WIPR	1	CORS	43.863	-89.142	0.01	0.38	1.02	0.29	-4.27	1.18		0.18	-0.39	-0.23
WIRB	1	CORS	44.959	-92.610	-0.53	0.17	2.02	0.13	-3.72	0.49		0.04	-0.03	0.16
WIS1	1	CORS	46.705	-92.015	-1.23	0.06	2.17	0.04	-1.97	0.17	DC	-0.01	-0.02	0.85
WIS2	1	CORS	46.705	-92.016	-0.51	0.2	2.23	0.14	-1.12	0.61	NED	0.70	0.05	1.70
WISS	1	CORS	46.705	-92.015	-1.32	0.06	2.34	0.04	-3	0.14	DC	-0.10	0.15	-0.18
WIS6	1	CORS	46.705	-92.016	-1.07	0.06	2.07	0.04	-2.53	0.14	DC	0.14	-0.12	0.28
WISB	1	CORS	44.795	-87.314	-1.38	0.15	1.05	0.11	-1.7	0.5	DC	0.09	-0.93	0.88
WISN	1	CORS	45.822	-92.369	-1.55	0.07	2.12	0.05	-5.27	0.17		-0.11	-0.05	-0.56
WISR	1	CBN	42.250	-83.020	-0.81	0.16	1.64	0.13	-2.34	0.53		0.01	-0.04	0.43
WIWB	1	CORS	43.421	-88.149	-0.54	0.54	2.72	0.41	-5.27	1.69		-0.29	0.50	-1.75
WLCI	1	CORS	40.808	-87.052	-0.84	0.05	1.15	0.03	-2.54	0.09	NNC			
WLOO	1	ACS	43.473	-80.560	2.73	0.2	-0.18	0.15	1.13	0.72	EP	4.19	-1.83	2.43
WMTW	1	CORS	44.154	-87.693	-1.16	0.74	2.7	0.55	-9.86	2.28	NED	-0.16	0.85	-6.52
WOLK	1	CBN	58.060	-103.799	-1.39	0.15	2.83	0.11	6.47	0.45		0.00	0.00	0.33
WOLV	1	CAMP	61.629	-140.090	7.82	0.89	4.57	0.6	4.31	2.68		-0.23	1.18	0.74
WOOD	1	ACS	46.162	-67.591	-2.02	0.06	1.67	0.04	-0.92	0.13		-0.04	-0.03	-0.33
WOOS	1	CORS	40.799	-81.963	-1.26	0.06	1.95	0.04	-2.64	0.15				
WOST	1	ACS	50.212	-126.605	4.42	0.08	6.03	0.05	2.73	0.19		-0.20	-0.01	0.57
WRUN	1	CORS	42.235	-83.542	-0.76	0.05	1.35	0.04	-2.66	0.12		-0.05	-0.14	-0.12
WSLR	1	ACS	50.127	-122.921	2.83	0.05	5.61	0.04	3.08	0.09		-0.06	0.14	0.42
WTHL	1	CBN	45.487	-62.733	-1.74	0.1	1.63	0.07	-1.85	0.29		-0.02	0.06	-0.20
WVN3	1	CBN	49.352	-123.251	4.27	0.32	6.19	0.24	-0.02	1.05		-0.05	-0.12	0.55
Y565	1	CAMP	61.593	-139.445	6.51	0.93	6.33	0.61	1.79	2.89		-0.07	1.71	-1.42
YAKA	1	CAMP	54.071	-131.837	3.81	0.32	2.19	0.21	-0.46	0.96	PS	-4.70	0.94	1.13
YE5	1	CBN	62.467	-114.376	-0.42	0.31	2.86	0.22	5.37	0.93		0.31	0.18	0.24
YELL	1	ACS	62.481	-114.481	-0.83	0.04	2.61	0.03	5.05	0.07		-0.03	-0.02	-0.03
YFB1	1	ACS	63.732	-68.543	-0.38	0.05	0.76	0.04	3.42	0.11	EP	1.76	-1.98	0.13
YKTT	1	CORS	59.511	-139.649	49.56	1.96	-20.9	1.36	20.68	6.09		15.53	-3.10	3.06
YOU1	1	CORS	43.231	-78.970	-1.81	0.09	1.92	0.07	-1.69	0.26	DC	-0.14	0.18	-0.36
YOU2	1	CORS	43.231	-78.970	-1.63	0.18	2.16	0.14	0.04	0.62	DC	0.03	0.42	1.37
YOU5	2	CORS	43.231	-78.970	-1.79	0.09	1.44	0.06	-2.19	0.25	DC	-0.12	-0.30	-0.86
YOU6	1	CORS	43.231	-78.970	-1.71	0.06	1.69	0.04	-3.33	0.15	DC	-0.04	-0.04	-2.00

			Velocities (mm/yr) and Uncertainties (1σ , mm/yr)						Outlier rationale	Residuals (mm/yr)				
Site	Solution	Type	Latitude	Longitude	v_{North}	σ_{North}	v_{East}	σ_{East}	v_{Up}	σ_{Up}	$\text{res}_{\text{North}}$	res_{East}	res_{Up}	
YQX1	1	ACS	48.967	-54.598	-3.27	0.06	0.88	0.04	0.31	0.1	EP	-1.85	-0.13	0.80
YRKT	1	CBN	51.219	-102.404	-1.21	0.13	2.64	0.09	-1.23	0.39		-0.01	0.01	0.00
YWG1	2	ACS	49.901	-97.259	-8.56	0.08	-2.67	0.06	-0.81	0.21	EP	-7.23	-4.85	0.04
YYR1	1	ACS	53.309	-60.420	-1.13	0.07	2.24	0.05	4.76	0.16		0.17	0.04	-0.12
ZAN1	1	CORS	61.229	-149.780	9.46	0.09	-5.04	0.07	0.52	0.22				
ZAN1	2	CORS	61.229	-149.780	1.2	0.13	-6.85	0.09	3.41	0.34	PS			
ZAU1	1	CORS	41.783	-88.331	0.02	0.05	1.8	0.03	-3.09	0.09		0.01	-0.01	-0.27
ZMP1	1	CORS	44.638	-93.152	-0.35	0.05	2.16	0.03	-3.27	0.09		0.04	-0.02	0.19
ZOB1	1	CORS	41.297	-82.206	-0.82	0.05	1.8	0.03	-2.48	0.09		0.18	-0.03	-0.01